AD-A075 401 MASSACHUSETTS INST OF TECH CAMBRIDGE DEPT OF CIVIL E--ETC F/G 8/11
STATE-OF-THE-ART FOR ASSESSING EARTHQUAKE HAZARDS IN THE UNITED--ETC(U)
AUG 79 E H VANMARCKE DACW39-78-M-3907
UNCLASSIFIED WES-MP-S-73-1 NL

| OF |
ADA
075401

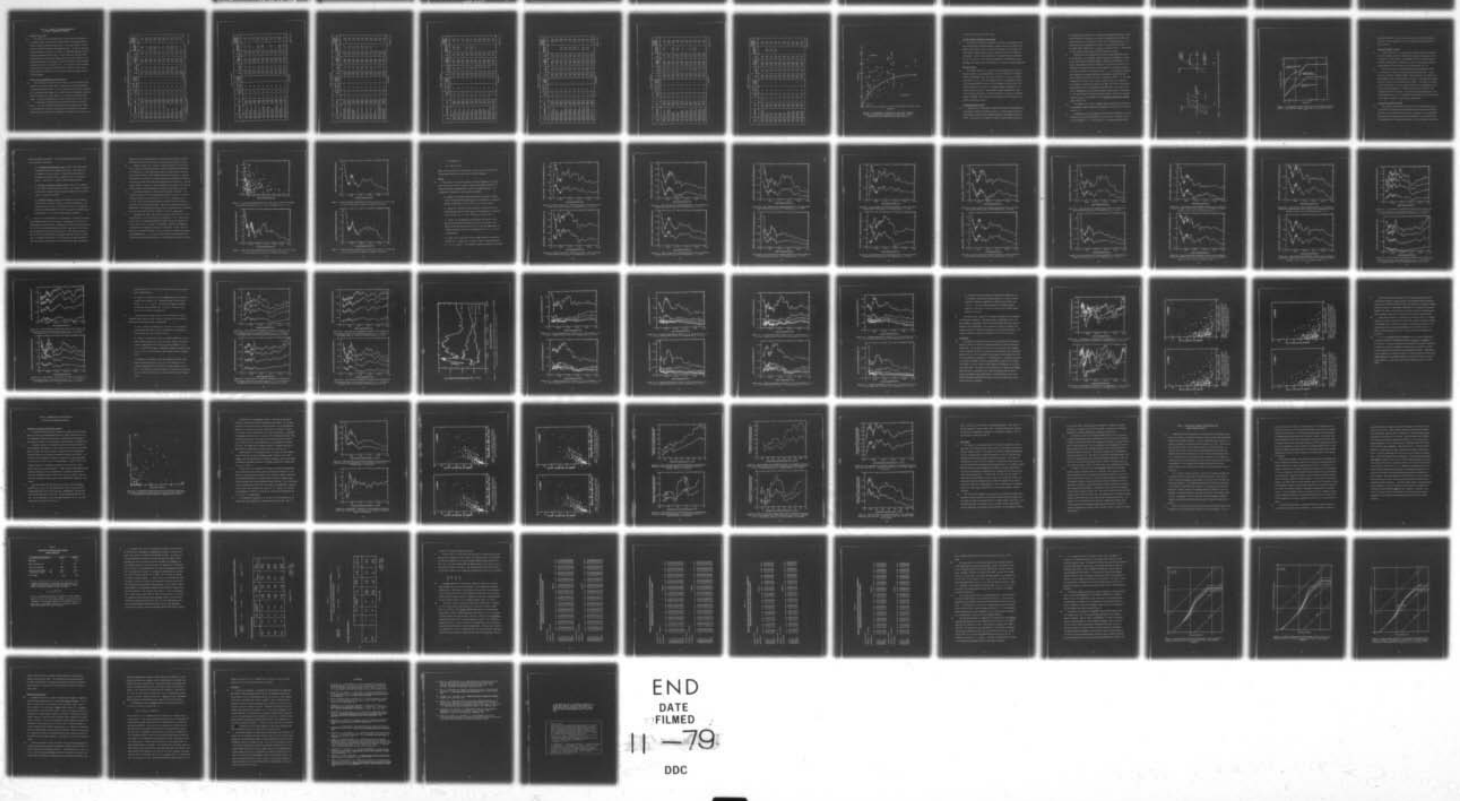

END
DATE
FILMED
11-79
DDC

MISCELLANEOUS PAPER S-73-1

STATE-OF-THE-ART FOR ASSESSING EARTHQUAKE HAZARDS IN THE UNITED STATES

Report 14

REPRESENTATION OF EARTHQUAKE GROUND MOTION: SCALED ACCELEROGRAMS AND EQUIVALENT RESPONSE SPECTRA

by

Erik H. Vanmarcke
Department of Civil Engineering
Massachusetts Institute of Technology
Cambridge, Massachusetts 02139

August 1979
Report 14 of a Series

Prepared for Office, Chief of Engineers, U. S. Army
Washington, D. C. 20314

Under Purchase Order No. DACW39-78-M-3907

Monitored by Geotechnical Laboratory
U. S. Army Engineer Waterways Experiment Station
P. O. Box 631, Vicksburg, Miss. 39180

M. P. S-73-1 STATE-OF-THE-ART FOR ASSESSING EARTHQUAKE HAZARDS IN THE UNITED STATES REPORT 14 AUG. 1979

When this report is no longer needed, return it to the originator.

The findings in this report are not to be construed as an official Department of the Army position unless so designated by other authorized documents.

Unclassified

SECURITY CLASSIFICATION OF THIS PAGE *(When Data Entered)*

REPORT DOCUMENTATION PAGE

READ INSTRUCTIONS BEFORE COMPLETING FORM

1. REPORT NUMBER
Miscellaneous Paper S-73-1

2. GOVT ACCESSION NO.

3. RECIPIENT'S CATALOG NUMBER

4. TITLE *(and Subtitle)*
STATE-OF-THE-ART FOR ASSESSING EARTHQUAKE HAZARDS IN THE UNITED STATES, Report 14, REPRESENTATION OF EARTHQUAKE GROUND MOTION: SCALED ACCELEROGRAMS AND EQUIVALENT RESPONSE SPECTRA

5. TYPE OF REPORT & PERIOD COVERED
Report 14 of a series

6. PERFORMING ORG. REPORT NUMBER

7. AUTHOR(s)
Erik H. Vanmarcke

8. CONTRACT OR GRANT NUMBER(s)
Purchase Order No.
DACW39-78-M-3907

9. PERFORMING ORGANIZATION NAME AND ADDRESS
Department of Civil Engineering
Massachusetts Institute of Technology
Cambridge, Mass. 02139

10. PROGRAM ELEMENT, PROJECT, TASK AREA & WORK UNIT NUMBERS

11. CONTROLLING OFFICE NAME AND ADDRESS
Office, Chief of Engineers, U. S. Army
Washington, D. C. 20314

12. REPORT DATE
August 1979

13. NUMBER OF PAGES
83

14. MONITORING AGENCY NAME & ADDRESS *(if different from Controlling Office)*
U. S. Army Engineer Waterways Experiment Station
Geotechnical Laboratory
P. O. Box 631, Vicksburg, Miss. 39180

15. SECURITY CLASS. *(of this report)*
Unclassified

15a. DECLASSIFICATION/DOWNGRADING SCHEDULE

16. DISTRIBUTION STATEMENT *(of this Report)*
Approved for public release; distribution unlimited.

(12) 88

17. DISTRIBUTION STATEMENT *(of the abstract entered in Block 20, if different from Report)*

18. SUPPLEMENTARY NOTES

19. KEY WORDS *(Continue on reverse side if necessary and identify by block number)*

Accelerograms
Earthquake engineering
Earthquake hazards
Earthquakes
Ground Motion
Seismic analysis
State-of-the-art studies

20. ABSTRACT *(Continue on reverse side if necessary and identify by block number)*

Alternative representations of earthquake ground motion for the purpose of seismic analysis and design are reviewed and critically examined, with emphasis on the relation between earthquake time histories and response spectra. The results of a study on the effects of scaling earthquake records on peak acceleration are presented. Errors attributable to scaling are evaluated in terms of the response for one-degree elastic and elasto-plastic systems and

(Continued)

DD FORM 1 JAN 73 1473 EDITION OF 1 NOV 65 IS OBSOLETE

Unclassified

SECURITY CLASSIFICATION OF THIS PAGE *(When Data Entered)*

220 010

20. ABSTRACT (Continued)

CONT

the equivalent number of cycles of uniform shear stress. The significance of duration and frequency content is assessed in this context. The pitfalls of the practice of using "standard" design response spectra are pointed out, and methodology is proposed for developing site-specific design response spectra based on appropriate accelerograms from past earthquakes.

PREFACE

This report was prepared by Dr. Erik H. Vanmarcke, Professor of Civil Engineering at Massachusetts Institute of Technology (MIT), as part of on-going work at the U. S. Army Engineer Waterways Experiment Station (WES) in Civil Works Investigation Studies, "Methodologies for Selecting Design Earthquakes," sponsored by the Office, Chief of Engineers, U. S. Army. This is the fourteenth of a series of state-of-the-art reports on methodologies for determining the severity of bedrock motion during earthquakes.

Preparation of the report was under the direction of Dr. E. L. Krinitzsky, Engineering and Rock Mechanics Division (EG&RMD), Geotechnical Laboratory (GL). General direction was by Mr. J. P. Sale, Chief, GL, and Dr. D. C. Banks, Chief, EG&RMD. The author wishes to express his appreciation to Professor Robert V. Whitman of MIT for his helpful advice during the conduct of the study and the preparation of this report. Mr. Paul Lai of MIT assisted in carrying out many of the computations.

COL J. L. Cannon, CE, and COL Nelson P. Conover, CE, were Directors of WE during the period of this study. Mr. F. R. Brown was Technical Director.

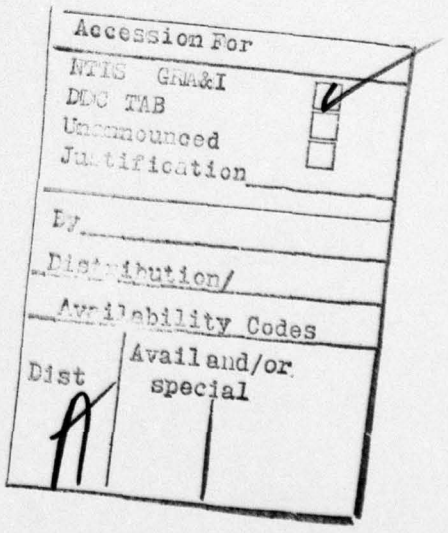

CONTENTS

STATE-OF-THE-ART FOR ASSESSING EARTHQUAKE HAZARDS IN THE UNITED STATES

REPRESENTATION OF EARTHQUAKE GROUND MOTION: SCALED ACCELEROGRAMS AND EQUIVALENT RESPONSE SPECTRA

PART I: INTRODUCTION

1. A most important step in seismic safety evaluation of civil engineering facilities is the specification of the seismic input. Depending on the type of structure, its importance, and the type of analysis contemplated, different characterizations of the input earthquake motion are appropriate. In present earthquake engineering practice, the seismic input will likely be expressed either in terms of a set of smooth response spectra or by a selection of one or more representative "time histories" of earthquake motion.

2. At a given site, different representations of essentially the same seismic input may be required to investigate different classes of structures or to perform different types of analysis. For example, at a dam site, the engineer may want to assess the seismic safety of an earth embankment by time history analysis, and the concrete spillway and miscellaneous appurtenant structures by the response spectrum method of analysis. In a study of seismic behavior of the earth embankment itself for stability, deformation and liquefaction potential, the engineer might alternately represent the earthquake by a pseudo-static force, a response spectrum and a time history.

3. This report is concerned with the question of <u>compatibility</u> between different representations for essentially the same seismic input. But since different modes of specifying the seismic input are intimately related to different procedures of analysis, it seems logical that criteria for compatibility be applied to the end product of the seismic analysis, i.e., to the predicted performance or the predicted seismic load effect. The aim (of the search for compatibility) is to permit achievement of consistent

levels of safety, independent of the representation of seismic input and of the mode of seismic analysis.

4. The report examines the alternatives for specifying earthquake ground motions which serve as input for seismic analysis and design. The focus is not on how the characteristics of the design earthquake (say, magnitude and source-to-site distance) are selected, or on how the maximum ground acceleration is obtained. Rather, the report deals with the characterization of ground motions conditional on the "design" maximum ground acceleration (or velocity), or conditional on magnitude, distance and local site geological condition.

5. The report presents the results of a major study aimed at evaluating the consequences of the widespread practice of scaling accelerograms and smooth response spectra on maximum acceleration. In the WES report series on "Methodologies for Selecting Design Earthquakes," Krinitzsky and Chang (1) propose that maximum motion levels (acceleration or velocity) be used as a basis for rescaling selected existing records or for the generation of appropriate synthetic records. With respect to limitations on scaling, they state: "Because of uncertainties concerning the appropriateness of rescaling any single earthquake record, several records should be used. However, strong-motion records should be selected that require as little rescaling as possible. If a record has to be rescaled by as much as a factor of 4, the records should be discarded." The study of the effect of scale factors consists of a series of statistical analyses of the response of simple systems to a set of 140 horizontal components of 70 earthquake records. Its purpose is to bring about a better understanding of the effects of scaling earthquake records or response spectra, and to assess

the degree of conservatism inherent in design procedures that are based on the use of scaled response spectra or scaled earthquake records.

6. In parallel with the study on the effect of scaling, and in an attempt to explain its results, the frequency content and the strong-motion duration of the set of 140 accelerograms are also examined. The dependence of duration and dominant frequency on magnitude and distance, and their (indirect) correlation with maximum acceleration, are discussed in Part IV of this report.

7. Significant biases are indeed found to be in evidence in the study of the effect of accelerogram scaling. These biases can be avoided if the earthquake engineer uses smooth response spectra that are site-specific, i.e., compatible with the site seismic condition under study. In pursuit of this idea, the last part of the report develops and illustrates a procedure for obtaining site-specific smooth response spectra. It is intended to serve the needs of engineers who must assess the seismic safety of projects (such as dams and appurtenant structures) for which seismic input is required in the form of smooth response spectra as well as time histories.

8. It is assumed that a catalog of strong-motion earthquake records is available, from which the engineer selects a number of time histories that are, as much as possible, representative of the site seismic condition being investigated. The proposed procedure generates a set of smooth response spectra that can represent the site seismic condition as well as the time histories. The proposed procedure is illustrated for two site conditions characterized in terms of magnitude, source-to-site distance and local geology (soil vs rock). In the illustration, it is assumed that the family of available accelerograms is the set of 140 accelerograms mentioned earlier.

PART II: REPRESENTATION OF EARTHQUAKE GROUND MOTION

9. From the perspective of earthquake engineering, the most important parameter characterizing ground motion is the maximum ground acceleration. Seismic design criteria are most often expressed in terms of maximum acceleration. A design value of maximum acceleration may be obtained from an attenuation relationship in function of a specified magnitude and distance, from correlations with a specified M. Mercalli Intensity, or directly from a regional seismic risk map which corresponds to an appropriate mean return period.

10. The maximum acceleration serves as an anchor for more detailed ground motion descriptions. The precise seismic input format obviously depends on the type of analysis to be performed. At present, whenever some form of dynamic (as opposed to pseudo-static) analysis is contemplated, the seismic input takes the form of either time histories or smooth response spectra. Both can be conveniently scaled w.r.t. maximum acceleration.

11. Time history analysis is commonly used to evaluate the response of earth structures (to check stability, deformation, liquefaction potential), secondary systems (equipment) attached to major structures, or systems whose complex, often nonlinear, behavior is under study.

An advantage of time history analysis is that it is quite generally applicable. Repeated time history calculations of response to different accelerograms (all scaled to the same maximum acceleration) can provide important information about variability of seismic response, but such extensive calculations are often prohibitively expensive in practice.

12. The response spectrum method of analysis yields response predictions for multidegree linear (or linearized) systems by combining modal responses that are taken directly from a smooth response spectrum. For

an important class of multidegree inelastic systems, the response spectrum method also provides useful predictions if the (elastic) response spectrum is first modified by an "inelastic response ratio" which depends on the natural period and on the amount of inelastic action permitted in the structure (i.e., on the "design" ductility factor).

13. A common procedure for generating design response spectra is to multiply the design maximum ground acceleration by a set of scaled (unit acceleration) response spectra. It is well known that the shape of the scaled response spectra presently used in seismic design of nuclear power plants (prescribed by NRC Reg. Guide 1.60) was obtained from the results of statistical processing of the response spectra of a large number of accelerograms, all scaled to a common maximum acceleration (2,3). The background studies by Newmark and Blume (see Ref. 2) involved calculations of response spectra of 33 and 28 components of horizontal motion, respectively. The mean and the mean plus one standard deviation of the spectral amplification factors were computed. The latter level was selected as the level appropriate for use in design.

14. A third method of analysis which has not yet found its way into practice, but which holds considerable promise, is based on random vibration. This method shares the qualities of simplicity and economy with the response spectrum method, and it does permit assessment of the variability of seismic response predictions (and the probability that extreme, or permissible, response levels will be exceeded). The input for a seismic random vibration analysis takes the form of the spectral density function and the duration of strong ground motion. A basic property of the spectral density function is that its integral over all frequencies is equal to the rms ground acceleration. This quantity is in turn proportional to the maximum

ground acceleration. The point is that the seismic input required for random vibration analysis can also be scaled on peak acceleration by adjusting the area under the spectral density function (4,5).

15. Spectral density functions can serve as a starting point for generating artificial earthquake time histories. Moreover, all three modes of ground motion representation (response spectra, spectral density functions, and time histories) come into play when time histories are synthesized based on the criterion that their corresponding response spectra must closely match a set of prescribed smooth response spectra (5).

PART III: EFFECTS OF ACCELEROGRAM SCALING ON SEISMIC PERFORMANCE PARAMETERS

Purpose of the Study

16. The purpose of the study described in this section of the report is to quantify errors that may result from scaling of earthquake records or response spectra on maximum acceleration - a procedure which is so much a part of current earthquake engineering practice. The idea is that maximum acceleration is only one of a number of significant parameters characterizing earthquake ground motion. Other parameters that may affect the amplitude and the shape of response spectra (and more generally, the seismic performance of structures) are the strong-motion duration and the predominant period of the ground motion. To the extent that the maximum acceleration is correlated, either directly or indirectly, with one of these parameters, biases will be introduced by scaling response spectra or accelerograms.

The Set of Accelerograms Used in the Analysis

17. The studies were carried out using a data set of 140 horizontal components of 70 western United States strong-motion records corresponding to different event/site pairs. It is the same data set selected by McGuire (6,7) and McGuire and Barnard (8) to avoid bias due to unusually large numbers of records from a single event, i.e., the 1971 San Fernando earthquake. Pertinent characteristics of these records are listed in Table 1.

18. A scattergram of magnitudes and epicentral distances is shown in Fig. 1. The near-field/far-field demarcation line, based on the tabulation presented in the report by Krinitzsky and Chang (9) is also shown. Eleven sites (22 records) were classified by McGuire as "rock" sites, and

Table 1

Pertinent Characteristics of 70 Western United States Strong Motion Records

C.I.T. NO.	EARTHQUAKE	COMP.	M	R (km)	F. Field or N. Field	SITE r=rock s=soil	a_p (g)	v_p (cm/sec)	I_o $10^4\left(\frac{cm^2}{sec^3}\right)$	T_o (sec)	Bracketed Duration	Strong-Motion Duration s_o
A002-1	Northwest	S44W	6.0	53	FF	s	0.104	4.8	0.5616	0.18	2.89	4.11
A002-2	California	N46W					0.112	7.4	0.7047	0.24	2.90	4.12
A003-1	Kern County	S00E	7.7	127	FF	s	0.047	6.2	0.4068	0.44	-	16.00
A003-2		S90W					0.053	9.1	0.7132	0.52	0.16	23.59
A004-1	Kern County	N21E	7.7	43	NF	s	0.156	15.7	3.4020	0.26	19.60	13.66
A004-2		S69E					0.179	17.7	3.6887	0.24	15.58	10.72
A005-1	Kern County	N42E	7.7	89	FF	s	0.090	11.8	1.485	0.43	13.86	16.80
A005-2		S48E					0.131	19.3	1.802	0.66	9.02	6.62
A006-1	Kern County	S00W	7.7	119	FF	s	0.055	6.1	0.6191	0.40	0.04	19.32
A006-2		N90E					0.044	9.4	0.6473	0.40	-	35.41
A007-1	Kern County	S00W	7.7	119	FF	s	0.059	6.6	0.6343	0.35	0.06	17.09
A007-2		N90E					0.042	8.9	0.6372	0.37	-	40.08
A008-1	Eureka	S00W	6.6	24	NF	s	0.168	31.6	2.1154	0.32	4.34	5.47
A008-2		N90E					0.258	29.4	4.4298	0.42	6.12	4.23
A009-1	Eureka	N44E	6.6	40	FF	s	0.159	35.6	3.4131	0.39	10.58	11.53
A009-2		N46W					0.201	26.0	2.3542	0.37	8.52	3.52
A010-1	San Jose	N31W	5.8	10	NF	s	0.102	10.8	0.4675	0.25	0.54	2.97
A010-2		N59E					0.108	4.4	0.3323	0.19	1.44	1.78
A014-1	San Francisco	N09W	5.3	15	FF	s	0.043	2.9	0.1012	0.21	-	4.07
A014-2		N81E					0.046	2.1	0.8769	0.27	-	2.42

(Continued)

Note: M = magnitude, R = distance, a_p = peak acceleration, v_p = peak velocity, I_o = Arias Intensity, and T_o = predominant period.

Table 1 (Continued)

C.I.T. NO.	EARTHQUAKE	COMP.	M	R (km)	F. Field or N. Field	SITE r=rock s=soil	a_p (g)	v_p (cm/sec)	I_o $10^4\left(\frac{cm^2}{sec^3}\right)$	T_o (sec)	Bracketed Duration	Strong-Motion Duration s_o
A015-1	San	N10E	5.3	12	FF	r	0.083	4.9	0.1751	0.21	0.40	1.34
A015-2	Francisco	S80E					0.105	4.6	0.3114	0.16	1.62	2.02
A016-1	San	S09E	5.3	14	FF	s	0.085	5.1	0.3302	0.29	1.42	2.76
A016-2	Francisco	S81W					0.056	4.0	0.2122	0.26	1.28	5.16
A017-1	San	N26E	5.3	24	FF	s	0.040	2.0	0.0600	0.21	-	2.48
A017-2	Francisco	S64E					0.024	1.2	0.0360	0.22	-	4.82
A018-1	Hollister	S01W	5.6	21	FF	s	0.065	7.8	0.8371	0.47	10.84	18.05
A018-2		N89W					0.179	17.1	1.6319	0.42	9.18	2.72
A019-1	Borrego	S00W	6.5	64	FF	s	0.130	25.8	1.5104	0.34	3.08	7.07
A019-2	Mountain	S90W					0.057	14.7	0.9603	0.34	0.06	31.55
A020-1	Borrego	S00W	6.5	96	FF	s	0.030	6.0	0.1375	0.42	-	12.90
A020-2	Mountain	S90W					0.029	6.1	0.1818	0.52	-	18.73
B021-1	Long	S08W	6.3	53	FF	s	0.133	28.7	1.4159	0.30	6.34	6.44
B021-2	Beach	N82W					0.154	17.0	1.1565	0.31	7.62	2.91
B023-1	Southern	N00E	5.5	38	FF	s	0.033	2.0	0.0617	0.35	-	3.53
B023-2	California	N90W					0.027	2.2	0.0649	0.35	-	6.76
B024-1	Lower	S00W	6.5	64	FF	s	0.160	20.5	3.4234	0.23	16.08	13.30
B024-2	California	S90W					0.183	11.5	3.8876	0.30	18.14	10.19
B026-1	1st N.W.	N45E	5.5	55	FF	s	0.144	6.6	0.6262	0.27	1.52	1.74
B026-2	California	S45E					0.089	6.6	0.4604	0.20	1.26	4.64

(Continued)

Table 1 (Continued)

C.I.T. NQ.	EARTHQUAKE	COMP.	M	R (km)	F. Field or N. Field	SITE r=rock s=soil	a_p (g)	v_p (cm/sec)	I_o $10^4\left[\frac{cm^2}{sec^3}\right]$	T_o (sec)	Bracketed Duration	Strong-Motion Duration s_o
B027-1	2nd N.W.	N45E	6.6	104	FF	s	0.062	3.5	0.2566	0.32	0.06	4.34
B027-2	California	S45E					0.039	3.4	0.2004	0.36	-	11.23
B030-1	Northern	N44E	5.4	43	FF	s	0.054	6.9	0.3256	0.27	0.04	9.67
B030-2	California	S46E					0.068	4.7	0.3296	0.23	0.42	4.01
B031-1	Wheeler	N21E	5.9	43	FF	s	0.065	5.8	0.2434	0.34	0.42	3.64
B031-2	Ridge	S69E					0.068	3.6	0.2653	0.26	0.14	4.12
B034-1	Parkfield	N05W	5.3	5	NF	s	0.355	22.5	3.8963	0.26	7.90	1.66
B034-2		N85E					0.434	25.4	5.3081	0.38	7.32	0.95
B035-1	Parkfield	N50E	5.3	9	NF	s	0.237	10.8	1.9147	0.16	7.90	2.37
B035-2		N40W					0.275	11.8	2.3601	0.18	5.90	1.99
B036-1	Parkfield	N50E	5.3	38	FF	s	0.053	7.0	0.3357	0.19	0.02	12.60
B036-2		N40W					0.064	8.0	0.3855	0.16	0.58	9.55
B037-1	Parkfield	N65W	5.3	6	NF	r	0.269	14.5	1.9059	0.21	3.72	1.39
B037-2		S25W					0.347	22.5	2.8140	0.33	3.46	0.65
B038-1	Parkfield	N36W	5.3	77	FF	r	0.014	1.1	0.0195	0.23	-	8.27
B038-2		S54W					0.012	0.8	0.0123	0.23	-	8.07
B039-1	2nd Northern	S11E	5.8	51	FF	s	0.021	2.3	0.0300	0.34	-	4.77
B039-2	California	N79E					0.020	2.8	0.0314	0.38	-	5.58
B040-1	Borrego	N33E	6.5	134	FF	r	0.041	3.7	0.1508	0.30	-	7.01
B040-2	Mountain	N57W					0.046	4.2	0.1737	0.33	-	5.65

(Continued)

Table 1 (Continued)

C.I.T. NO.	EARTHQUAKE	COMP.	M	R (km)	F. Field or N. Field	SITE r=rock s=soil	a_p (g)	v_p (cm/sec)	I_o $10^4\left(\frac{cm^2}{sec^3}\right)$	T_o (sec)	Bracketed Duration	Strong-Motion Duration s_o
C048-1	San	N00W	6.6	20	NF	s	0.255	30.0	7.9804	0.41	17.96	9.93
C048-2	Fernando	S90W					0.134	23.9	4.2129	0.41	22.12	22.88
D056-1	San	N21E	6.6	29	NF	r	0.315	16.5	4.3301	0.28	61.74	2.71
D056-2	Fernando	N69W					0.271	27.2	6.1760	0.25	19.66	7.07
E071-1	San	S00W	6.6	89	FF	s	0.027	1.9	0.0425	0.16	-	4.77
E071-2	Fernando	N90E					0.026	2.5	0.0451	0.16	-	6.14
F086-1	San	N83E	6.6	46	FF	s	0.107	17.4	1.1661	0.35	8.30	8.09
F086-2	Fernando	S07W					0.082	15.1	0.8030	0.27	9.14	11.09
G114-1	San	S60E	6.6	33	NF	s	0.113	14.0	2.0904	0.26	14.56	16.42
G114-2	Fernando	S30W					0.139	9.3	1.5509	0.18	11.54	7.51
T286-1	Borrego	North	6.5	48	FF	s	0.060	6.22	0.6205	0.27	2.16	17.63
T286-2	Valley	East					0.047	6.05	0.4517	0.28	-	20.24
T287-1	Imperial	North	5.6	30	FF	s	0.031	2.98	0.1415	0.30	-	13.90
T287-2	Valley	East					0.028	3.09	0.1523	0.39	-	17.72
T288-1	Imperial	North	5.5	11	NF	s	0.007	1.39	0.0060	0.38	-	8.99
T288-2	Valley	East					0.036	6.32	0.2194	0.29	-	16.26
T289-1	Lower	North	6.3	150	FF	s	0.025	3.76	0.0889	0.33	-	13.28
T289-2	California	East					0.028	3.17	0.1031	0.40	-	11.37
T290-1	Imp. County	North	7	22	NF	s	0.031	?	0.0233	0.17	-	1.37
T290-2	Foreshock	East					0.016		0.0277	0.20	-	9.95

(Continued)

Table 1 (Continued)

C.I.T. NQ.	EARTHQUAKE	COMP.	M	R (km)	F. Field or N. Field	SITE r=rock s=soil	a_p (g)	v_p (cm/sec)	I_o $10^4\left(\frac{cm^2}{sec^3}\right)$	T_o (sec)	Bracketed Duration	Strong-Motion Duration s_o
T293-1	Gulf of	North	6.3	147	FF	s	0.014	2.43	0.0907	0.73	-	48.70
T293-2	California	East					0.015	2.40	0.0799	0.51	-	35.85
U298-1	Humboldt	N45W	5.75	80	FF	s	0.039	4.07	0.1322	0.33	-	6.86
U298-2	Bay	S45W					0.037	2.71	0.1005	0.25	-	6.10
U299-1	Santa	N45E	5.9	16	NF	s	0.238	21.70	2.0100	0.27	3.26	2.03
U299-2	Barbara	S45E					0.176	21.60	1.5176	0.37	1.94	2.80
U300-1	Northern	N45W	6.4	50	FF	s	0.121	6.92	0.6519	0.29	2.66	2.79
U300-2	California	S45W					0.116	5.74	0.6519	0.27	2.64	3.33
U301-1	Northern	N89W	5.3	21	FF	s	0.197	11.70	1.0933	0.39	3.42	0.78
U301-2	California	S01W					0.122	8.26	1.1072	0.38	5.02	5.08
U305-1	Central	N89W	5.3	27	FF	s	0.053	4.19	0.2983	0.32	0.02	8.70
U305-2	California	S01W					0.050	4.52	0.3082	0.32	0.02	10.82
U307-1	Central	N89W	5.0	6	FF	s	0.057	5.25	0.2963	0.35	0.04	7.12
U307-2	California	S01W					0.036	3.64	0.1514	0.31	-	10.25
U308-1	Northern	N46W	5.7	59	FF	s	0.059	3.11	0.2011	0.26	4.54	4.00
U308-2	California	S44W					0.075	3.60	0.2351	0.30	0.28	2.54
U309-1	Central Cal.	N89W	5.6	21	NF	s	0.172	10.80	1.0012	0.37	8.62	1.43
U309-2	Aftershock	S01W					0.076	6.28	0.6454	0.43	5.20	8.46
U311-1	Parkfield	N21E	5.3	131	FF	s	0.008	2.10	0.0184	1.00	-	21.04
U311-2		S69E					0.011	2.21	0.0234	0.76	-	13.49

(Continued)

Table 1 (Continued)

C.I.T. NO.	EARTHQUAKE	COMP.	M	R (km)	F. Field or N. Field	SITE r=rock s=soil	a_p (g)	v_p (cm/sec)	I_o $10^4 \left(\frac{cm^2}{sec^3}\right)$	T_o (sec)	Bracketed Duration	Strong-Motion Duration s_o
U312-1	Ferndale	N46W	5.8	32	FF	s	0.105	11.80	0.4672	0.27	0.38	2.66
U312-2		S44W					0.237	11.90	0.6584	0.20	0.72	0.30
U313-1	Northern	N89W	5.2	39	FF	s	0.013	2.67	0.0357	0.43	-	18.60
U313-2	California	S01W					0.017	1.74	0.0448	0.41	-	14.74
V314-1	Long	N39E	6.3	59	FF	r	0.064	17.30	1.0251	0.72	10.38	21.62
V314-2	Beach	N51W					0.097	23.60	1.4550	0.39	12.56	13.48
V315-1	Long	South	6.3	27	NF	s	0.196	29.40	2.9709	0.30	6.6	5.81
V315-2	Beach	West					0.159	16.50	2.5643	0.26	8.24	8.88
V316-1	Torrance	North	5.4	6	NF	s	0.040	7.61	0.1376	0.35	-	6.47
V316-2	Gardena	East					0.055	9.32	0.2399	1.54	0.12	1.52
V317-1	Torrance	S50E	5.4	27	FF	s	0.015	1.33	0.0215	0.38	-	7.07
V317-2	Gardena	S40W					0.011	1.42	0.0201	0.38	-	13.64
V319-1	Southern	N36W	6	77	FF	r	0.054	3.35	0.1532	0.31	0.02	3.40
V319-2	California	S54W					0.036	2.89	0.1183	0.34	-	7.05
V329-1	Southern	South	5	6	FF	s	0.167	17.90	0.6101	0.43	0.52	0.67
V329-2	California	West					0.089	8.85	0.1506	0.48	0.44	0.49
V330-1	Northern	N79E	5	19	FF	s	0.046	3.52	0.0872	0.29	-	2.31
V330-2	California	S11E					0.048	2.67	0.0782	0.38	-	1.52
V331-1	Southern	South	4.5	18	FF	r	0.041	2.12	0.0465	0.19	-	1.63
V331-2	California	East					0.037	1.13	0.0283	0.15	-	1.27

(Continued)

Table 1 (Concluded)

C.I.T. NO.	EARTHQUAKE	COMP.	M	R (km)	F. Field or N. Field	SITE r=rock s=soil	a_p (g)	v_p (cm/sec)	I_o $10^4\left(\frac{cm^2}{sec^3}\right)$	T_o (sec)	Bracketed Duration	Strong-Motion Duration s_o
V332-1	Northern	South	6.25-	151	FF	s	0.015	1.57	0.0235	0.37	-	8.59
V332-2	California	East	6.5				0.013	1.74	0.0189	0.46	-	9.07
W334-1	Lytle	S65E	5.4	13	NF	r	0.142	8.87	0.8279	0.25	2.80	2.42
W334-2	Creek	S25W					0.198	9.63	0.9002	0.18	2.08	1.26
W335-1	Lytle	S85E	5.4	19	FF	r	0.071	5.55	0.1854	0.12	0.72	2.98
W335-2	Creek	S05W					0.056	1.96	0.0950	0.13	0.44	2.26
W336-1	Lytle	S54E	5.4	22	FF	r	0.057	2.94	0.1412	0.16	0.14	3.36
W336-2	Creek	S36W					0.071	3.96	0.1466	0.16	0.06	1.90
W339-1	Lytle	South	5.4	18	FF	s	0.041	2.55	0.1452	0.25	-	7.32
W339-2	Creek	East					0.036	1.87	0.1328	0.25	-	9.12
W342-1	Lytle	North	5.4	56	FF	s	0.020	1.53	0.0364	0.24	-	8.18
W342-2	Creek	East					0.019	1.44	0.0287	0.20	-	7.05
Y370-1	Borrego	South	6.5	144	FF	s	0.022	3.53	0.0762	0.31	-	15.41
Y370-2	Mountain	East					0.029	2.71	0.0704	0.31	-	6.57
Y371-1	Borrego	S04E	6.5	174	FF	s	0.013	4.38	0.0660	0.73	-	34.50
Y371-2	Mountain	S86W					0.012	4.28	0.0560	0.65	-	38.51
Y373-1	Borrego	S82E	6.5	205	FF	s	0.008	1.35	0.0095	0.75	-	12.01
Y373-2	Mountain	S08W					0.007	1.32	0.0087	0.55	-	13.95
Y379-1	Borrego	N83W	6.5	214	FF	s	0.019	4.27	0.0905	0.72	-	22.21
Y379-2	Mountain	S07W					0.019	4.65	0.0813	0.73	-	18.62

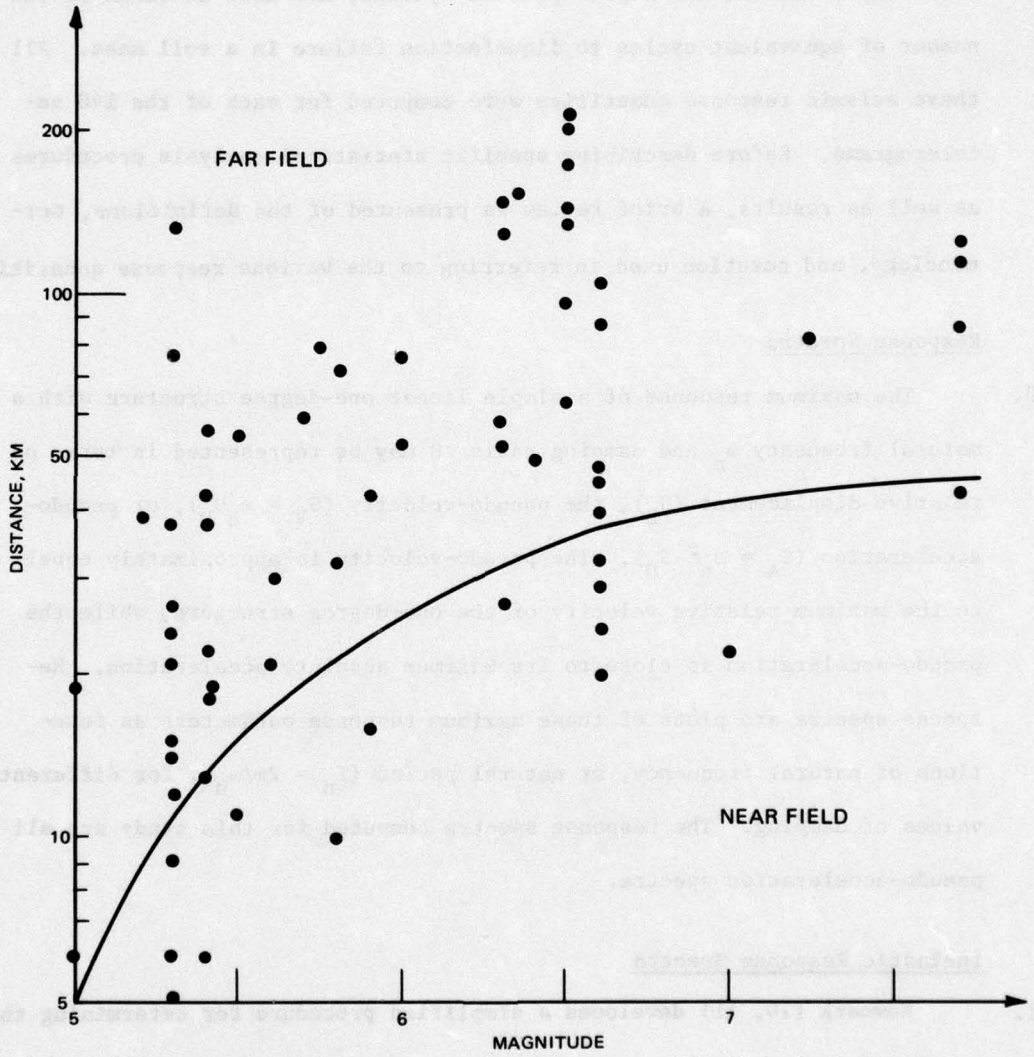

Figure 1. Scattergram of magnitudes and epicentral distances for the 70 strong-motion records used in this study. Curve represents the near-field/far-field demarcation line

59 sites (118 records) as "soil" sites.

Seismic Response Quantities Investigated

19. The effect of scaling was evaluated in terms of the response of various simple elastic and elasto-plastic systems, and also in terms of the number of equivalent cycles to liquefaction failure in a soil mass. All these seismic response quantities were computed for each of the 140 accelerograms. Before describing specific statistical analysis procedures as well as results, a brief review is presented of the definitions, terminology, and notation used in referring to the various response quantities.

Response Spectra

20. The maximum response of a simple linear one-degree structure with a natural frequency ω_n and damping ratio β may be represented in terms of relative displacement (S_D), the pseudo-velocity ($S_V = \omega_n S_D$), or pseudo-acceleration ($S_A = \omega_n^2 S_D$). The pseudo-velocity is approximately equal to the maximum relative velocity of the one-degree structure, while the pseudo-acceleration is close to its maximum absolute acceleration. Response spectra are plots of these maximum response parameters as functions of natural frequency, or natural period ($T_n = 2\pi/\omega_n$), for different values of damping. The response spectra computed for this study are all pseudo-acceleration spectra.

Inelastic Response Spectra

21. Newmark (10, 11) developed a simplified procedure for determining the relationship between the maximum response of a single-degree-of-freedom elasto-plastic system and the maximum response of the associated elastic system. The result is the inelastic response spectrum which consists of

an "acceleration spectrum" and a "(relative) displacement spectrum." These may be plotted as a function of the (initial undamped) natural period for a specified level of the ductility ratio μ and the damping factor β. The ductility ratio μ is defined as the ratio of the maximum deflection to the limit elastic deflection, $\mu = y_{max}/y_e$, as shown in Fig. 2. The inelastic acceleration response spectrum will be denoted by $S_A(\mu)$.

22. Starting from the pseudo-velocity elastic response spectrum plotted on log-log paper, the inelastic response spectrum is developed as follows. In the period range where displacement or velocity are amplified, the inelastic displacement spectrum is identical to the elastic spectrum. The inelastic acceleration spectrum in these regions is obtained by dividing the elastic spectrum by the ductility ratio μ. In the amplified acceleration range of the response spectrum, the inelastic acceleration spectrum is obtained by dividing the elastic spectrum by $\sqrt{2\mu-1}$. At very high frequencies, the elastic and inelastic response spectra are identical. The spectrum is completed by drawing a straight line from the zero-period acceleration line to the amplified acceleration line. Note that the inelastic displacement and acceleration spectra always differ by the factor μ. The ratio between the elastic and the inelastic acceleration response spectra, $S_A/S_A(\mu)$, is referred to as the <u>inelastic acceleration response ratio</u> (see Fig. 2b).

23. For example, Fig. 3 shows a smooth elastic response spectrum and the corresponding response spectrum for a damping of 2 percent and a ductility ratio of 4.

24. Requirements to resist damage for structures and components are often expressed in terms of an allowable ductility factor. The elastic condition corresponds to $\mu = 1$, while values $\mu \geq 5$ may be appropriate when a

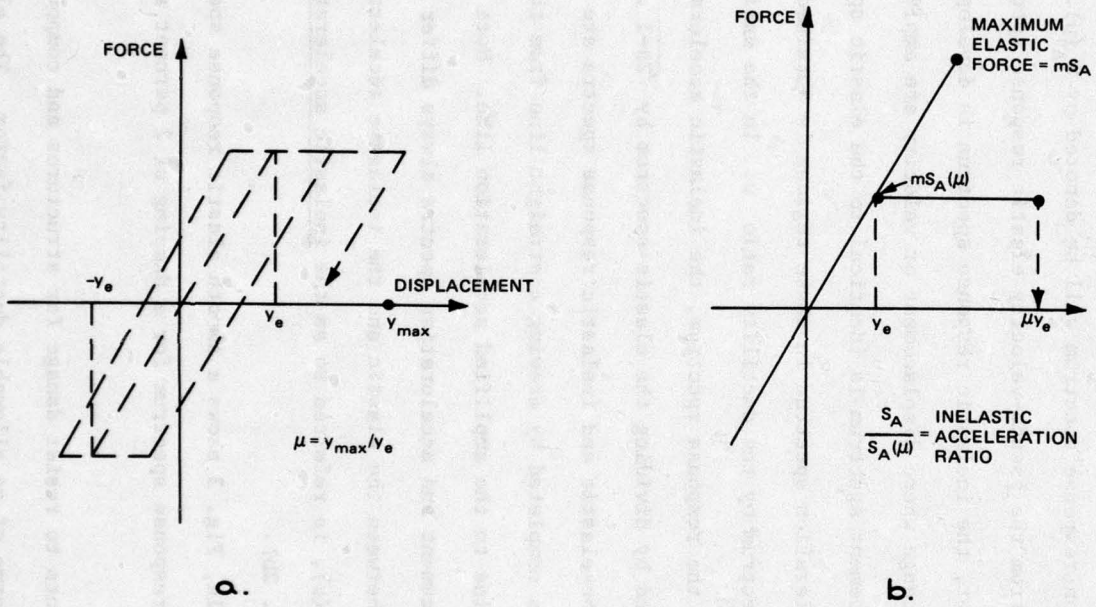

Figure 2. Force-deformation relationship for a one-degree elasto-plastic system

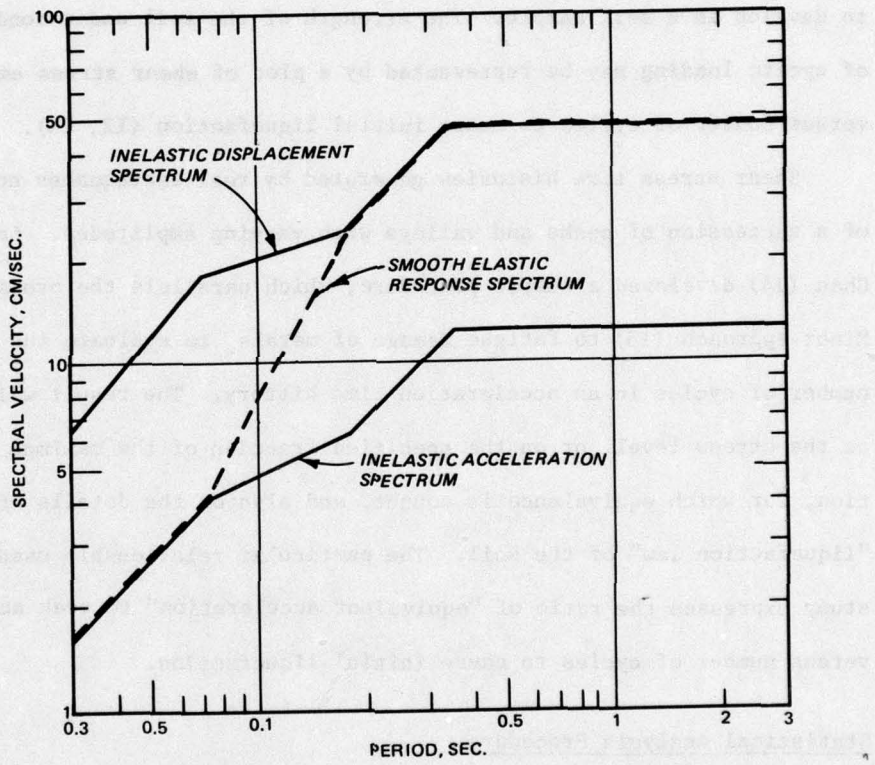

Figure 3. Relationship between smooth elastic and inelastic response spectra. The inelastic response spectrum is for a ductility factor $\mu = 4$

considerable amount of energy can be absorbed in inelastic deformation. Ductility factors appropriate for use in design are discussed in References 10 and 11.

Equivalent Number of Cycles

25. Dynamic tests for soil liquefaction potential measure the number of cycles at constant shear stress amplitude necessary for excessive strain to develop in a soil sample. The strength of the soil under conditions of cyclic loading may be represented by a plot of shear stress amplitude versus number of cycles to cause initial liquefaction (12, 13).

26. Shear stress time histories generated by real earthquakes consist of a succession of peaks and valleys with varying amplitudes. Lee and Chan (14) developed a simple procedure, which parallels the probabilistic Miner approach (15) to fatigue damage of metals, to evaluate the equivalent number of cycles in an acceleration time history. The result will depend on the stress level, or on the specified fraction of the maximum acceleration, for which equivalence is sought, and also on the details of the "liquefaction law" of the soil. The particular relationship used in this study expresses the ratio of "equivalent acceleration" to peak acceleration versus number of cycles to cause initial liquefaction.

Statistical Analysis Procedure

27. The specific response quantities selected for the statistical study of the effect of scaling are all defined in such a way that they have the property of being "invariant with respect to scaling of the accelerogram." This means that scaling a particular accelerogram (i.e., multiplying all its accelerations by a common scale factor) will not change the calculated

values (for that accelerogram). The following response quantities have this property of invariance:

a) Acceleration amplification factor = ratio of the acceleration response spectrum to the maximum acceleration. This factor can be evaluated for either elastic or inelastic response spectra. It depends on natural period T_n, damping ratio β, and ductility factor μ. The value $\mu = 1$ implies elastic response spectra.

b) Inelastic acceleration response ratio = ratio of the ordinate of the elastic response spectrum to that of the inelastic response spectrum (for the same natural period and damping, and for a given value of the ductility factor).

c) Equivalent number of cycles corresponding to an acceleration level that is a specified fraction of the peak acceleration. The invariance property rests on the assumption that the "liquefaction laws" can be represented by a plot of a/a_p versus N (in which $a/a_p = 1$ corresponds to $N = 1$, and N increases as a/a_p decreases).

28. Given a set of accelerograms, it is possible to calculate the average, the standard deviation, and to construct a histogram, for any of the response measures just mentioned. [Precisely this kind of statistical analysis (for the acceleration amplification factor) gave rise to the development of NRC Reg. Guide 1.60 response spectra.] The question at hand is whether these response measures are in fact independent of peak acceleration. To examine this question, the 140 records are ranked according to their actual peak acceleration, and the (conditional) mean and standard

deviation of each response measure are calculated for subsets of records whose peak accelerations lie within a relatively narrow range of values.

29. Formally, suppose that Y denotes a response quantity of interest and that a_p denotes the peak acceleration. Does the conditional distribution of Y depend on a_p? The conditional response statistics can be estimated from a subset of records with maximum accelerations close to a_p. Subsets are chosen so that half of the records have peak accelerations less than or equal to a_p, and the other half peak accelerations that exceed a_p. The size of each subset of records (n = 20) was selected on the basis of a brief sensitivity study in which the number of records in each subset was varied.

30. The analysis procedure is illustrated in Figures 4 through 7. The response parameter is the acceleration amplification factor for an elastic one-degree system with natural period T_n = 1.0 sec. and damping ratio β = 0.02. Fig. 4 shows the amplification factors of all 140 records as a function of their peak accelerations. For the same one-degree system, the sample mean of the amplification factor based on "moving" subsets comprising 10, 20 and 30 records is shown in Figures 5, 6 and 7, respectively.

31. Throughout the report, the statistics given are the mean m, the standard deviation σ, and the coefficient of variation $V = \sigma/m$. These are directly useful in evaluating exceedance probabilities if the random quantity at hand, say X, is assumed to be Gaussian. However, the lognormal distribution is frequently an attractive alternative. In that case, the mean and the standard deviation of log X are needed to evaluate the exceedance probabilities. If Y = log X, the mean and the standard deviation of Y and the mean m_X and the coefficient of variation V_X are related as follows:

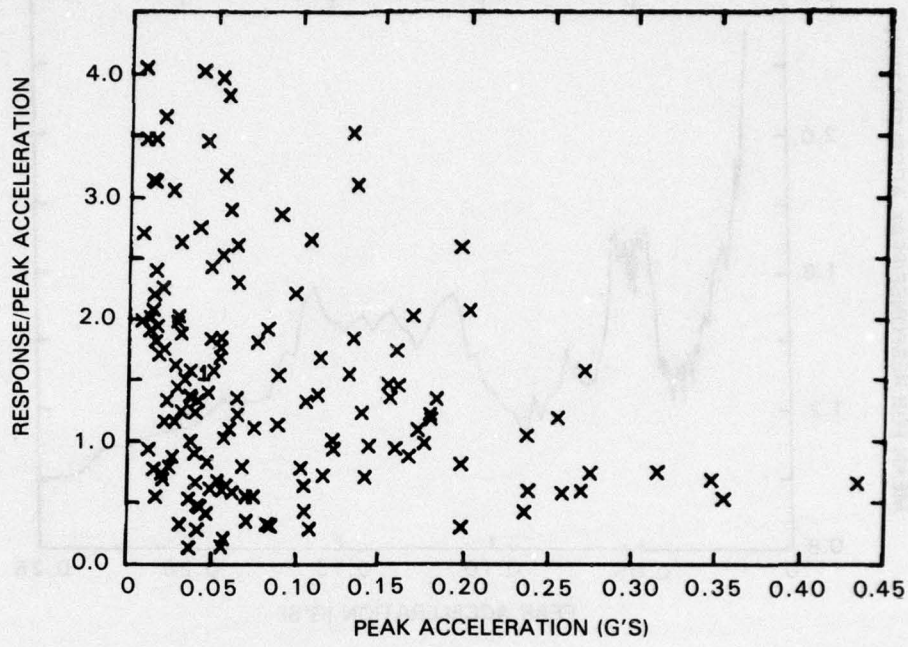

Figure 4. Acceleration amplification factor S_A/a_p for an elastic one-degree system with natural period T_n = 1.0 sec. and damping ratio β = 0.02

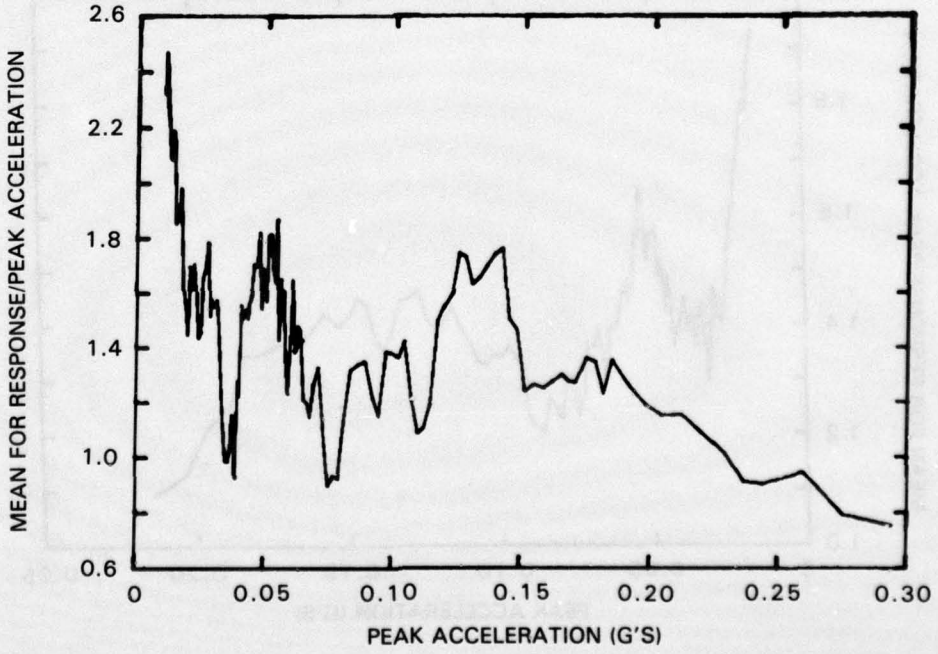

Figure 5. Mean acceleration amplification factor S_A/a_p for T_n = 1.0 sec. and β = 0.02. Each point is based on a subset of 10 records

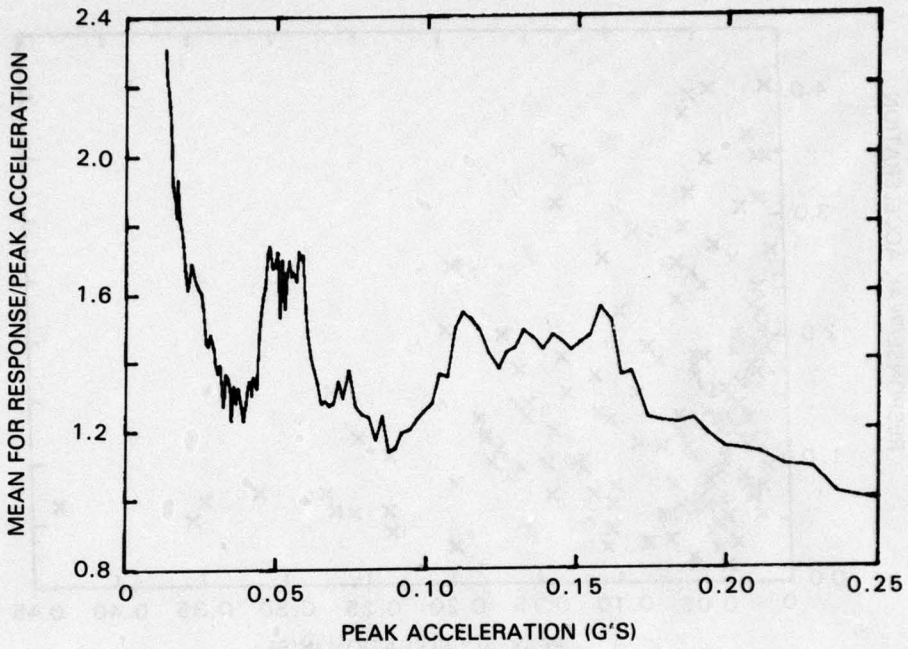

Figure 6. Mean acceleration amplification factor S_A/a_p for T_n = 1.0 sec. and β = 0.02. Each point is based on a subset of 20 records

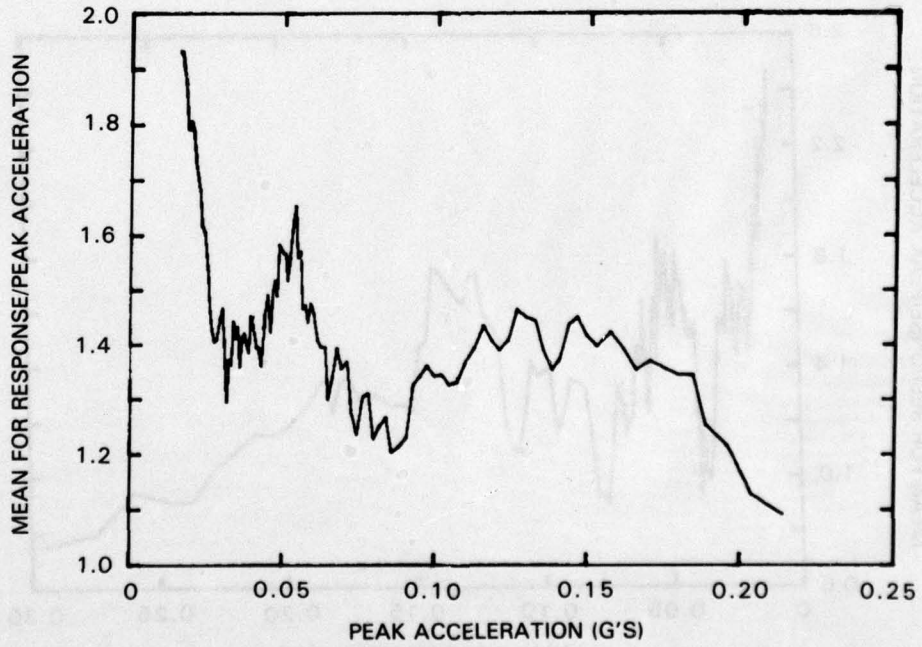

Figure 7. Mean acceleration amplification factor S_A/a_p for T_n = 1.0 sec. and β = 0.02. Each point is based on a subset of 30 records

$$\sigma_Y^2 = \log(V_x^2 + 1)$$

$$m_Y = \log m_x - \frac{1}{2}\sigma_Y^2$$

Hence, if the statistics of X are given (as they are in this report) the corresponding statistics of log X can be easily evaluated.

Results

32. This section of the report presents the major findings of the statistical study in the form of a series of figures showing the statistics of various performance parameters (i.e., mean m, standard deviation σ, or coefficient of variation V) versus peak acceleration.

a) Figures 8-1 through 8-6 show statistics (m and $m+\sigma$) of the acceleration amplification factor S_A/a_p for 2% damping for 6 different natural periods (T_n = 0.1, 0.2, 0.5, 1.0, 2.0 and 5.0 sec.).

b) Figures 9-1 through 9-6 show statistics (m and $m+\sigma$) of the acceleration amplification factor S_A/a_p for 5% damping for 6 different natural periods (T_n = 0.1, 0.2, 0.5, 1.0, 2.0 and 5.0 sec.).

c) Figures 10-1 through 10-4 show statistics (m and $m+\sigma$) of the inelastic acceleration amplification factor $S_A(\mu)/a_p$ for a one-degree system with natural period T_n = 0.5 sec. and damping 5%, for different specified values of the ductility factor μ = 2, 3, 4 and 5, respectively.

d) Figures 11-1 through 11-4 show the mean inelastic acceleration response ratio $S_A/S_A(\mu)$ for 4 different values of ductility factor μ (μ = 2, 3, 4 and 5). The different figures correspond to different

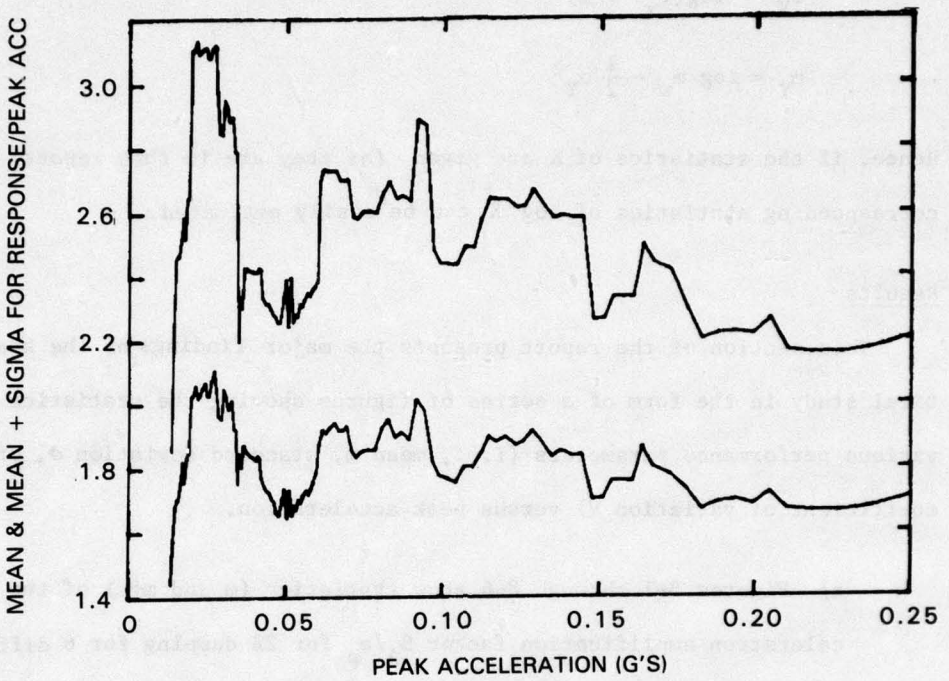

Figure 8-1. Mean and mean plus standard deviation of the acceleration amplification factor S_A/a_p for 2% damping and T_n = 0.1 sec.

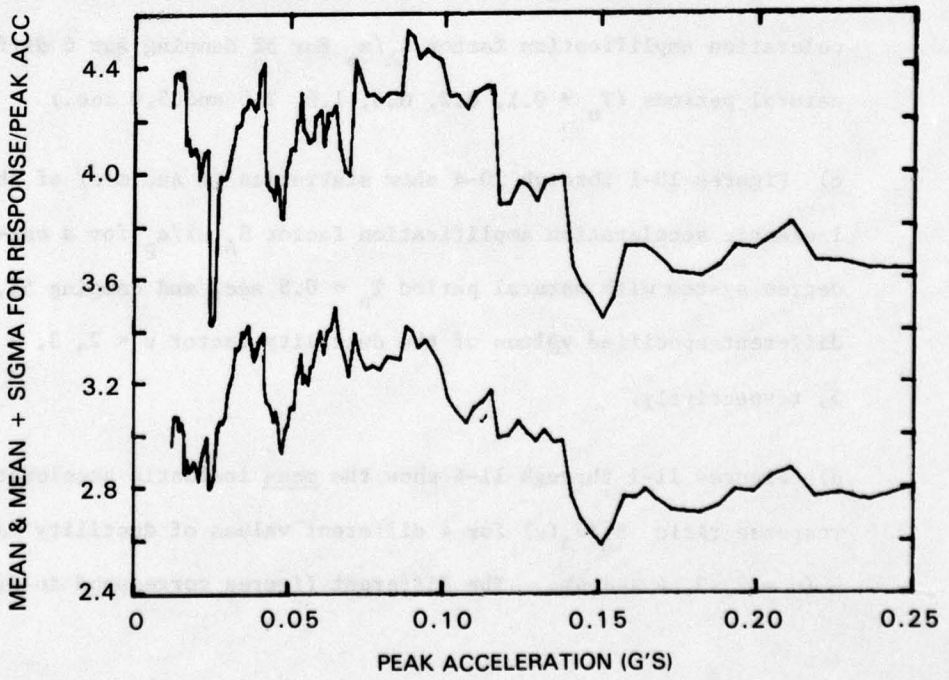

Figure 8-2. Mean and mean plus standard deviation of the acceleration amplification factor S_A/a_p for 2% damping and T_n = 0.2 sec.

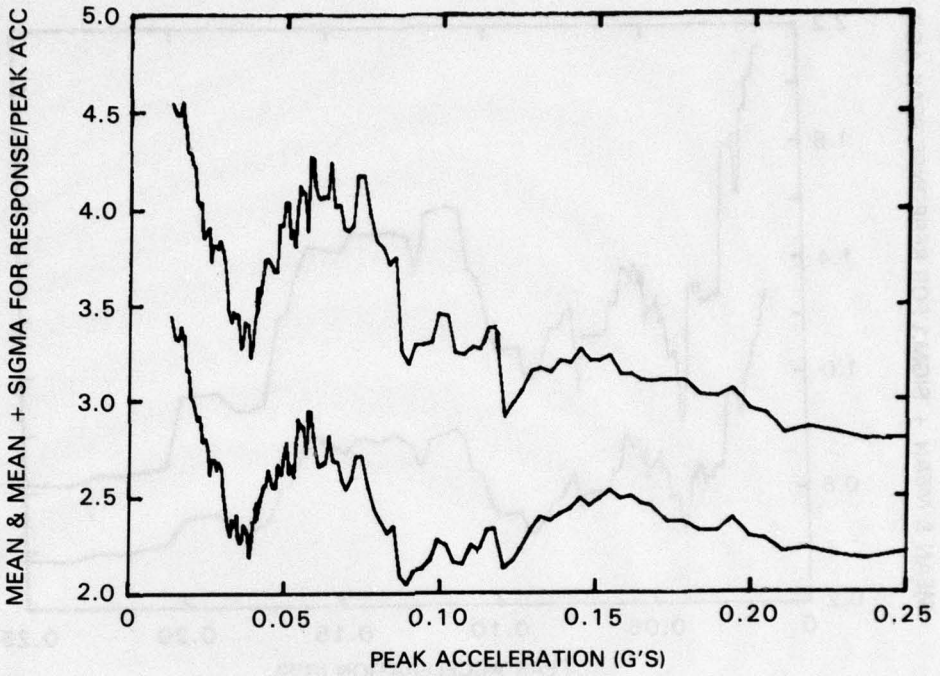

Figure 8-3. Mean and mean plus standard deviation of the acceleration amplification factor S_A/a_p for 2% damping and T_n = 0.5 sec.

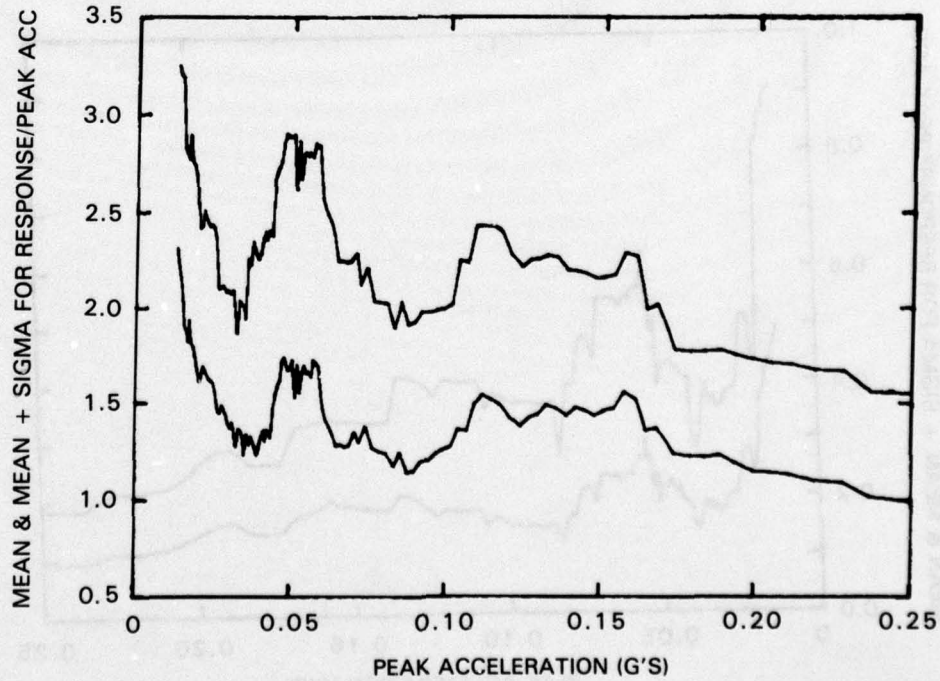

Figure 8-4. Mean and mean plus standard deviation of the acceleration amplification factor S_A/a_p for 2% damping and T_n = 1.0 sec.

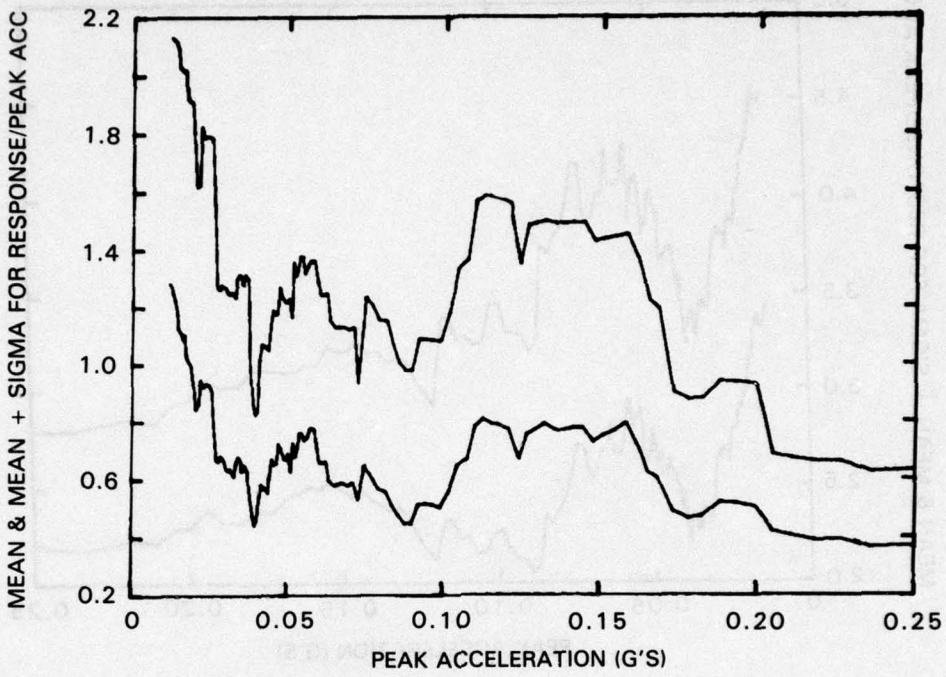

Figure 8-5. Mean and mean plus standard deviation of the acceleration amplification factor S_A/a_p for 2% damping and T_n = 2.0 sec.

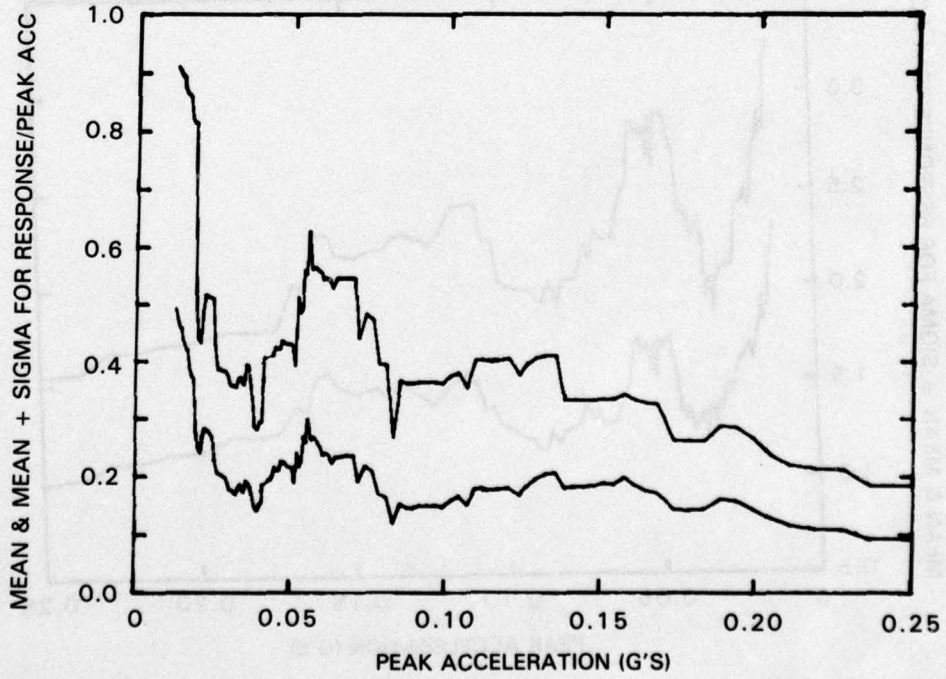

Figure 8-6. Mean and mean plus standard deviation of the acceleration amplification factor S_A/a_p for 2% damping and T_n = 5.0 sec.

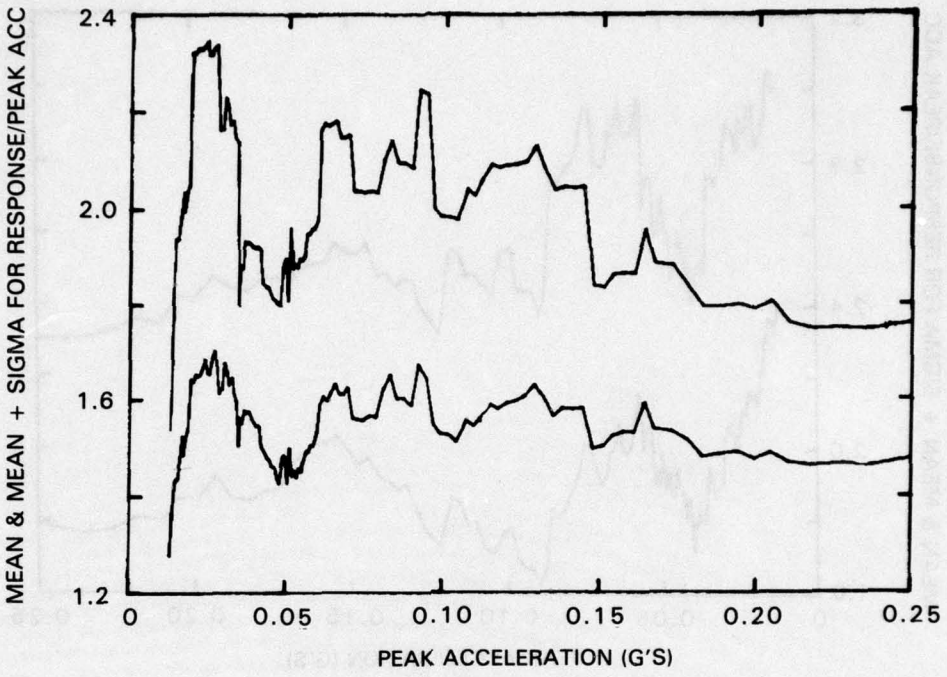

Figure 9-1. Mean and mean plus standard deviation of the acceleration amplification factor S_A/a_p for 5% damping and T_n = 0.1 sec.

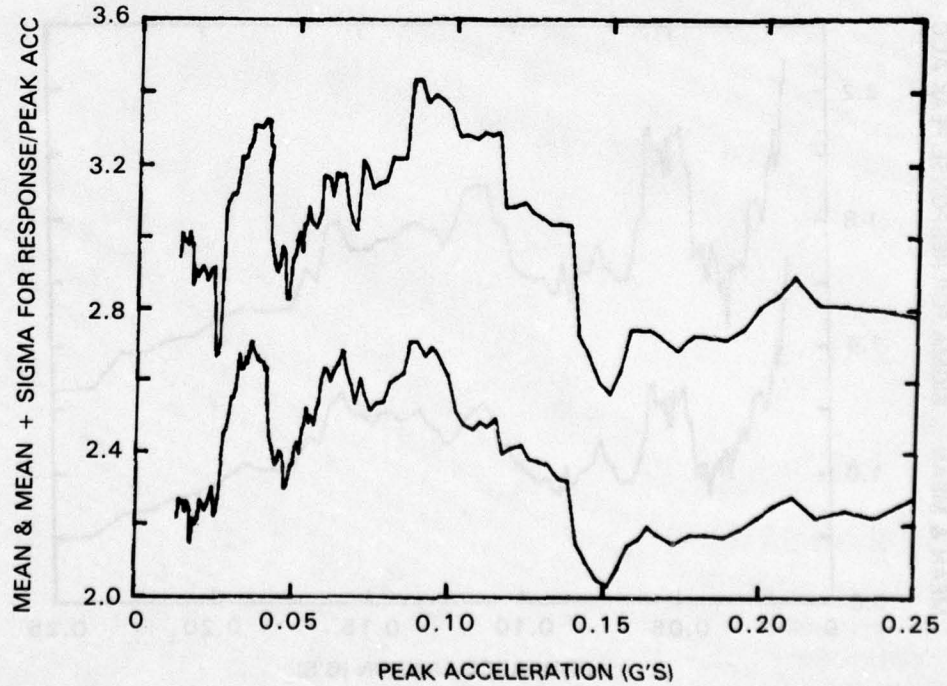

Figure 9-2. Mean and mean plus standard deviation of the acceleration amplification factor S_A/a_p for 5% damping and T_n = 0.2 sec.

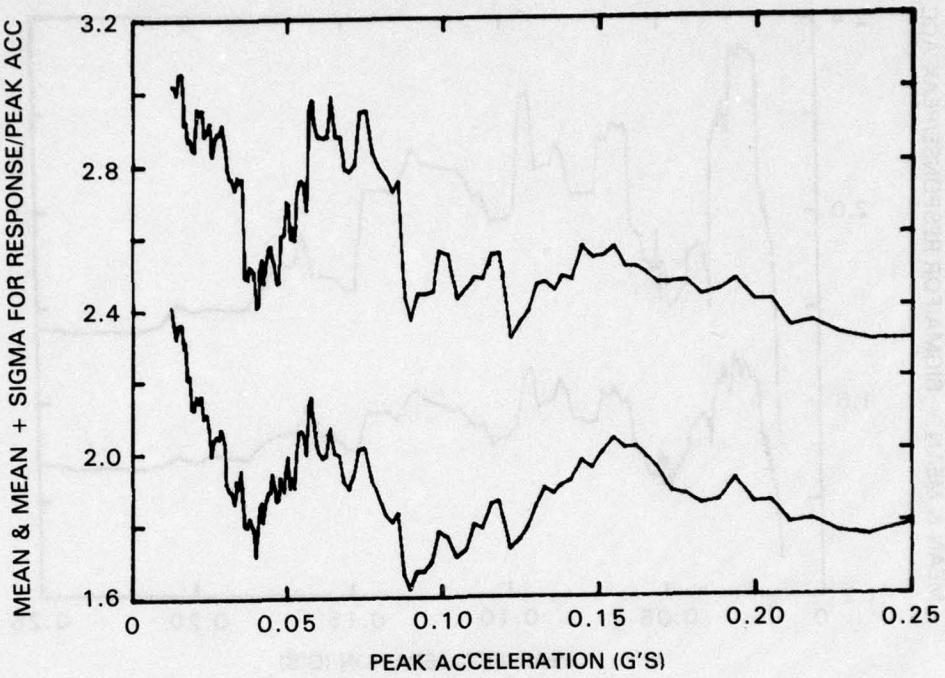

Figure 9-3. Mean and mean plus standard deviation of the acceleration amplification factor S_A/a_p for 5% damping and T_n = 0.5 sec.

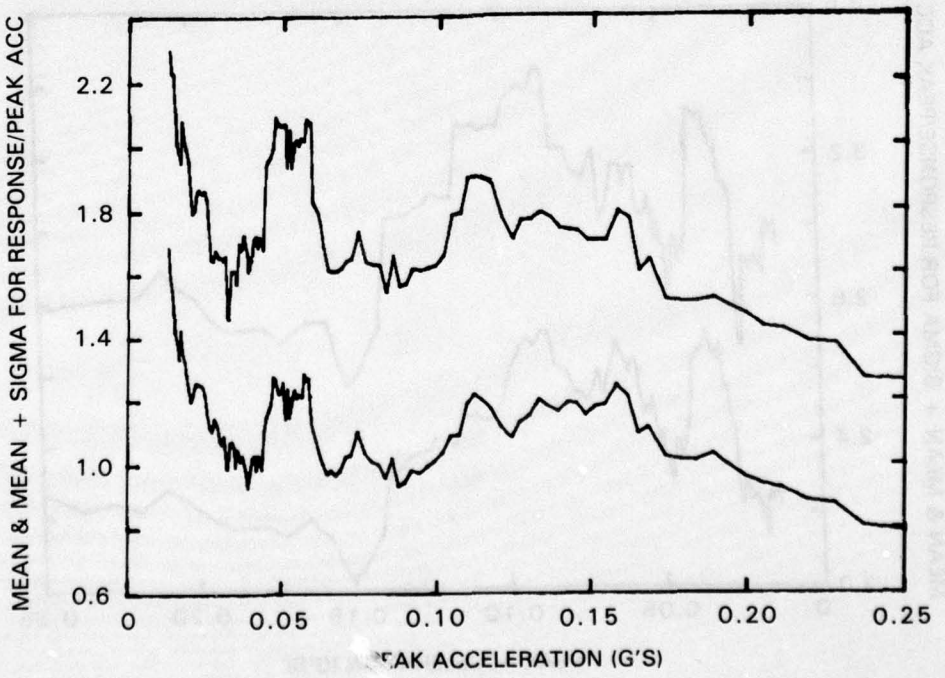

Figure 9-4. Mean and mean plus standard deviation of the acceleration amplification factor S_A/a_p for 5% damping and T_n = 1.0 sec.

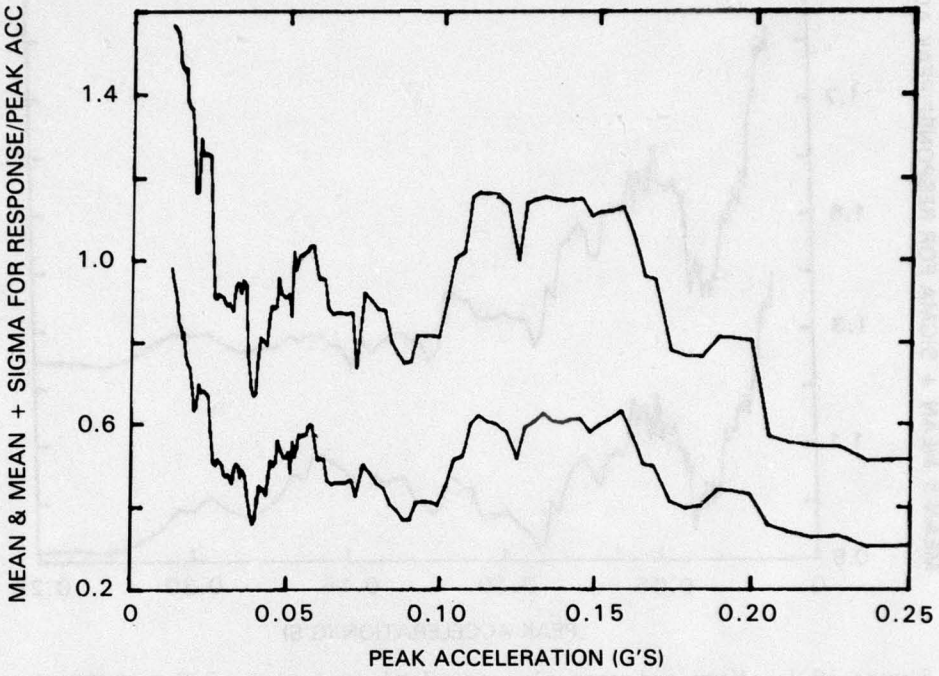

Figure 9-5. Mean and mean plus standard deviation of the acceleration amplification factor S_A/a_p for 5% damping and T_n = 2.0 sec.

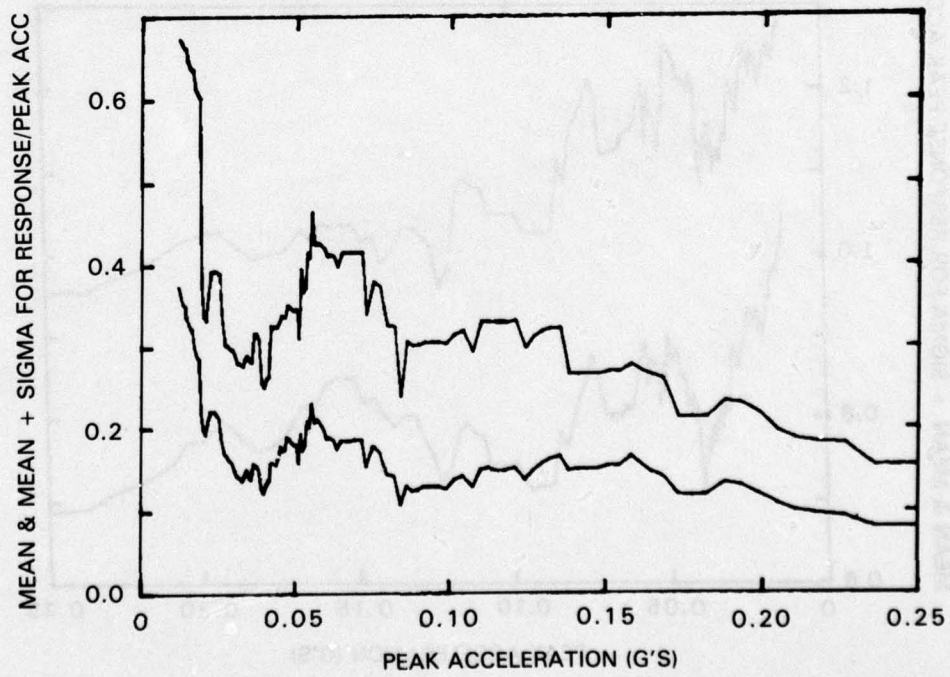

Figure 9-6. Mean and mean plus standard deviation of the acceleration amplification factor S_A/a_p for 5% damping and T_n = 5.0 sec.

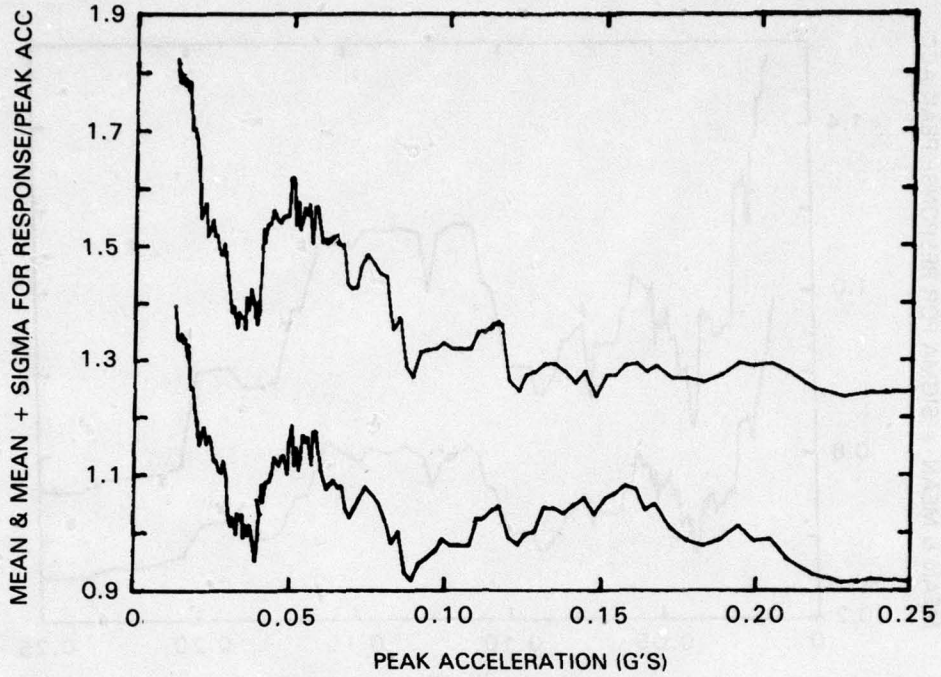

Figure 10-1. Mean and mean plus standard deviation of the inelastic acceleration amplification factor $S_A(\mu)/a_p$ for 5% damping and natural period 0.5 sec., and for a ductility factor $\mu = 2$

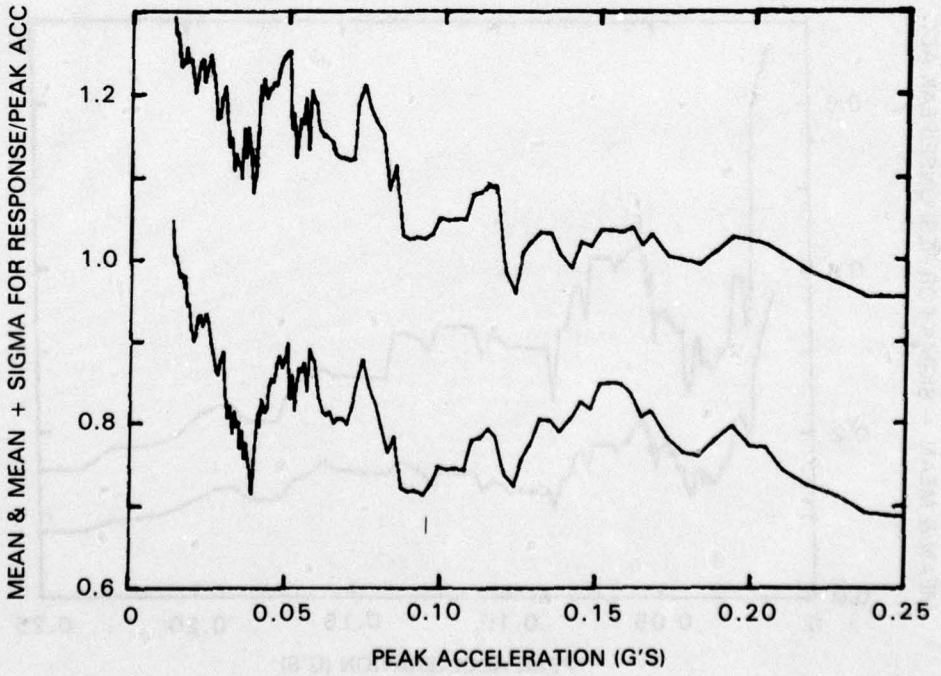

Figure 10-2. Mean and mean plus standard deviation of the inelastic acceleration amplification factor $S_A(\mu)/a_p$ for 5% damping and natural period 0.5 sec., and for a ductility factor $\mu = 3$

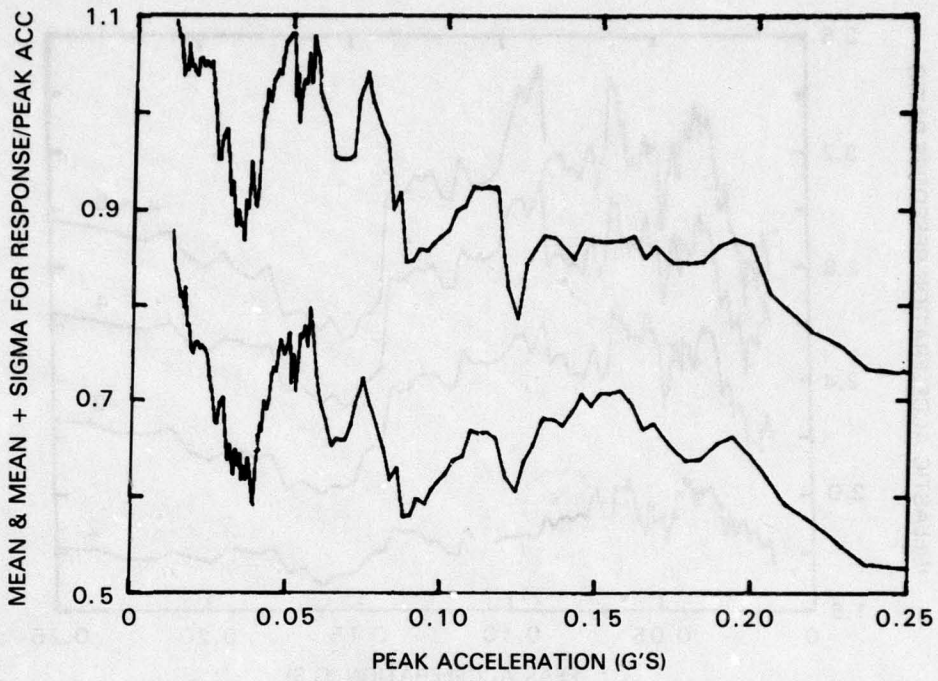

Figure 10-3. Mean and mean plus standard deviation of the inelastic acceleration amplification factor $S_A(\mu)/a_p$ for 5% damping and natural period 0.5 sec., and for a ductility factor $\mu = 4$

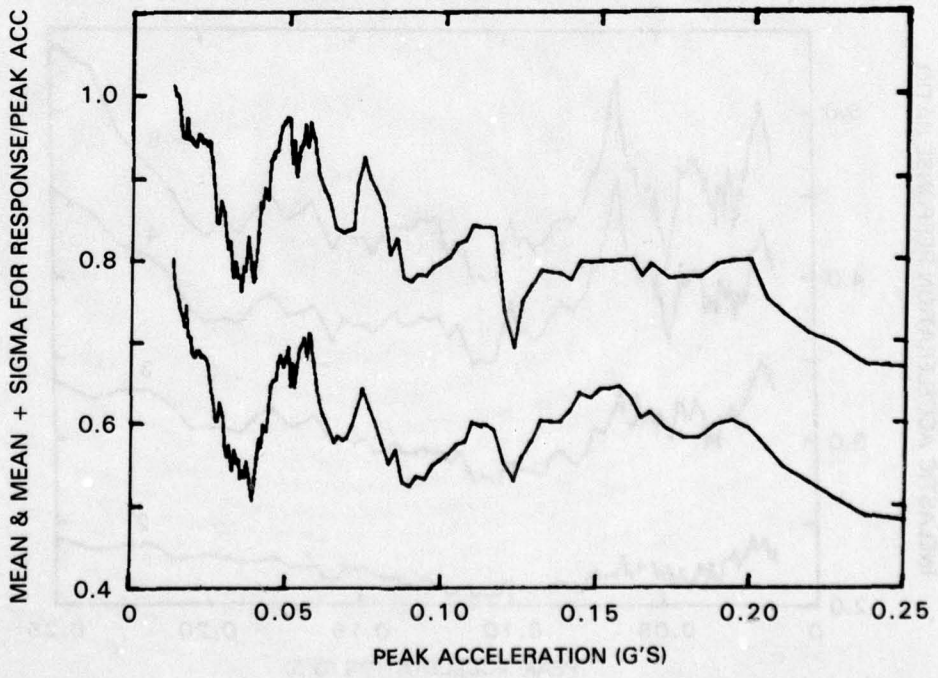

Figure 10-4. Mean and mean plus standard deviation of the inelastic acceleration amplification factor $S_A(\mu)/a_p$ for 5% damping and natural period 0.5 sec., and for a ductility factor $\mu = 5$

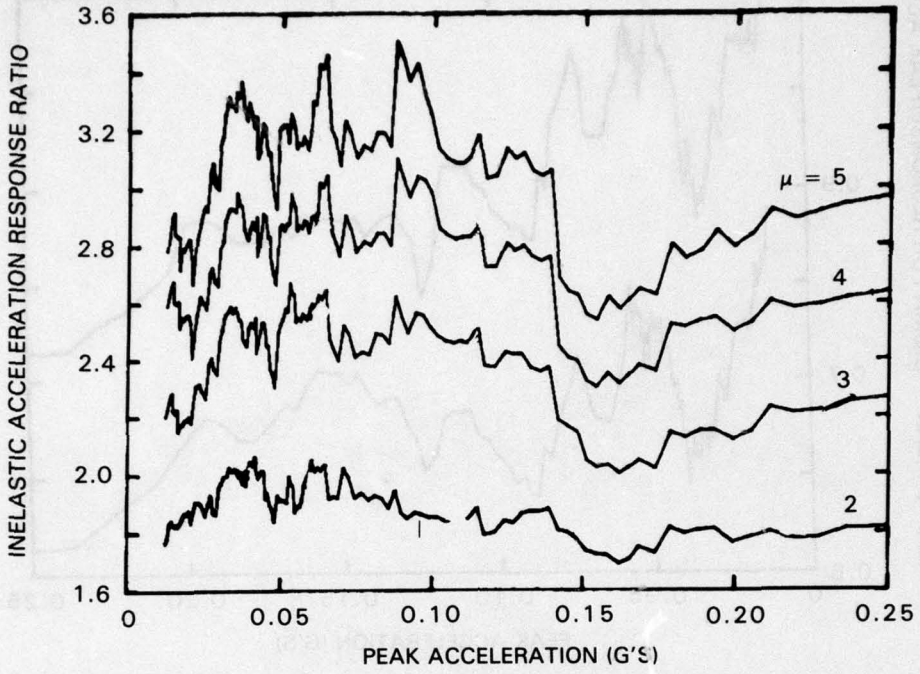

Figure 11-1. Mean inelastic acceleration response ratio $S_A/S_A(\mu)$ for four different values of the ductility factor μ (μ = 2, 3, 4 and 5). The damping ratio is 2% and the natural period T_n = 0.2 sec.

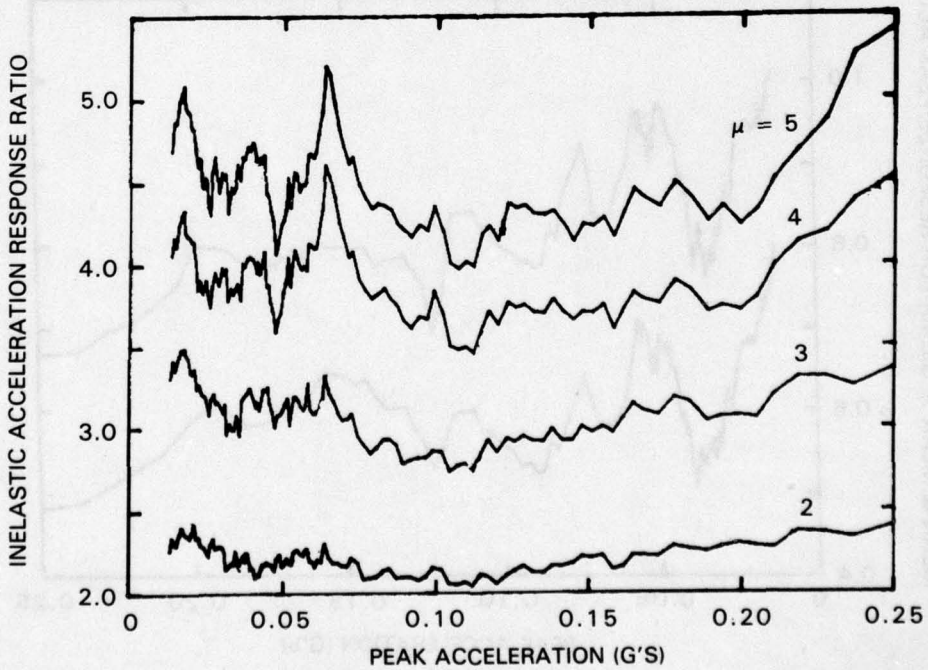

Figure 11-2. Mean inelastic acceleration response ratio $S_A/S_A(\mu)$ for four different values of the ductility factor μ (μ = 2, 3, 4 and 5). The damping ratio is 2% and the natural period T_n = 0.5 sec.

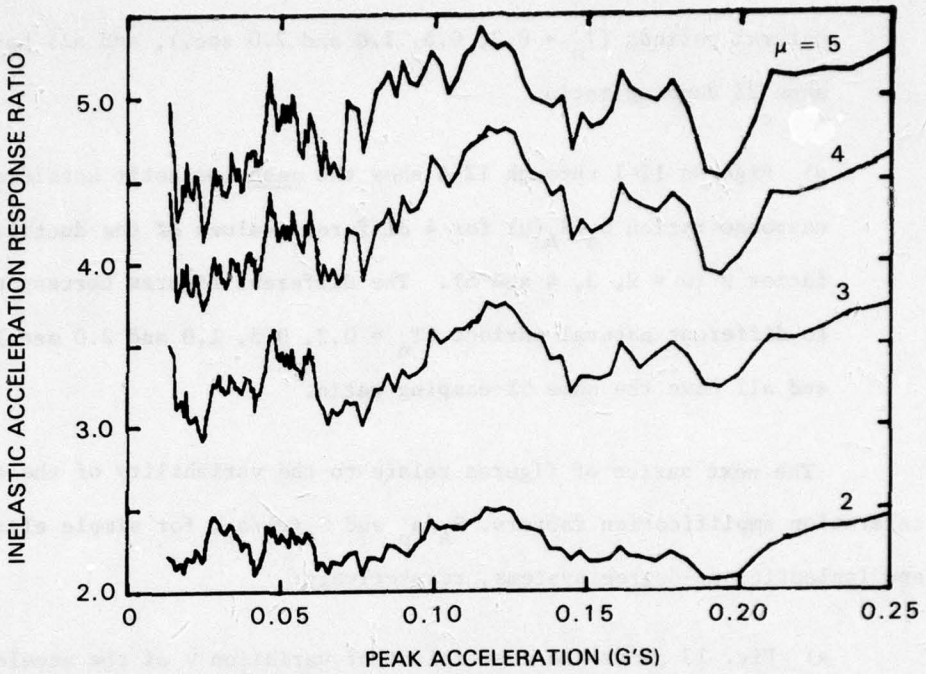

Figure 11-3. Mean inelastic acceleration response ratio $S_A/S_A(\mu)$ for four different values of the ductility factor μ (μ = 2, 3, 4 and 5). The damping ratio is 2% and the natural period T_n = 1.0 sec.

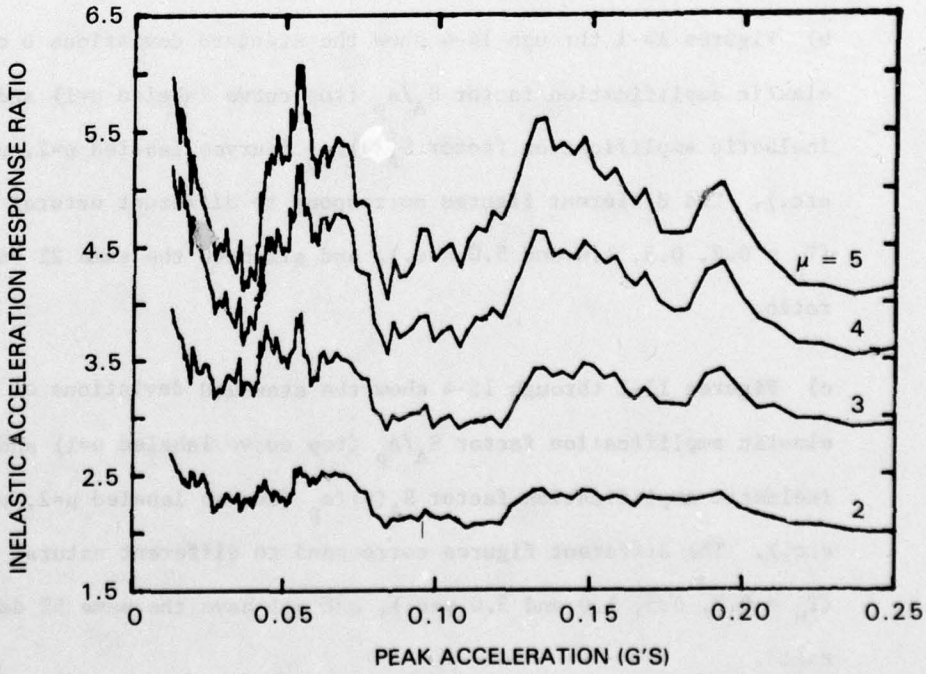

Figure 11-4. Mean inelastic acceleration response ratio $S_A/S_A(\mu)$ for four different values of the ductility factor μ (μ = 2, 3, 4 and 5). The damping ratio is 2% and the natural period T_n = 5.0 sec.

natural periods (T_n = 0.2, 0.5, 1.0 and 2.0 sec.), and all have the same 2% damping ratio.

e) Figures 12-1 through 12-4 show the mean inelastic acceleration response ration $S_A/S_A(\mu)$ for 4 different values of the ductility factor μ (μ = 2, 3, 4 and 5). The different figures correspond to different natural periods (T_n = 0.2, 0.5, 1.0 and 2.0 sec.), and all have the same 5% damping ratio.

33. The next series of figures relate to the variability of the acceleration amplification factors, S_A/a_p and $S_A(\mu)/a_p$, for simple elastic and inelastic one-degree systems, respectively:

a) Fig. 13 shows the coefficient of variation V of the acceleration amplification factor S_A/a_p for 2% damping for 3 different natural periods (T_n = 0.2, 1.0 and 5.0 sec.).

b) Figures 14-1 through 14-4 show the standard deviations σ of the elastic amplification factor S_A/a_p (top curve labeled μ=1) and the inelastic amplification factor $S_A(\mu)/a_p$ (curves labeled μ=2, μ=3, etc.). The different figures correspond to different natural periods (T_n = 0.2, 0.5, 1.0 and 5.0 sec.), and all have the same 2% damping ratio.

c) Figures 15-1 through 15-4 show the standard deviations of the elastic amplification factor S_A/a_p (top curve labeled μ=1) and inelastic amplification factor $S_A(\mu)/a_p$ (curves labeled μ=2, μ=3, etc.). The different figures correspond to different natural periods (T_n = 0.2, 0.5, 1.0 and 5.0 sec.), and all have the same 5% damping ratio.

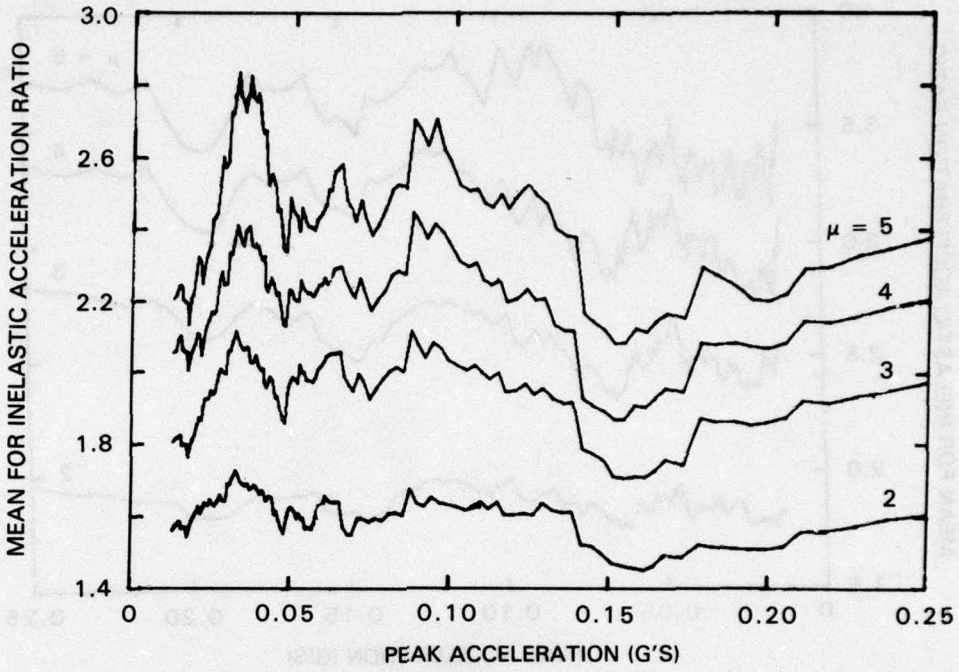

Figure 12-1. Mean inelastic acceleration response ratio $S_A/S_A(\mu)$ for four different values of the ductility factor μ (μ = 2, 3, 4 and 5). The damping ratio is 5% and the natural period is T_n = 0.2 sec.

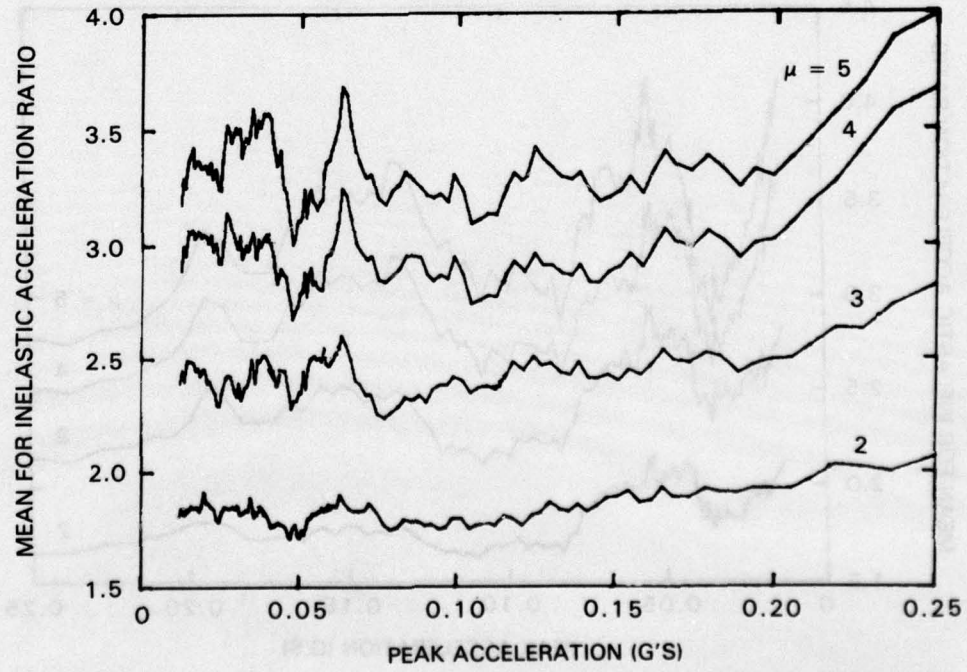

Figure 12-2. Mean inelastic acceleration response ratio $S_A/S_A(\mu)$ for four different values of the ductility factor μ (μ = 2, 3, 4 and 5). The damping ratio is 5% and the natural period T_n = 0.5 sec.

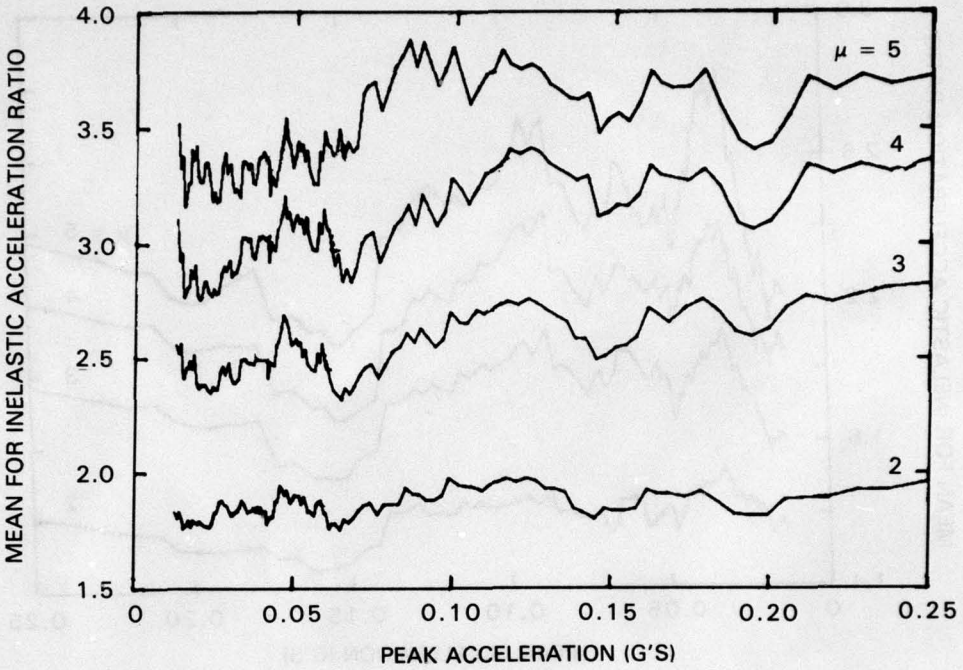

Figure 12-3. Mean inelastic acceleration response ratio $S_A/S_A(\mu)$ for four different values of the ductility factor μ (μ = 2, 3, 4 and 5). The damping ratio is 5% and the natural period T_n = 1.0 sec.

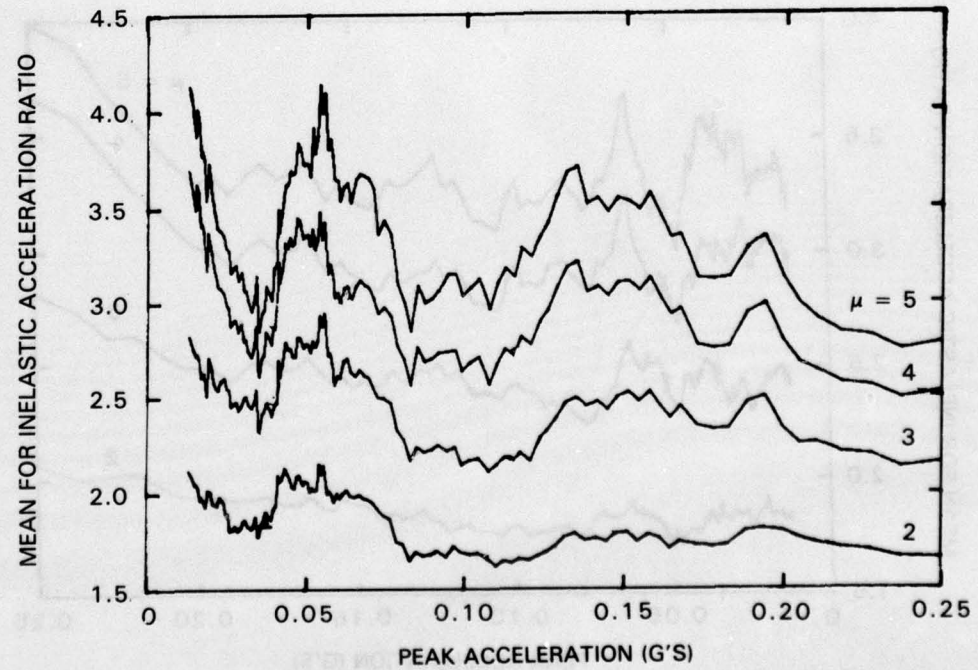

Figure 12-4. Mean inelastic acceleration response ratio $S_A/S_A(\mu)$ for four different values of the ductility factor μ (μ = 2, 3, 4 and 5). The damping ratio is 5% and the natural period T_n = 5.0 sec.

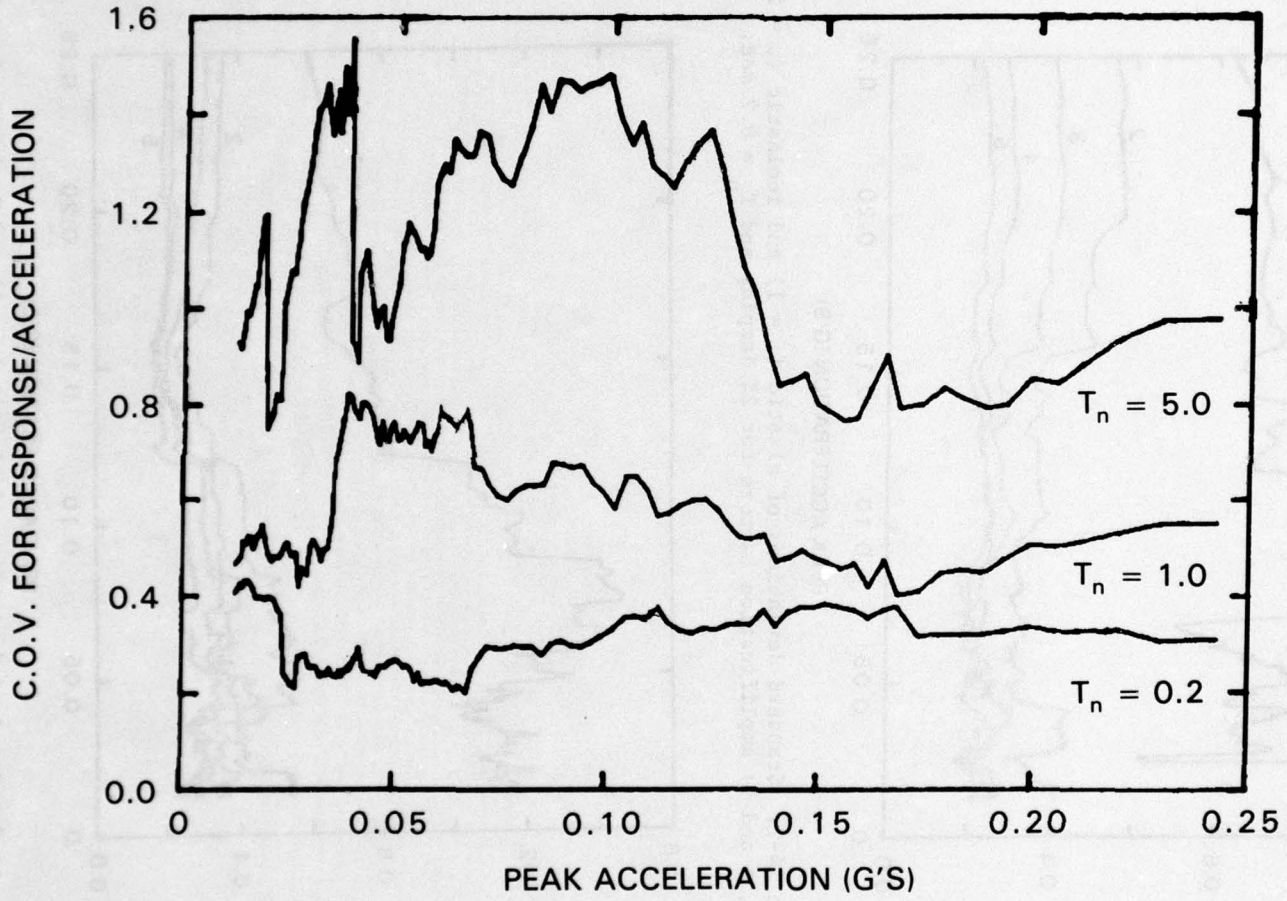

Figure 13. Coefficient of variation of the acceleration amplification factor S_A/a_p for 2% damping for three different natural periods, T_n = 0.2, 1.0 and 5.0 sec.

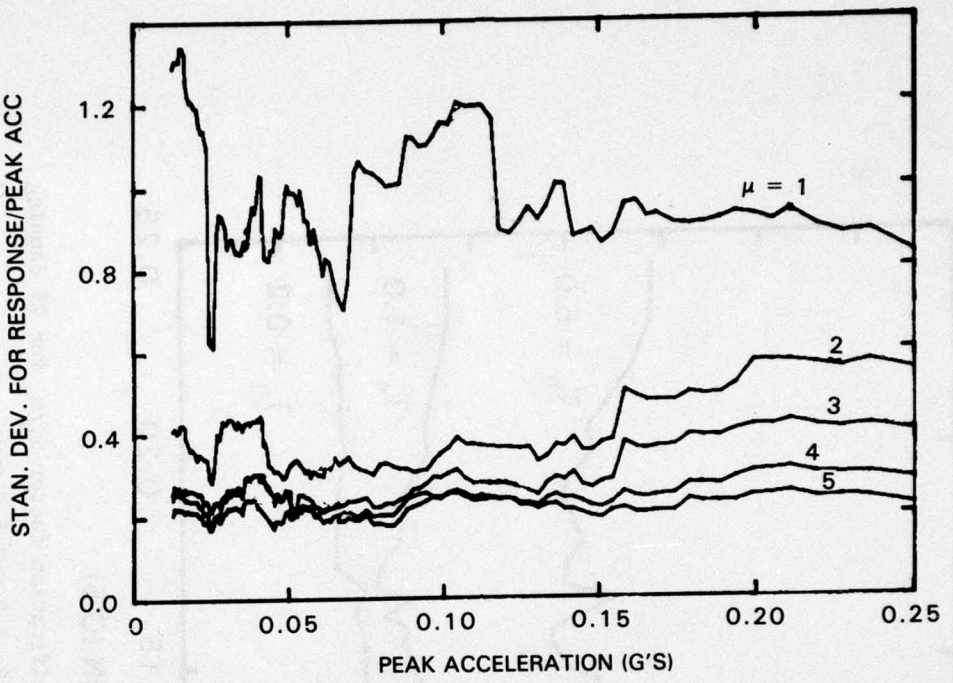

Figure 14-1. Standard deviations of elastic ($\mu = 1$) and inelastic ($\mu = 2$, 3, 4 and 5) amplification factors for 2% damping and $T_n = 0.2$ sec.

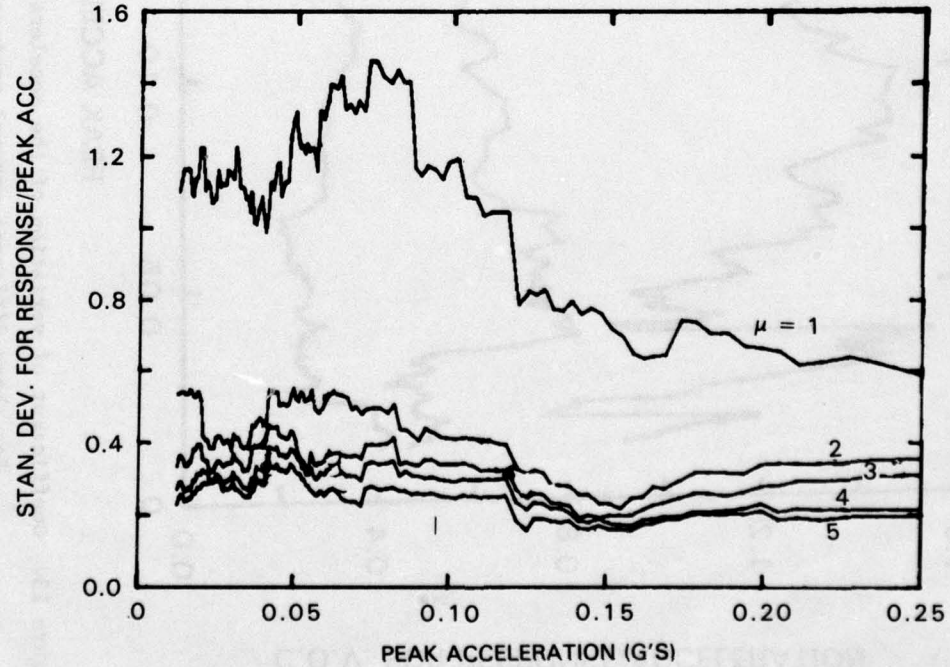

Figure 14-2. Standard deviations of elastic ($\mu = 1$) and inelastic ($\mu = 2$, 3, 4 and 5) amplification factors for 2% damping and $T_n = 0.5$ sec.

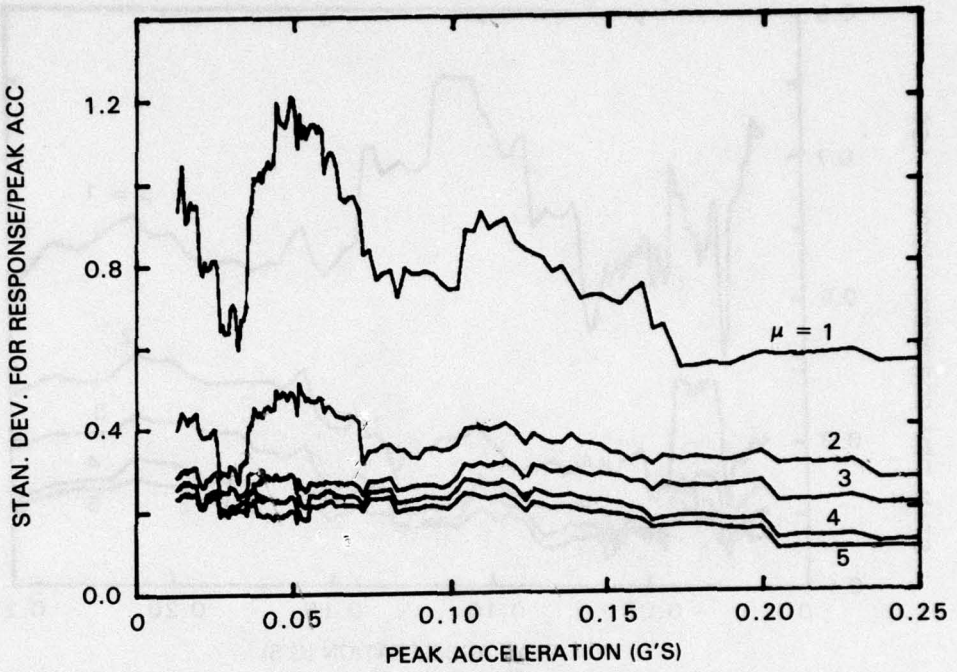

Figure 14-3. Standard deviations of elastic (μ = 1) and inelastic (μ = 2, 3, 4 and 5) amplification factors for 2% damping and T_n = 1.0 sec.

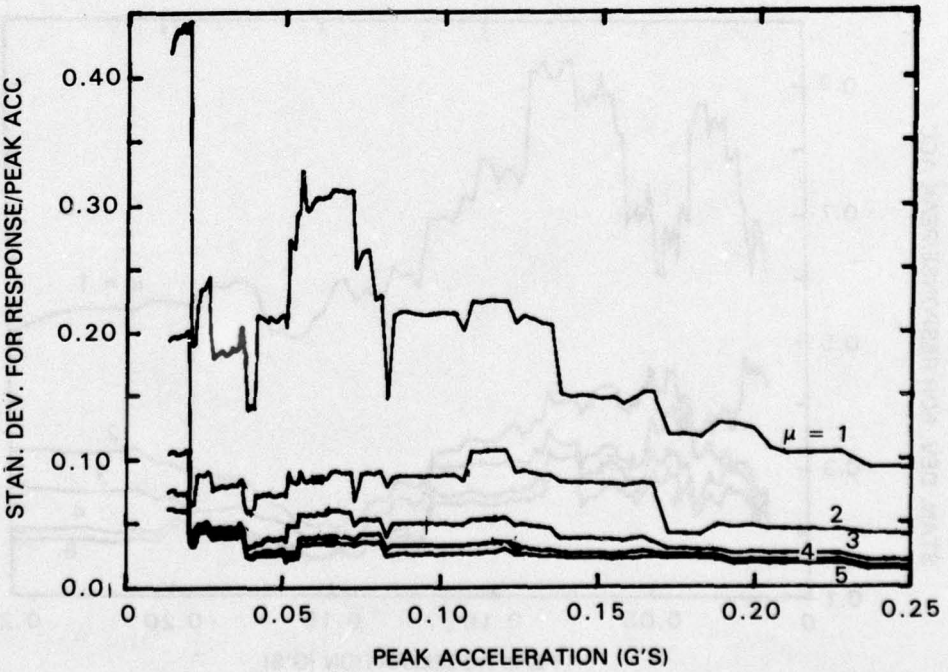

Figure 14-4. Standard deviations of elastic (μ = 1) and inelastic (μ = 2, 3, 4 and 5) amplification factors for 2% damping and T_n = 5.0 sec

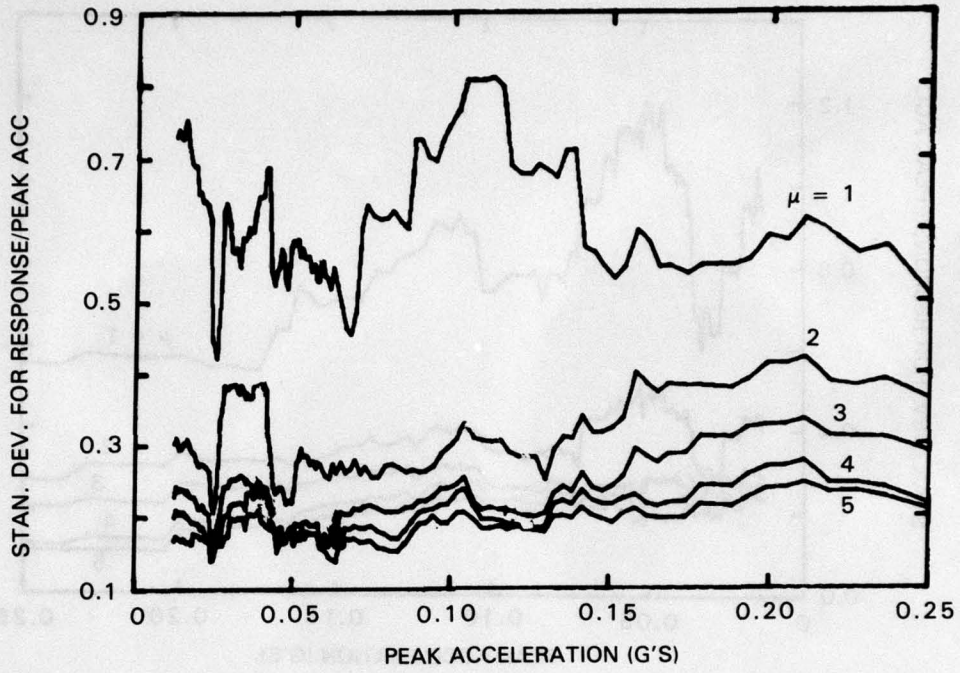

Figure 15-1. Standard deviations of elastic ($\mu = 1$) and inelastic ($\mu = 2$, 3, 4 and 5) amplification factors for 5% damping and $T_n = 0.2$ sec.

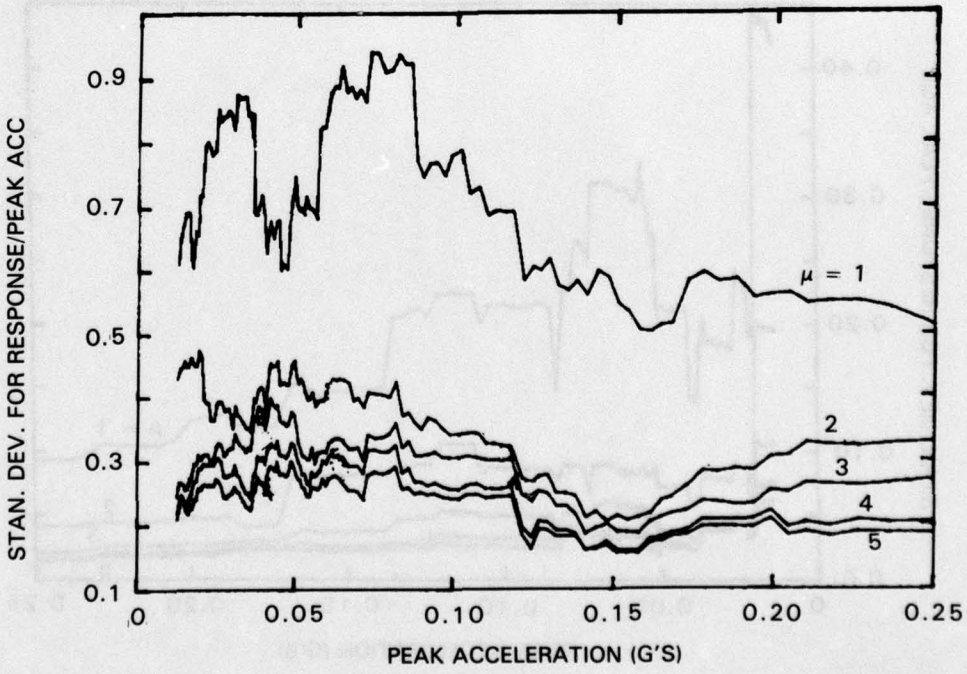

Figure 15-2. Standard deviations of elastic ($\mu = 1$) and inelastic ($\mu = 2$, 3, 4 and 5) amplification factors for 5% damping and $T_n = 0.5$ sec.

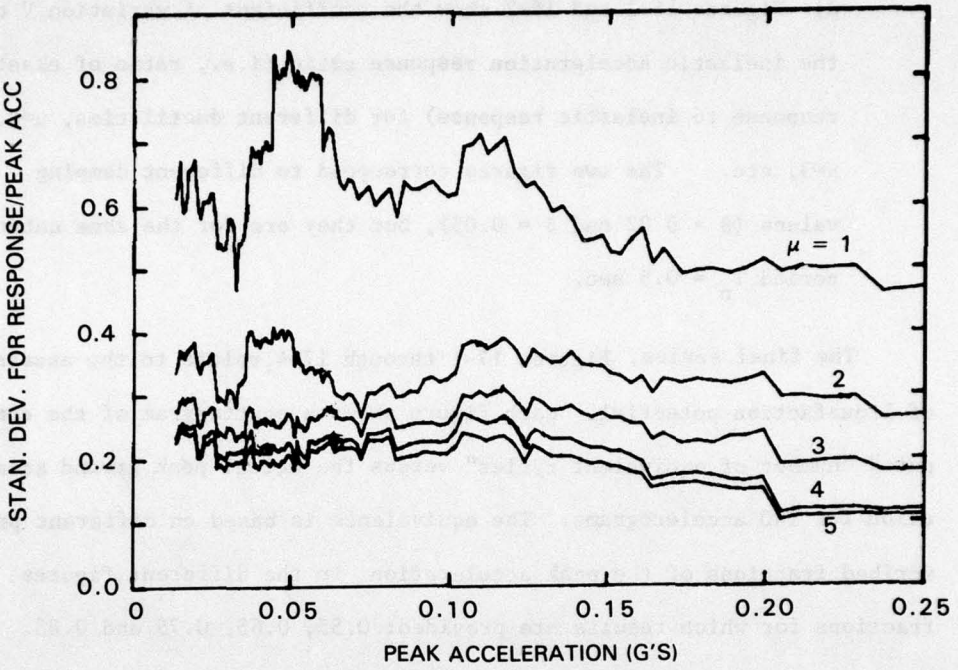

Figure 15-3. Standard deviations of elastic (μ = 1) and inelastic (μ = 2, 3, 4 and 5) amplification factors for 5% damping and T_n = 1.0 sec.

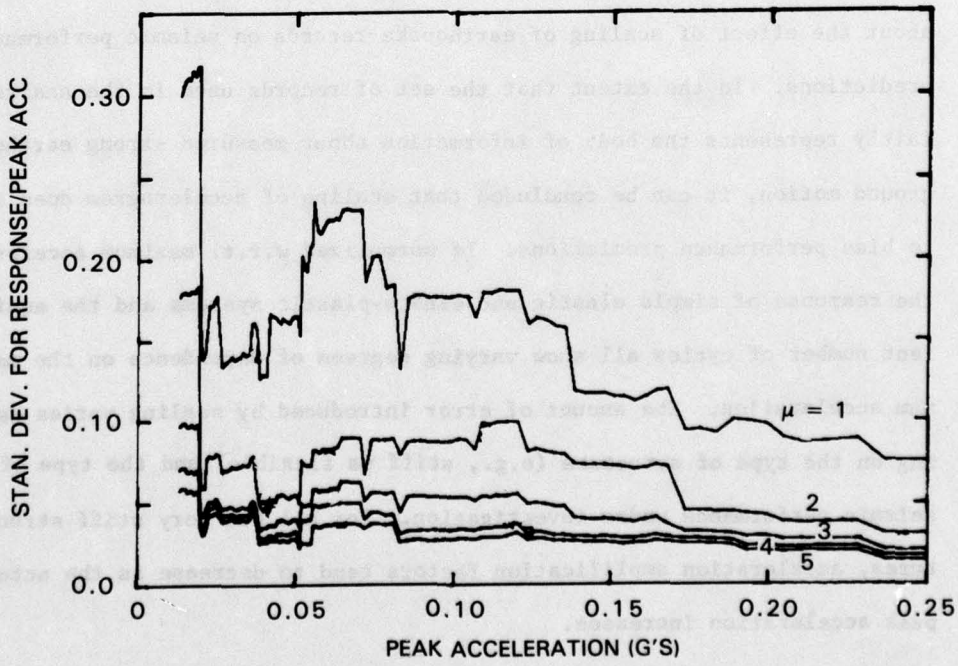

Figure 15-4. Standard deviations of elastic (μ = 1) and inelastic (μ = 2, 3, 4 and 5) amplification factors for 5% damping and T_n = 5.0 sec.

d) Figures 16-1 and 16-2 show the coefficient of variation V of the inelastic acceleration response ratio (i.e., ratio of elastic response to inelastic response) for different ductilities, μ=2, μ=3, etc. The two figures correspond to different damping values (β = 0.02 and β = 0.05), but they are for the same natural period T_n = 0.5 sec.

34. The final series, Figures 17-1 through 17-4, relate to the assessment of liquefaction potential. Each figure shows a scattergram of the computed "number of equivalent cycles" versus the actual peak ground acceleration for 140 accelerograms. The equivalence is based on different prescribed fractions of the peak acceleration in the different figures. The fractions for which results are provided: 0.55, 0.65, 0.75 and 0.85.

Conclusions

35. The results just presented provide specific quantitative information about the effect of scaling of earthquake records on seismic performance predictions. To the extent that the set of records used in the analysis fairly represents the body of information about measured strong earthquake ground motion, it can be concluded that scaling of accelerogram does tend to bias performance predictions. If normalized w.r.t. maximum acceleration, the response of simple elastic and elasto-plastic systems and the equivalent number of cycles all show varying degrees of dependence on the maximum acceleration. The amount of error introduced by scaling varies depending on the type of structure (e.g., stiff vs flexible) and the type of seismic performance under investigation. For all but very stiff structures, acceleration amplification factors tend to decrease as the actual peak acceleration increases.

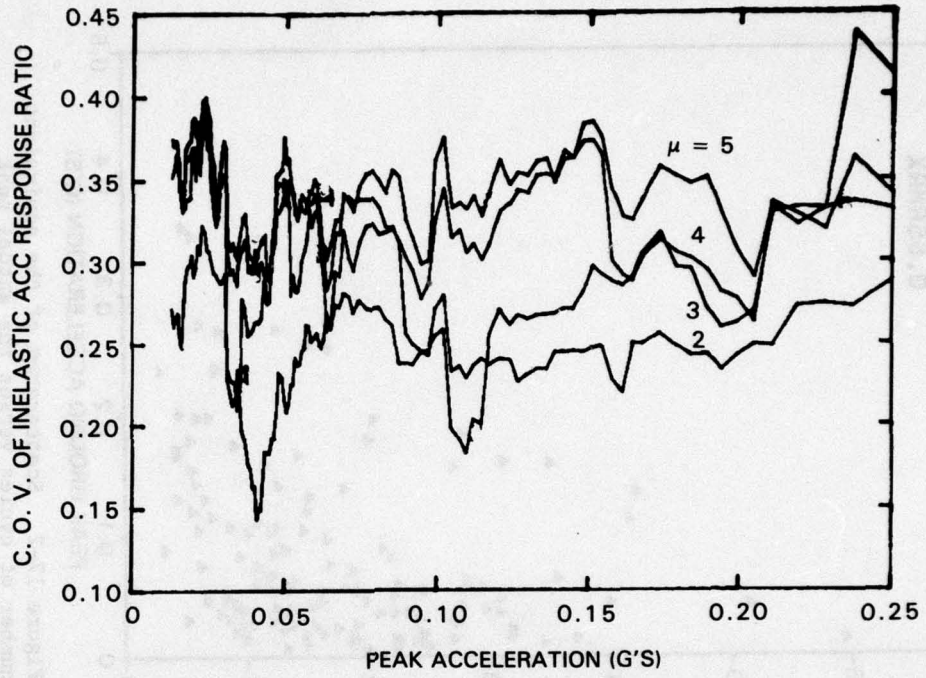

Figure 16-1. Coefficients of variation of the inelastic (μ = 2, 3, 4 and 5) acceleration amplification factor for 2% damping and T_n = 0.5 sec.

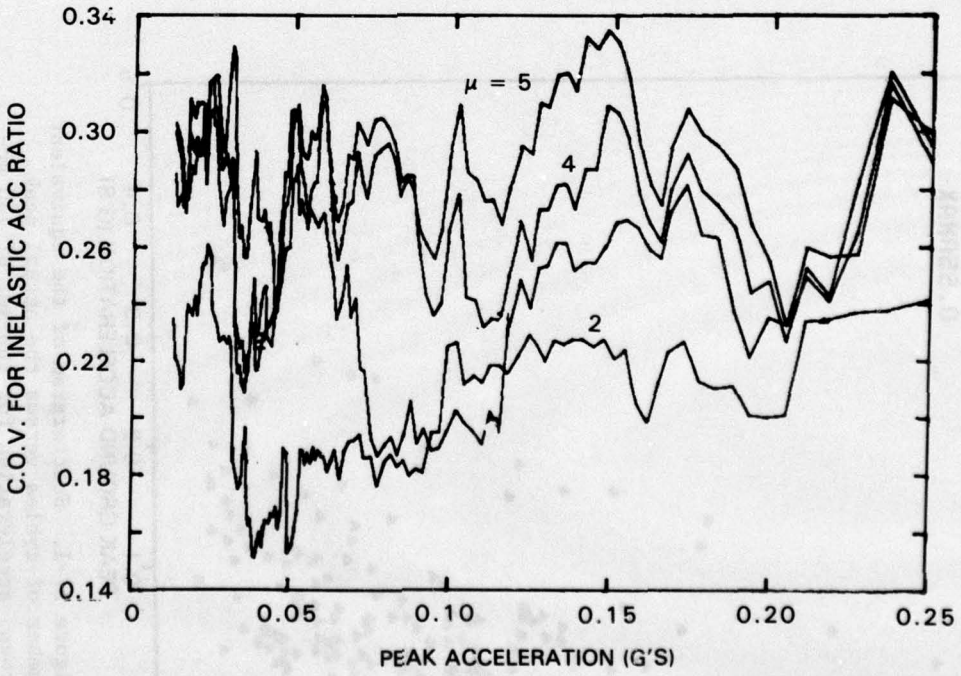

Figure 16-2. Coefficients of variation of the inelastic (μ = 2, 3, 4 and 5) acceleration amplification factor for 5% damping and T_n = 0.5 sec.

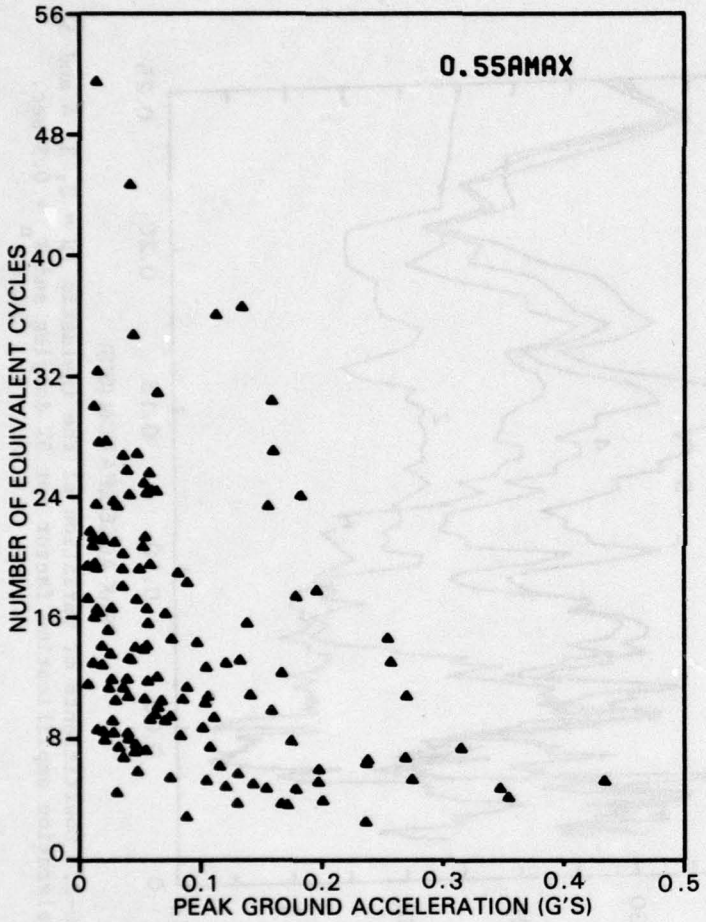

Figure 17-1. Scattergram of the equivalent number of cycles versus the actual peak ground acceleration for the set of 140 accelerograms. The equivalence is based on the acceleration level 0.55 a_p

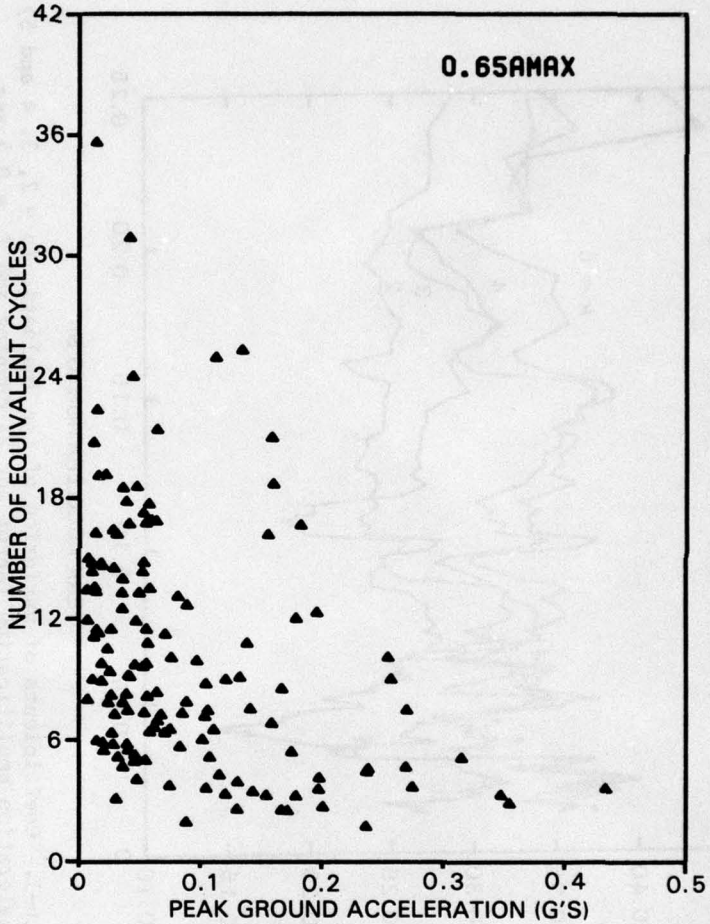

Figure 17-2. Scattergram of the equivalent number of cycles versus the actual peak ground acceleration for the set of 140 accelerograms. The equivalence is based on the acceleration level 0.65 a_p

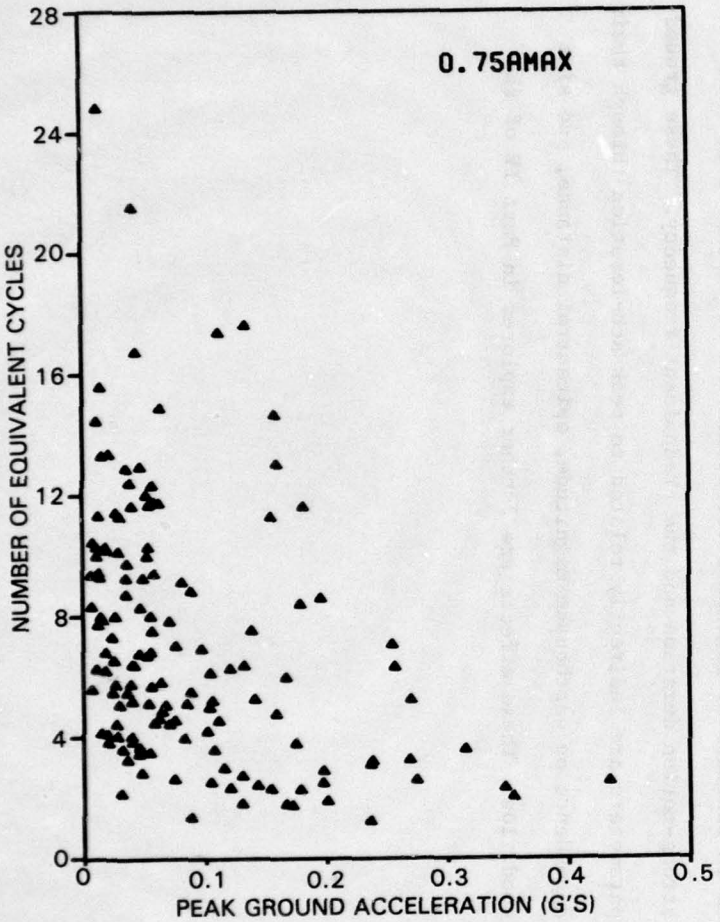

Figure 17-3. Scattergram of the equivalent number of cycles versus the natural peak ground acceleration for the set of 140 accelerograms. The equivalence is based on the acceleration level 0.75 a_p

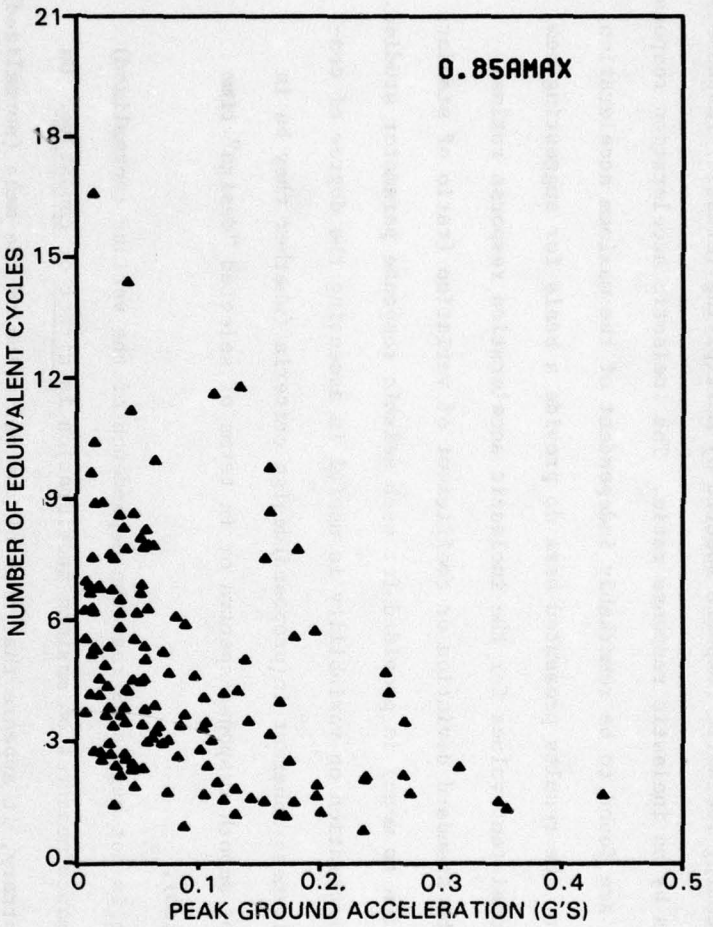

Figure 17-4. Scattergram of the equivalent number of cycles versus the natural peak ground acceleration for the set of 140 accelerograms. The equivalence is based on the acceleration level 0.85 a_p

37. The results confirm the validity of the Newmark-Hall procedure for constructing inelastic response spectra by multiplying (elastic) response spectra by an inelastic response ratio. The inelastic acceleration response ratios are found to be remarkably independent of the maximum acceleration. However, the results presented here do provide a basis for suggesting new, more consistent values for the inelastic acceleration response ratios.

38. The standard deviation or coefficient of variation (ratio of standard deviation to mean) is provided for each seismic response parameter studied. This information on variability is useful in assessing the degree of conservativeness inherent in (proposed) design criteria (whether they be in terms of smooth response spectra or in terms of selected "design" time histories).

39. It is not suggested that the dependence of the various (normalized) performance measures on maximum acceleration is direct or causative. On the contrary, it appears that much of the variation of the mean (normalized) responses in function of maximum acceleration can be explained in terms of the strong-motion duration and the predominant frequency. These ground motion parameters are indirectly related to peak acceleration through their common dependence on earthquake magnitude, epicentral distance, and site ground condition. These effects are further explored in Part IV of the report.

PART IV: INTERPRETATION OF THE RESULTS OF THE STUDY ON ACCELEROGRAM SCALING

Influence of Duration and Frequency Content

40. A second statistical study was carried out, based on the 140 accelerograms, to relate the strong-motion duration to peak acceleration as well as to magnitude and epicentral distance. Parameters which characterize the frequency content of the ground motion were analyzed in a parallel way.

41. In earlier reports in this series (1, 9, 16), duration was taken as the "bracketed" time interval in which acceleration is greater than 0.05g. These durations are listed in Table 1, together with the strong-motion durations based on the definition proposed by Vanmarcke and Lai (17). According to this definition, duration is related to the peak acceleration $a_p = \max |a(t)|$ as well as to the Arias Intensity $I_o = \int_0^{t_o} a^2(t)dt$. The resulting duration is essentially proportional to the factor I_o/a_p^2. (Both I_o and a_p are listed in Table I). Fig. 18 shows a scattergram of the durations according to the two definitions for those accelerograms for which the "bracketed duration" exists (i.e., when $a_p \geq 0.05g$). The correlations presented below are based on the Vanmarcke-Lai definition of duration.

42. The mean duration for all records is 9.27 sec., and the standard deviation is 8.7 sec. For the 32 near-field records, the mean and the standard deviation are 6.34 and 5.55 sec., respectively. For the far-field records, the mean is 10.2 sec., and the standard deviation is 9.4 sec. For the records on "rock," the mean duration is 4.7 sec., and for the records on "soil," it is 10.1 sec.

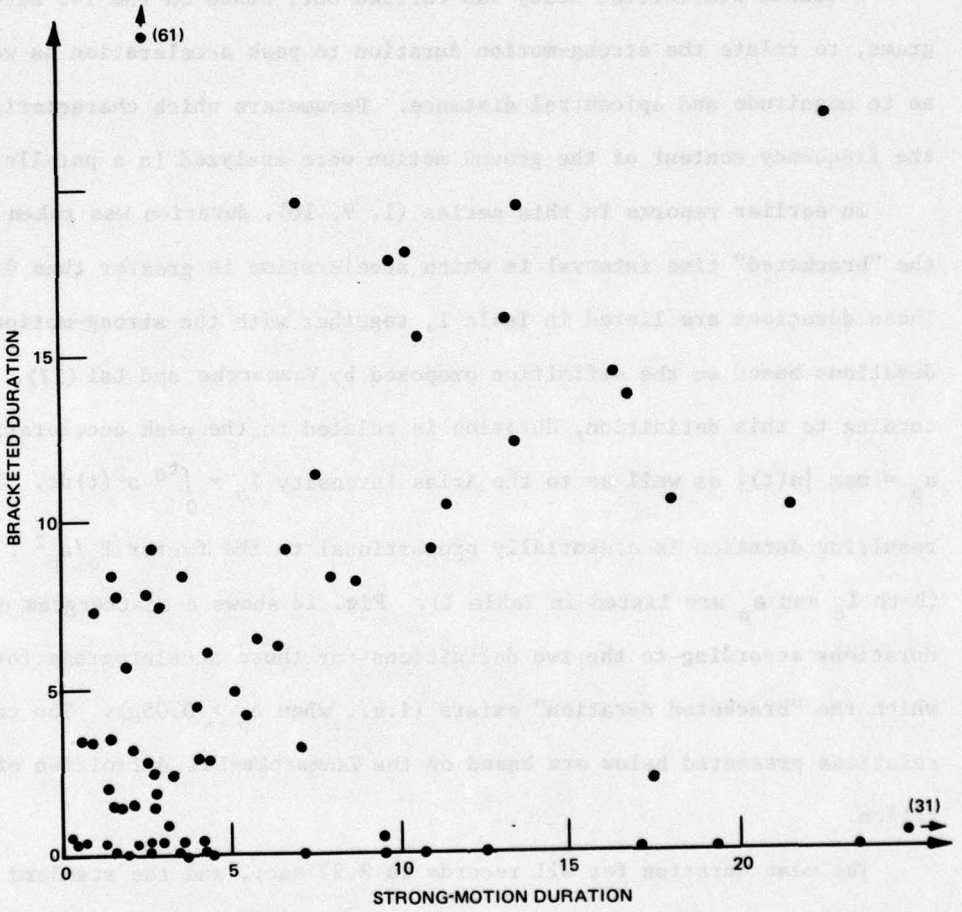

Figure 18. Scattergram of durations based on two different definitions, the "bracketed duration" (which exists for records with $a_p \geq 0.05g$) and the strong-motion duration proposed by Vanmarcke and Lai (17)

43. Although there is considerable scatter, large peak accelerations tend to be associated with small strong-motion durations. Fig. 19 shows the mean, and the mean plus one standard deviation, of the strong-motion duration as a function of the peak acceleration. As before, the point on the "mean" curve corresponding to the peak acceleration a_p is obtained by averaging the durations for a subset of 20 records whose "median" peak acceleration equals a_p. Note that the mean duration decreases from 18 sec. to about 3 sec. as the (median) value of a_p increases from 0.015g to 0.25g. The coefficient of variation (ratio of standard deviation to mean) does not change much with peak acceleration (see Fig. 20).

44. Scattergrams of the "equivalent number of cycles" and the strong-motion duration for the 140 accelerograms shown in Figures 21 through 24 suggest that these quantities are strongly correlated. These scattergrams correspond to different fractions of the peak acceleration, ranging from $0.55\ a_p$ to $0.85\ a_p$.

45. We now turn to the dependence of duration on distance and magnitude. Fig. 25 shows that the duration tends to increase with distance R. The points in this plot again correspond to the statistics (mean or mean plus one standard deviation) of a "moving subset" of 20 accelerograms whose actual distances are clustered around a target distance. Fig. 26 indicates that the mean duration also tends to increase as the magnitude M increases, but in a much less pronounced way (than for R). Figures 27 and 28 show the dependence of duration on distance for records from earthquakes with $M \geq 6$ and $M < 6$, respectively.

46. The predominant frequencies of the set of 140 accelerograms do not display any clear dependence on peak acceleration (Fig. 29). There is

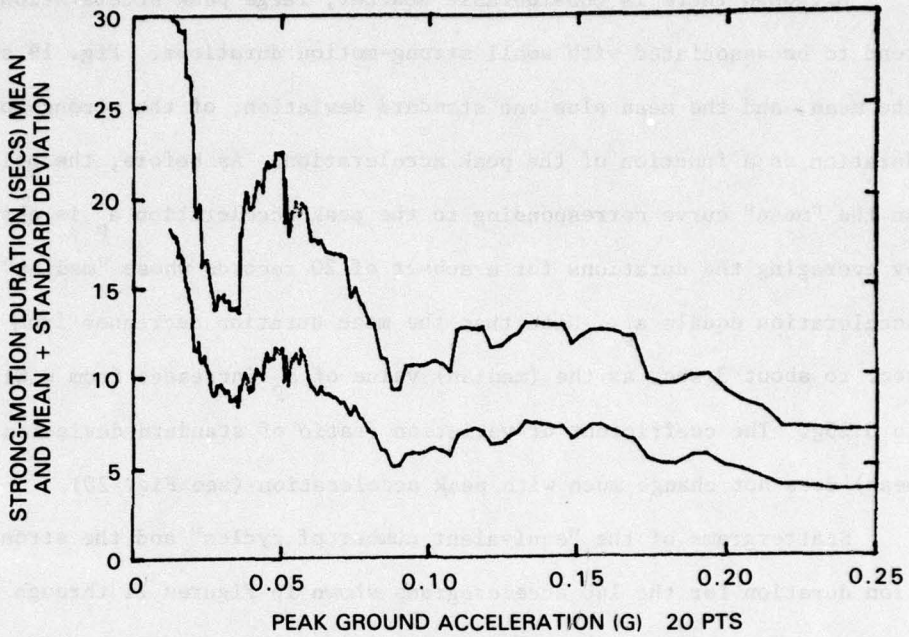

Figure 19. Mean and mean plus standard deviation of the strong-motion duration versus peak acceleration. (Calculations are based on a "moving" subset of 20 records)

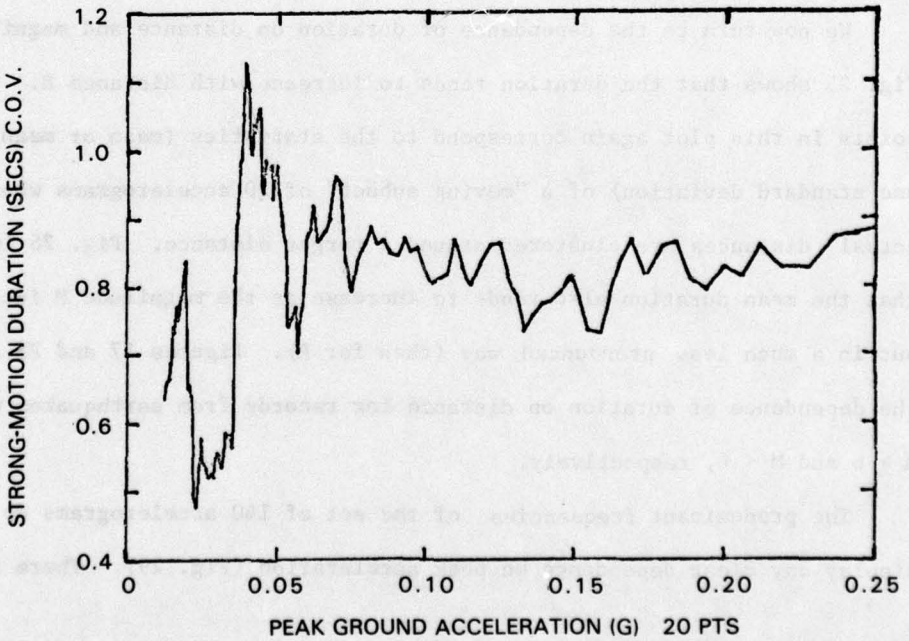

Figure 20. Coefficient of variation of the strong-motion duration versus peak acceleration. (Calculations are based on a "moving" subset of 20 records)

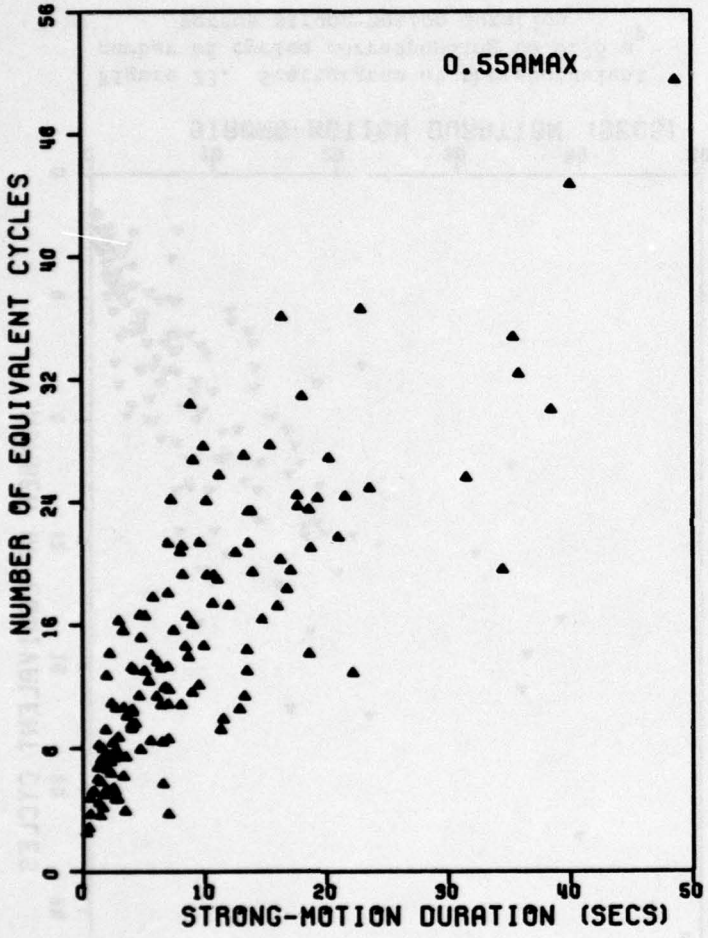

Figure 21. Scattergram of the equivalent number of cycles corresponding to 0.55 a_p versus strong-motion duration

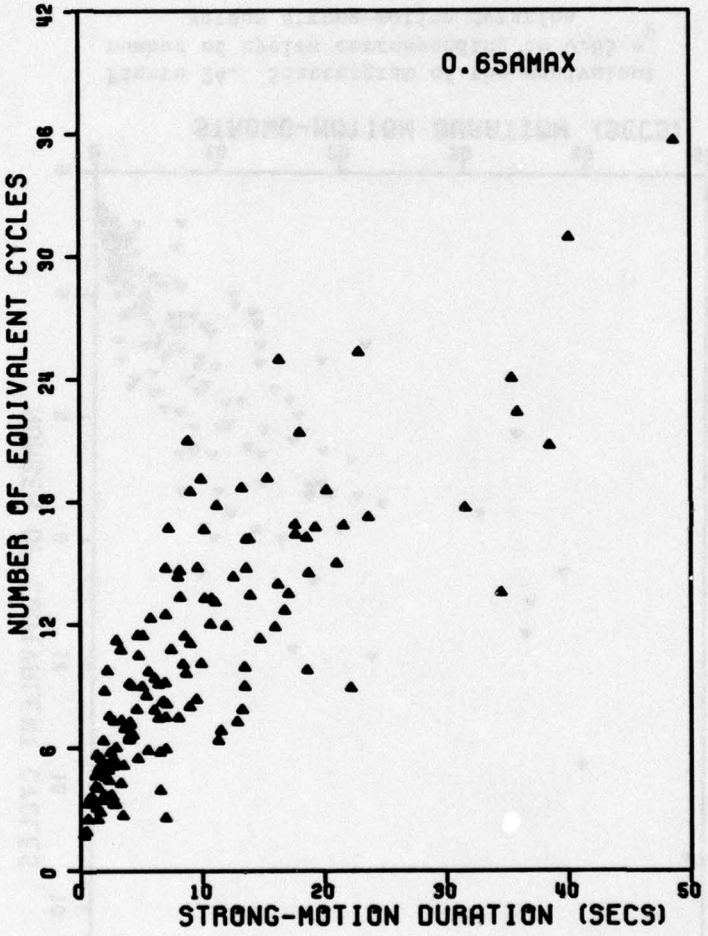

Figure 22. Scattergram of the equivalent number of cycles corresponding to 0.65 a_p versus strong-motion duration

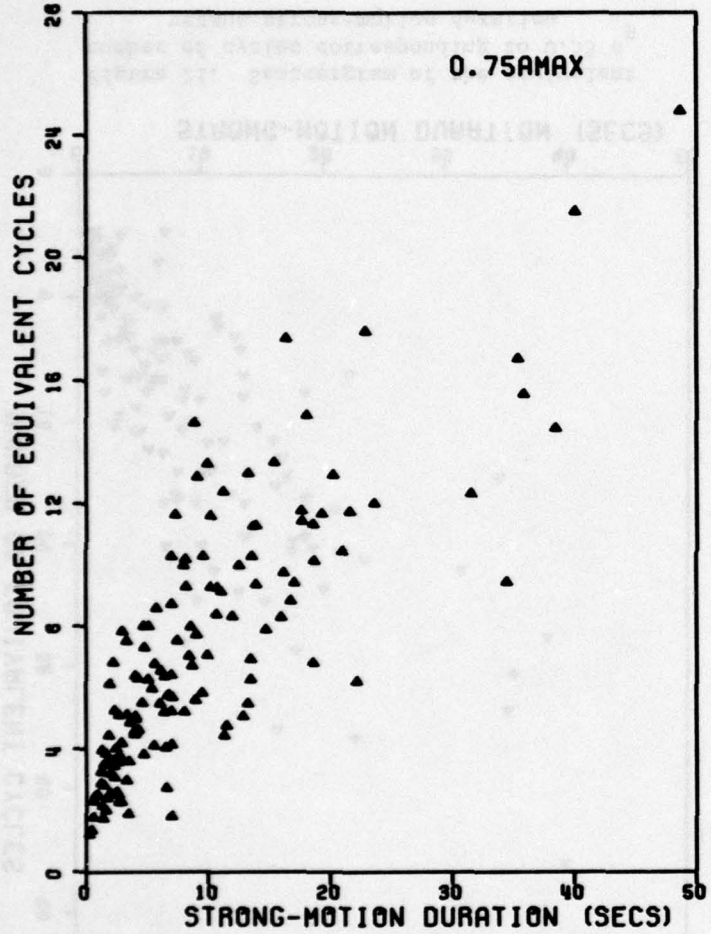

Figure 23. Scattergram of the equivalent number of cycles corresponding to 0.75 a_p versus strong-motion duration

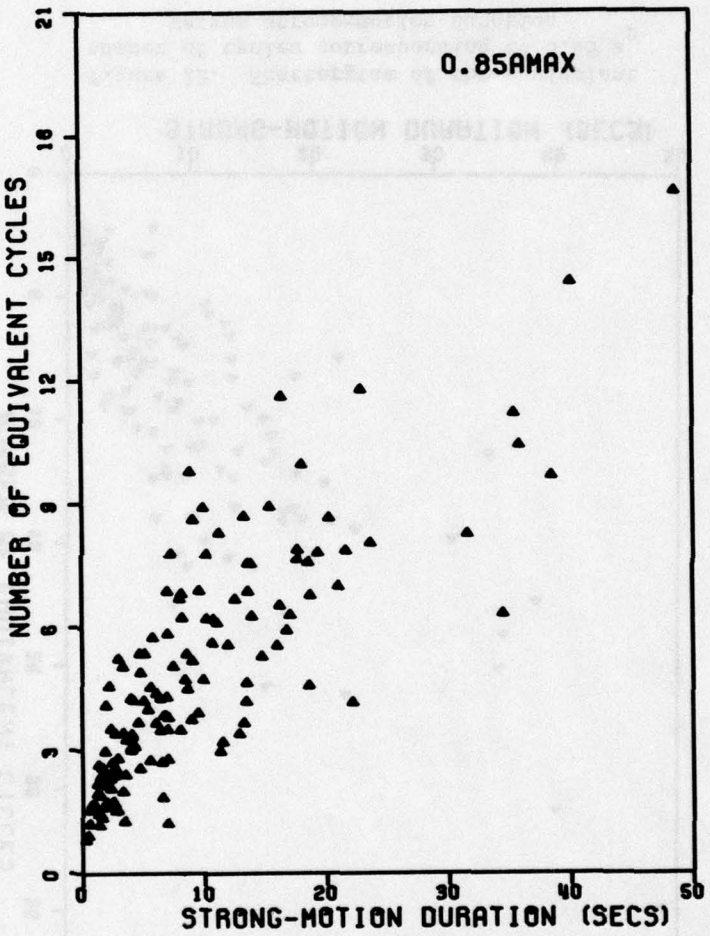

Figure 24. Scattergram of the equivalent number of cycles corresponding to 0.85 a_p versus strong-motion duration

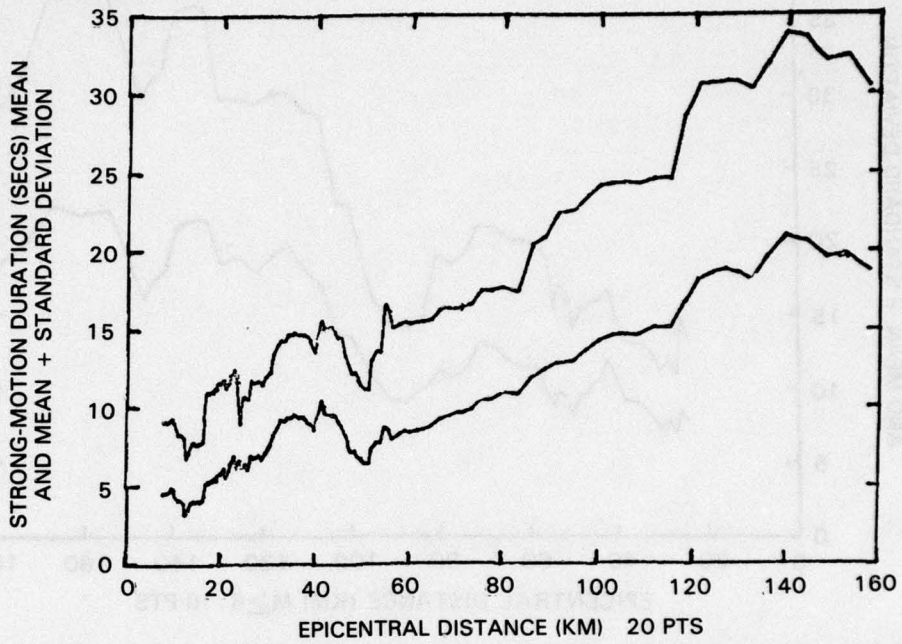

Figure 25. Mean and mean plus standard deviation of strong-motion duration versus epicentral distance. (Calculations based on a "moving" subset of 20 records)

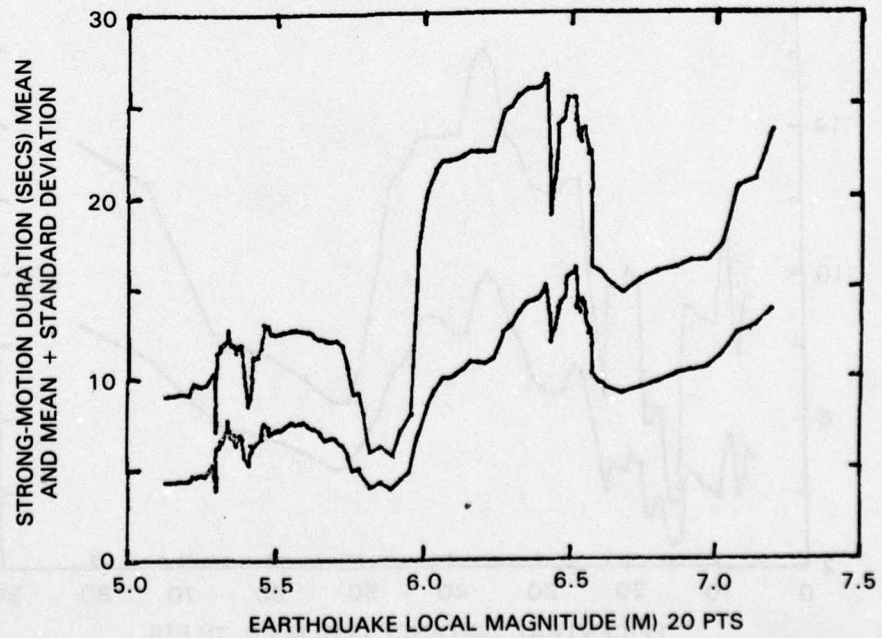

Figure 26. Mean and mean plus standard deviation of strong-motion duration versus Richter magnitude. (Calculations based on a "moving" subset of 20 records)

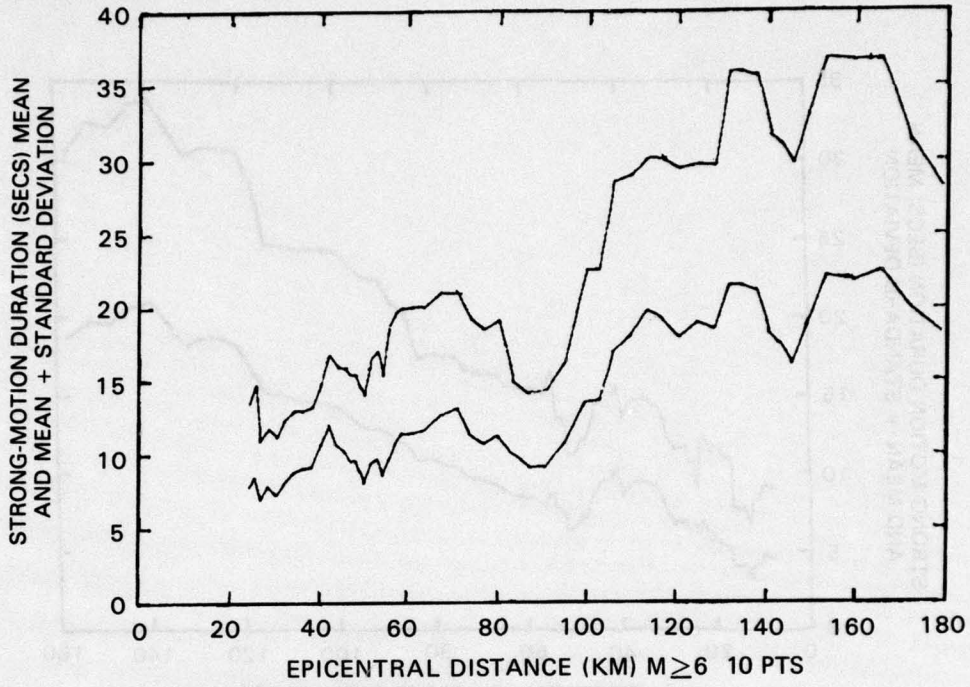

Figure 27. Mean and mean plus standard deviation of strong-motion duration versus epicentral distance for records from events with Richter magnitude $M \geq 6$. (Calculations based on a "moving" subset of 10 records)

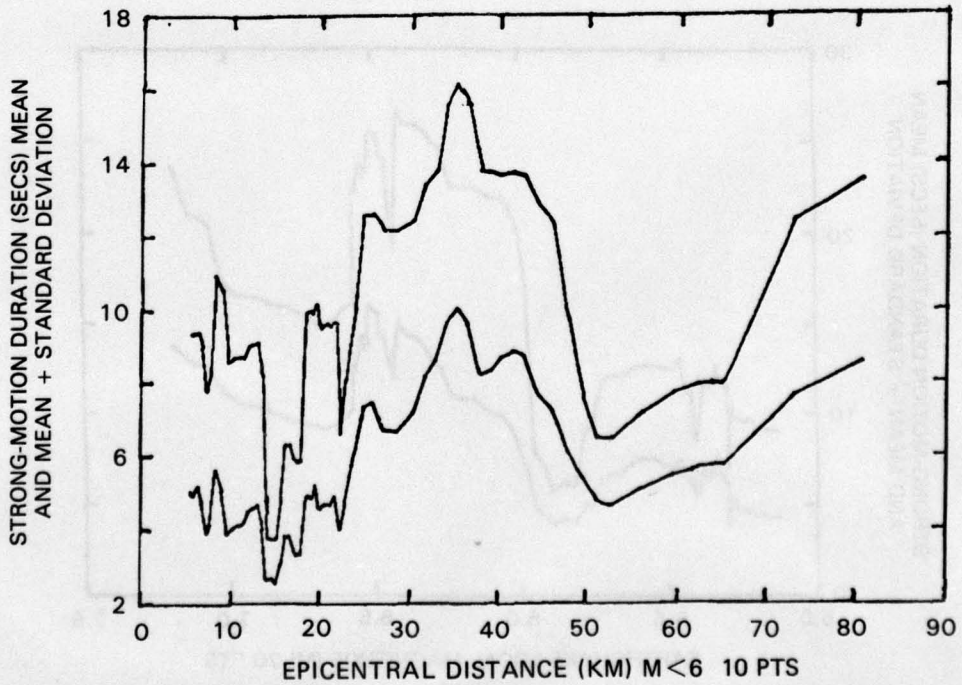

Figure 28. Mean and mean plus standard deviation of strong-motion duration versus epicentral distance for records from events with Richter magnitude $M < 6$. (Calculations based on a "moving" subset of 10 records)

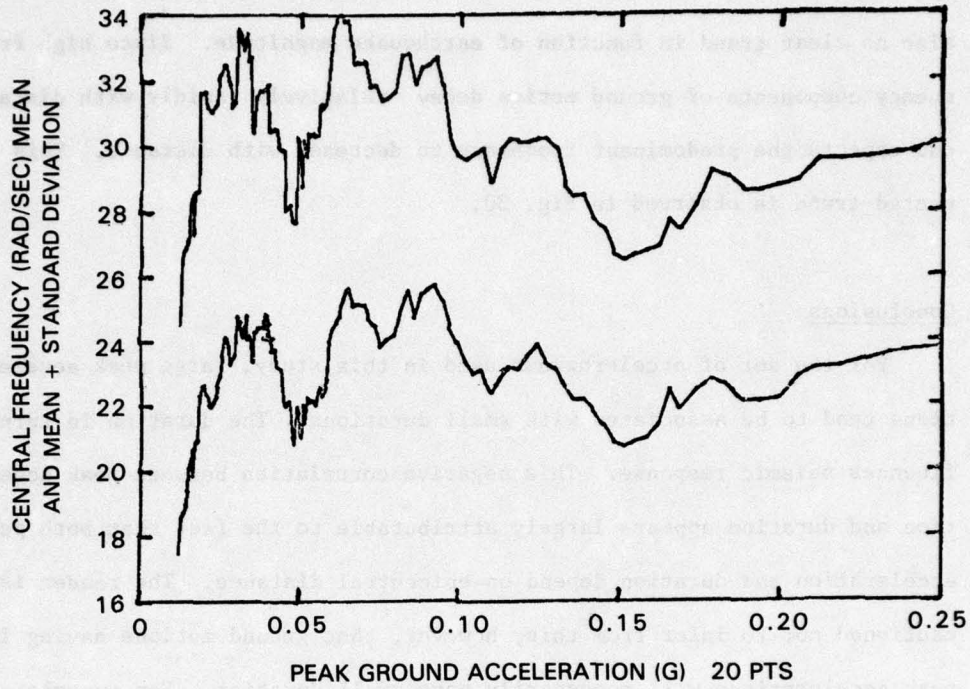

Figure 29. Mean and mean plus standard deviation of predominant frequency versus peak acceleration. (Calculations are based on a "moving" subset of 20 records)

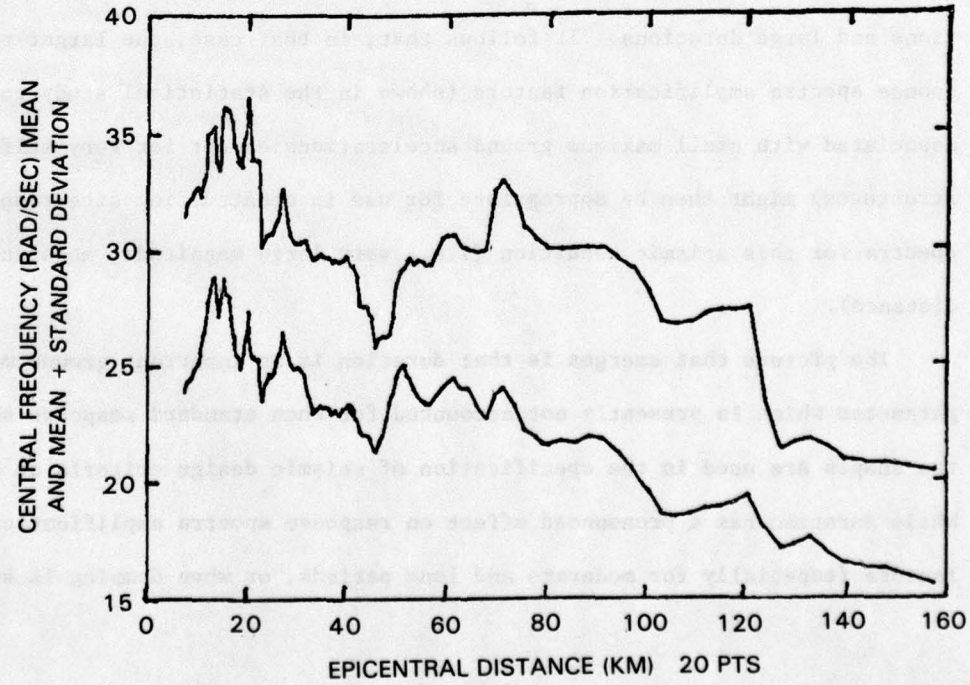

Figure 30. Mean and mean plus standard deviation of the predominant frequency versus distance. (Calculations based on a "moving" subset of 20 records)

also no clear trend in function of earthquake magnitude. Since high frequency components of ground motion decay relatively rapidly with distance, one expects the predominant frequency to decrease with distance. This expected trend is observed in Fig. 30.

Conclusions

47. For the set of accelerograms used in this study, large peak accelerations tend to be associated with small durations. The duration in turn influences seismic response. This negative correlation between peak acceleration and duration appears largely attributable to the fact that both peak acceleration and duration depend on epicentral distance. The reader is cautioned not to infer from this, however, that ground motions having large peak accelerations will necessarily have small duration. For example, ground motions from very large magnitude events (which are hardly represented in the body of instrumental strong-motion data) might have both large accelerations and large durations. It follows that, in that case, the larger response spectra amplification factors (shown in the statistical study to be associated with small maximum ground accelerations except for very stiff structures) might then be appropriate for use in constructing site response spectra for this seismic condition (i.e., very large magnitude, moderate distance).

48. The picture that emerges is that duration is an important ground motion parameter which is presently not accounted for when standard response spectra shapes are used in the specification of seismic design criteria at a site. While duration has a pronounced effect on response spectra amplification factors (especially for moderate and long periods, or when damping is small),

it will often have a decisive effect on measures of response of systems susceptible to liquefaction, low-cycle fatigue, accumulation of permanent deformation, stiffness degradation, progressive failure, etc.

49. The observed trends of the response amplification factor in function of peak acceleration can also be explained in part in terms of the indirect correlation that exists between the predominant frequency of a ground motion and its peak acceleration. For an earthquake of given magnitude, both the peak acceleration and the predominant frequency tend to decrease when the epicentral distance increases. This makes it appear that the predominant frequency increases, i.e., that there is relatively more high-frequency content in the ground motion, when the peak acceleration increases. This explains why the spectral amplification factor tends to increase with a_p for very stiff structures, while it decreases with a_p for long-period structures.

50. In summary, the practice of using <u>standard</u> response spectra shapes scaled on peak acceleration fails to account for other important ground motion parameters, such as duration and predominant frequency, that influence response spectra shapes. By the same token, scaling of accelerograms and response spectra on peak acceleration introduces systematic errors attributable to indirect correlations between the peak acceleration and these other ground motion parameters. Estimates of these errors may be obtained from the plots presented in Part III. The sizes of these errors and the permissable values of scale factors will vary depending on the seismic response quantity under study and on the range of peak accelerations involved. For example, if the time histories are used for liquefaction studies, scale factors applied to accelerograms should perhaps not exceed 2, while for seismic investigation of linear elastic systems, factors as large as 4 might be tolerated.

PART V: COMPATIBILITY BETWEEN TIME HISTORIES AND SMOOTH RESPONSE SPECTRA

51. Compatibility between alternative representations of earthquake ground motion at a site is an important practical concern in earthquake engineering. Consider the following situation. A set of earthquake records has been selected to represent a prescribed seismic condition at a site. These records will be used as input for time history analyses of seismic response. At the same site, smooth response spectra representing essentially the same seismic condition are also needed to permit response spectrum-based analysis. The question is how one should proceed to derive a set of smooth response spectra that are compatible with the seismic criteria and the selected accelerograms. It is assumed that the time histories as well as the response spectra will be scaled with respect to a prescribed peak ground acceleration.

52. It is common in present practice to make use of standard response spectra shapes, derived on the basis of statistical analysis of many strong-motion records representing a wide range of source and site conditions and epicentral distances. The standard response spectra shapes may correspond to the mean of the amplification factors or to the mean plus one standard deviation. Which of these is used depends largely on whether or not it is desirable to add conservatism at this particular step in the seismic design process. An argument can also be made for always using mean (or median) response spectra and scaling the spectra upward if greater conservatism is sought.

53. There is no unique "best way" to construct smooth response spectra that represent a set of time histories (scaled to peak acceleration). It is as

much an art as it is a science. Obvious factors to be considered are: (a) the size and quality of the (recorded ground motion) data base, (b) desired simplicity and uniformity of the response spectra shapes, and (c) accuracy in representing expected ground motion spectral content. Statistical uncertainty decreases in function of the number of time histories that are used to estimate the mean and the standard deviation of the response spectra ordinates. But systematic errors or biases are introduced when the set of time histories contains records with source or site characteristics that deviate significantly from the seismic condition the response spectra are supposed to represent.

54. Much the same argument can be made when one analyzes the decision about how to subdivide the frequency range for the purpose of computing means and standard deviations of spectral amplification factors. In this case, the number of choices can be limited considerably by making use of a strong body of "prior information" that indicates that response spectra are approximately proportional to ground acceleration, ground velocity and ground displacement in different, adjacent frequency ranges. In other words, it may be assumed at the outset that the smooth response spectra will be piecewise linear, and alternately parallel to the constant acceleration, velocity and displacement lines in the usual tripartite logarithmic representation of response spectra. It will therefore suffice to calculate (for each damping) the mean and the standard deviation of a single amplification factor that can be applied throughout the frequency range where (that factor is) essentially constant.

55. The proposed methodology is introduced through an example involving two hypothetical seismic design situations. Each site/source condition is

specified in terms of magnitude, epicentral distance, and local site condition (soil vs rock). Also, based on information about motion attenuation with distance and dependence on magnitude, a "design" maximum ground acceleration is specified for each case. The criteria for the (hypothetical) seismic conditions are summarized in Table 2. In the first case, a moderate magnitude - short distance event is specified, while the second case involves a large magnitude - long distance event. The particular attenuation relations used in Table 2 are based on western United States data. It must be emphasized that they serve only an illustrative purpose here. Detailed discussion about methodology to obtain ground motion amplitudes given a seismic condition, or to obtain design amplitudes, is beyond the scope of this report. A pertinent reference is the report by Krinitzsky and Chang in this series (1). It summarizes information about the relations between epicentral M.M. Intensity and magnitude, between M.M. Intensity and distance, and between maximum ground motion amplitudes and M.M. Intensity. The report emphasizes the distinction that exists between the near field and the far field as regards the relation between motion amplitudes and M.M. Intensity. It presents upper bounds of observed ground motion amplitudes as well as estimates of the conditional probability of exceeding a motion amplitude given the M.M. Intensity. Needless to say, this is precisely the kind of information the engineer needs to make an assessment of site ground motion amplitudes during a specified seismic condition.

Table 2

Criteria for Two Hypothetical Seismic Design Conditions

Site/Source Conditions		Case I	Case II
Magnitude		6.5	8.0
Focal distance, km		50	150
Local site geology		Soil	Soil
Maximum acceleration* predicted, cm/sec^2	(1)	99.5	69.9
	(2)	118	102
For design		0.1g	0.1g

* Maximum accelerations are predicted from attenuation relationships proposed by Donovan (1973) and Orphal and Lahoud (1974). These relationships all have the form:

$$a_p = b_1 e^{b_2 M} R_o^{-b_3}$$

where a_p = maximum acceleration in cm/sec^2, M = Richter Magnitude, $R_o = R + c$, R = focal distance (km), b_1, b_2, b_3 and c are constants. The respective values of the constants (b_1, b_2, b_3 and c) are: (1) Donovan: 1080, 0.51, 1.32 and 25; and (2) Orphal and Lahoud: 69, 0.92, 1.39 and 0.

56. It is assumed that the pool of available earthquake records consists of 140 horizontal components of strong-motion records, the same data set used in the study of the effect of accelerogram scaling. The records selected to represent the site ground motion are given in Tables 3 and 4. Obviously, the selection process requires compromise and judgement, but the following objective criteria were used: (a) agreement of site geology (rock vs soil), (b) close matching of the specified magnitude and distance, and (c) minimizing the amount of accelerogram scaling required. In general, other constraints may have to be added, e.g., the type of faulting, focal depth, regional geology. Of course, the more constrained the search, the harder it will be to find the desired number of motions without deviating too much from the specified site condition. In the cases at hand, 8 accelerograms (2 x 4 horizontal components) were selected to represent the moderate magnitude - short distance event (Case I). For the large magnitude - large distance event (Case II) only 4 accelerograms (2 x 2 horizontal components) were found that came reasonably close to the prescribed site/source condition. Tables 3 and 4 list, for each accelerogram selected, the peak acceleration and velocity (a_p and v_p), event magnitude, source-to-site distance, the site condition, and the scale factor required

Table 3

Characteristics of the Ground Motions Selected to Represent the "Case I" Site Seismic Condition

Case I M = 6.5 R = 50 km Soil Site a_{design} = 0.1 g

Selected Earthquake Records

	M	R (km)	Local Site Geology	a_p (g)	Scale Factor	v_p (cm/sec)	v_p/a_p (cm/sec x g)
U300	6.4	50	Soil	0.121 0.116	0.83 0.86	6.92 5.74	57.19 49.48
T286	6.5	48	Soil	0.060 0.047	1.67 2.13	6.22 6.05	103.67 128.72
F086	6.6	46	Soil	0.107 0.082	0.93 1.22	17.4 15.1	162.12 184.15
A009	6.6	40	Soil	0.159 0.201	0.63 0.50	35.6 26.0	223.89 129.35

Average: 0.11 g

Mean: 129.8
St. Dev: 60.11
C.o.v.: 0.463

Table 4

Characteristics of the Ground Motions Selected to Represent the "Case II" Site Seismic Condition

Case II M = 8.0 R = 150 km Soil Site a_{design} = 0.1g

Selected Earthquake Records

	M	R (km)	Local Site Geology	a_p (g)	Scale Factor	v_p (cm/sec)	v_p/a_p (cm/sec x g)
A003	7.7	127	Soil	0.047 0.053	2.13 1.89	6.2 9.1	131.9 171.7
A006	7.7	119	Soil	0.055 0.044	1.82 2.27	6.1 9.4	110.9 213.6

Average: 0.05

Mean: 157.0
St. Dev: 45.36
C.o.v.: 0.29

to match the "design" maximum acceleration.

57. The next step is to assess the implications of the selection of ground motions on the response spectra shapes. The response spectra are evaluated for 2% and 5% damping and for the 12 natural periods ranging between 0.05 and 2 sec. The corresponding spectral amplification factors S_A/a_p and S_V/v_p are listed in Tables 5 through 8. The velocity amplification factor S_V/v_p is directly related to the acceleration amplification factor S_A/a_p as follows:

$$\frac{S_V}{v_p} = \frac{T_n}{2\pi} \cdot \frac{a_p}{v_p} \cdot \frac{S_A}{a_p}$$

58. The mean amplification factors are listed just below each column of amplification factors in Tables 5 through 8. The corresponding standard deviations and coefficients of variation are listed below the mean values. It will now be shown how the data presented in these tables can be used to construct smooth response spectra. Consider as a specific example the data in Table 5 which pertain to the 2% damped response spectra for Case I.

59. In Table 5, consider first the values of the coefficient of variation (c.o.v.) of the ratios S_A/a_p and S_V/v_p as a function of natural period. The c.o.v. values of the velocity amplification factor are significantly lower within a range of moderate periods (from about 0.5 to 1.0 sec.) than on either side of this period range. The c.o.v. values of the acceleration amplification factor do not vary much between 0.1 and 0.4 sec. but make an upward jump (at T_n = 0.5 sec) just when the variability of the velocity amplification factor begins to decrease dramatically. Based on these patterns (of dependence of c.o.v. on natural period), the "corner period," which will separate the period ranges of amplified acceleration and amplified velocity,

Table 5

Response Spectra Amplification Factors and Their Statistics for 2% Damping for Earthquakes Selected for the "Case I" Site Seismic Condition

SA/AMAX RATIOS

DAMPING = 2 PERCENT

EARTHQUAKE	PERIODS											
	0.050	0.075	0.100	0.150	0.200	0.300	0.400	0.500	0.750	1.000	1.500	2.000
U300-1	1.050	0.959	1.413	1.678	2.281	2.562	2.793	1.702	1.281	1.008	0.317	0.127
U300-2	1.043	1.190	1.190	3.336	3.328	3.664	3.586	1.336	0.974	0.722	0.179	0.147
T286-1	1.247	1.602	2.050	2.850	3.733	3.300	3.033	3.733	1.783	1.068	1.717	1.092
T286-2	1.145	1.487	2.170	2.787	3.085	2.532	3.617	4.830	2.149	1.851	2.149	1.096
F086-1	1.019	1.037	1.280	1.785	2.991	3.617	2.224	2.533	1.626	2.645	1.318	0.771
F086-2	1.050	1.100	1.378	2.634	3.439	3.598	3.951	2.415	1.927	1.927	1.021	0.706
A009-1	1.013	1.145	1.541	1.767	1.956	2.874	4.440	2.723	3.239	1.730	3.214	1.956
A009-2	1.055	1.179	1.144	2.269	2.199	1.438	1.721	2.144	2.239	2.065	2.269	0.726
MEAN	1.078	1.212	1.521	2.388	2.876	2.948	3.171	2.677	1.902	1.627	1.523	0.828
STD.DEV.	0.079	0.221	0.386	0.609	0.652	0.767	0.906	1.126	0.687	0.643	1.028	0.585
C.O.V.	0.074	0.182	0.254	0.255	0.227	0.260	0.286	0.421	0.361	0.395	0.675	0.707

SV/VMAX RATIOS

DAMPING = 2 PERCENT

EARTHQUAKE	PERIODS											
	0.050	0.075	0.100	0.150	0.200	0.300	0.400	0.500	0.750	1.000	1.500	2.000
U300-1	0.143	0.196	0.385	0.686	1.244	2.096	3.047	2.322	2.620	2.750	1.295	0.694
U300-2	0.164	0.281	0.375	1.577	2.098	3.465	4.522	2.106	2.303	2.274	0.848	0.929
T286-1	0.094	0.181	0.308	0.643	1.123	1.490	1.826	2.808	2.012	1.607	3.374	3.285
T286-2	0.069	0.135	0.263	0.507	0.748	0.920	1.753	2.926	1.953	2.243	3.906	2.655
F086-1	0.049	0.075	0.123	0.257	0.574	1.041	0.853	1.215	1.170	2.537	1.896	1.479
F086-2	0.044	0.070	0.117	0.335	0.583	0.914	1.339	1.023	1.224	1.632	1.297	1.196
A009-1	0.035	0.060	0.107	0.185	0.273	0.601	1.237	0.949	1.692	1.205	3.358	2.725
A009-2	0.064	0.107	0.138	0.410	0.530	0.520	0.830	1.293	2.025	2.490	4.103	1.752
MEAN	0.083	0.138	0.227	0.575	0.896	1.381	1.926	1.830	1.875	2.092	2.572	1.839
STD.DEV.	0.048	0.077	0.120	0.442	0.581	0.983	1.265	0.808	0.499	0.545	1.369	0.943
C.O.V.	0.574	0.558	0.527	0.768	0.648	0.712	0.657	0.442	0.266	0.260	0.532	0.513

Table 6

Response Spectra Amplification Factors and Their Statistics for 5% Damping for Earthquakes Selected for the "Case I" Site Seismic Condition

SA/AMAX RATIOS

DAMPING = 5 PERCENT

EARTHQUAKE	PERIODS											
	0.050	0.075	0.100	0.150	0.200	0.300	0.400	0.500	0.750	1.000	1.500	2.000
U300-1	1.058	1.017	1.380	1.562	1.686	1.959	2.107	1.438	1.107	0.750	0.269	0.111
U300-2	1.052	1.095	1.069	2.716	2.474	2.664	2.621	1.017	0.741	0.367	0.170	0.110
T286-1	1.175	1.457	1.602	2.033	2.733	2.933	2.333	2.217	1.187	0.883	1.138	0.665
T286-2	1.036	1.268	1.557	1.834	2.255	2.191	2.298	2.787	1.281	1.121	1.523	0.911
P086-1	1.009	1.075	1.103	1.626	2.364	2.523	2.224	1.944	1.252	2.112	1.009	0.679
P086-2	1.021	1.072	1.354	2.171	2.622	2.598	3.951	1.793	1.561	1.463	0.762	0.567
A009-1	1.019	1.101	1.390	1.679	1.704	2.264	2.975	1.994	2.736	1.667	2.516	1.761
A009-2	1.050	1.095	1.104	1.975	1.796	1.184	1.478	1.672	2.104	1.915	1.438	0.642
MEAN	1.052	1.147	1.320	1.950	2.204	2.290	2.498	1.858	1.496	1.285	1.103	0.681
STD.DEV.	0.053	0.144	0.208	0.375	0.421	0.541	0.726	0.526	0.636	0.607	0.754	0.519
C.O.V.	0.050	0.125	0.157	0.192	0.191	0.236	0.291	0.283	0.425	0.472	0.683	0.762

SV/VMAX RATIOS

DAMPING = 5 PERCENT

EARTHQUAKE	PERIODS											
	0.050	0.075	0.100	0.150	0.200	0.300	0.400	0.500	0.750	1.000	1.500	2.000
U300-1	0.144	0.208	0.376	0.639	0.920	1.603	2.299	1.961	2.265	2.047	1.099	0.604
U300-2	0.166	0.259	0.337	1.284	1.560	2.519	3.304	1.603	1.753	1.158	0.803	0.696
T286-1	0.088	0.164	0.241	0.459	0.822	1.324	1.404	1.668	1.339	1.329	2.569	2.001
T286-2	0.063	0.115	0.189	0.333	0.547	0.797	1.114	1.689	1.164	1.359	2.769	2.207
P086-1	0.048	0.077	0.106	0.234	0.454	0.726	0.853	0.932	0.901	2.026	1.452	1.303
P086-2	0.043	0.068	0.115	0.276	0.444	0.660	1.339	0.759	0.992	1.240	0.968	0.961
A009-1	0.035	0.058	0.097	0.175	0.237	0.473	0.829	0.694	1.429	1.161	2.529	2.453
A009-2	0.063	0.099	0.133	0.357	0.433	0.428	0.713	1.008	1.903	2.310	2.601	1.548
MEAN	0.081	0.131	0.199	0.470	0.677	1.066	1.482	1.289	1.468	1.578	1.861	1.472
STD.DEV.	0.048	0.073	0.109	0.359	0.420	0.715	0.892	0.492	0.473	0.468	0.856	0.701
C.O.V.	0.595	0.554	0.547	0.765	0.620	0.670	0.602	0.382	0.322	0.296	0.460	0.476

Table 7

Response Spectra Amplification Factors and Their Statistics for 2% Damping for Earthquakes Selected for the "Case II" Site Seismic Condition

SA/AMAX RATIOS

DAMPING = 2 PERCENT

EARTHQUAKE	PERIODS											
	0.050	0.075	0.100	0.150	0.200	0.300	0.400	0.500	0.750	1.000	1.500	2.000
A003-1	1.043	1.079	1.313	1.345	1.668	2.617	3.085	3.851	3.170	2.447	1.353	1.857
A003-2	1.025	1.064	1.142	1.489	2.000	2.981	2.547	3.038	4.226	3.962	1.423	1.447
A006-1	1.009	1.136	1.069	1.891	2.309	3.764	4.091	5.073	2.545	3.182	1.700	1.016
A006-2	1.027	1.148	1.302	1.427	2.252	4.068	3.341	3.591	3.318	3.477	3.500	1.164
MEAN	1.026	1.107	1.206	1.538	2.057	3.357	3.266	3.888	3.315	3.267	1.994	1.371
STD.DEV.	0.014	0.041	0.121	0.243	0.292	0.673	0.642	0.859	0.694	0.634	1.015	0.370
C.O.V.	0.013	0.037	0.100	0.158	0.142	0.201	0.196	0.221	0.209	0.194	0.509	0.270

SV/VMAX RATIOS

DAMPING = 2 PERCENT

EARTHQUAKE	PERIODS											
	0.050	0.075	0.100	0.150	0.200	0.300	0.400	0.500	0.750	1.000	1.500	2.000
A003-1	0.062	0.096	0.155	0.238	0.394	0.928	1.459	2.277	2.811	2.893	2.400	4.392
A003-2	0.047	0.073	0.104	0.203	0.363	0.812	0.926	1.380	2.879	3.599	1.939	2.629
A006-1	0.071	0.120	0.150	0.399	0.649	1.588	2.301	3.567	2.685	4.475	3.586	2.859
A006-2	0.037	0.063	0.095	0.156	0.329	0.891	0.976	1.311	1.817	2.539	3.833	1.699
MEAN	0.054	0.088	0.126	0.249	0.434	1.055	1.415	2.134	2.548	3.376	2.939	2.895
STD.DEV.	0.015	0.025	0.031	0.105	0.146	0.359	0.638	1.052	0.494	0.855	0.915	1.117
C.O.V.	0.276	0.290	0.247	0.423	0.337	0.340	0.451	0.493	0.194	0.253	0.311	0.386

Table 8

Response Spectra Amplification Factors and Their Statistics for 5% Damping for Earthquakes Selected for the "Case II" Site Seismic Condition

SA/AMAX RATIOS

DAMPING = 5 PERCENT

EARTHQUAKE	PERIODS											
	0.050	0.075	0.100	0.150	0.200	0.300	0.400	0.500	0.750	1.000	1.500	2.000
A003-1	1.030	1.038	1.143	1.217	1.532	1.966	2.255	2.851	2.277	1.796	1.026	1.168
A003-2	1.011	1.036	1.089	1.349	1.677	2.075	2.113	2.302	3.453	3.170	1.355	1.070
A006-1	1.016	1.113	1.025	1.442	1.873	2.491	2.727	3.218	2.127	2.127	1.204	0.731
A006-2	1.011	1.070	1.243	1.220	1.955	3.159	2.239	2.364	2.545	2.318	2.341	0.989
MEAN	1.017	1.064	1.125	1.307	1.759	2.423	2.334	2.684	2.601	2.353	1.481	0.989
STD.DEV.	0.009	0.036	0.092	0.109	0.191	0.540	0.270	0.433	0.594	0.586	0.589	0.187
C.O.V.	0.009	0.034	0.082	0.083	0.109	0.223	0.116	0.161	0.228	0.249	0.397	0.189

SV/VMAX RATIOS

DAMPING = 5 PERCENT

EARTHQUAKE	PERIODS											
	0.050	0.075	0.100	0.150	0.200	0.300	0.400	0.500	0.750	1.000	1.500	2.000
A003-1	0.061	0.092	0.135	0.216	0.362	0.697	1.067	1.685	2.019	2.123	1.819	2.762
A003-2	0.046	0.071	0.099	0.184	0.305	0.566	0.768	1.046	2.352	2.879	1.346	1.944
A006-1	0.071	0.117	0.144	0.304	0.527	1.051	1.534	2.263	2.244	2.992	2.539	2.056
A006-2	0.037	0.059	0.091	0.134	0.285	0.692	0.654	0.863	1.394	1.692	2.564	1.444
MEAN	0.054	0.085	0.117	0.209	0.370	0.751	1.006	1.464	2.002	2.422	2.192	2.051
STD.DEV.	0.015	0.026	0.026	0.072	0.110	0.209	0.393	0.639	0.429	0.621	0.415	0.544
C.O.V.	0.286	0.305	0.225	0.342	0.296	0.278	0.391	0.436	0.214	0.256	0.189	0.265

can be roughly estimated (the corner period is about 0.5 sec. in this case).

60. The second step is to evaluate the mean and the standard deviation of the amplification factors S_A/a_p and S_V/v_p. Note the patterns of variation of the mean amplification factors with period. The mean values of S_A/a_p initially increase with period, then reach a plateau in the range 0.2 sec. $\leq T_n \leq$ 0.5 sec., and finally decrease rapidly as T_n increases beyond 0.5 sec. In the range 0.2 sec. $\leq T_n \leq$ 0.5 sec., the mean of the acceleration amplification factor is 2.9 and its standard deviation is about 0.8. Similarly, in the amplified velocity range, 0.5 sec. $\leq T_n \leq$ 2 sec., the mean of the velocity amplification factor is 2.05 and its standard deviation is about 0.8.

61. In the short period range of the response spectrum, a gradual transition must be made between the zero-period value $S_A/a_p = 1$ and the level prevailing in the period range where the acceleration amplification is constant. A solid guide is the array of computed mean acceleration amplification factors in this transition range (see Table 5). The corresponding standard deviations are also available to aid in constructing scaled spectra corresponding to the mean plus one standard deviation.

62. The following procedure is suggested for estimating the mean <u>acceleration</u> amplification factor in the amplified velocity range of the response spectrum: (a) estimate the ratio v_p/a_p either by averaging the values of this ratio for each of the records selected or by using the attenuation relationships (predictions of a_p and v_p in function of M and R), and (b) multiply this ratio by the mean amplification factor S_V/v_p, and (c) multiply the result by $\omega_n = (2\pi/T_n)$. A parallel procedure may be followed in the amplified displacement range of the response spectrum.

63. It is proposed that the uncertainty in the ratio v_p/a_p not be reflected in the standard deviation of the scaled response spectra in the amplified velocity range. The standard deviation need only reflect uncertainty in the amplification factor S_V/v_p. This stems from the fact that the maximum ground velocity can be estimated independently, just as well as the maximum ground acceleration. In the velocity range of the response spectrum, when it comes to assessing variability, one may view the ground velocity, not the ground acceleration, as the "anchor." The result is that the coefficient of variation of the scaled response spectra will not necessarily be larger for moderate and large periods than for relatively short periods.

64. The smooth response spectra for 2% and 5% damping (for natural periods below 2 sec.) corresponding to the two seismic conditions are shown in Figures 31 and 32, respectively. Each figure shows the response spectra corresponding to the mean and to the mean plus one standard deviation. A direct comparison of the mean 5% damped response spectra corresponding to the two seismic conditions is made in Fig. 33.

65 We have just outlined how "compatible" smooth response spectra can be estimated from a set of time histories representing a well-defined seismic condition. For the sake of completeness, it should be mentioned that it is also possible to obtain compatible seismic input in the form of the spectral density function and strong-motion duration, which constitute the input for seismic random vibration analysis of structures. The duration and the parameters of the spectral density function may now be viewed as random variables whose properties (mean, standard deviation) can be estimated partly from correlations with magnitude and distance, and

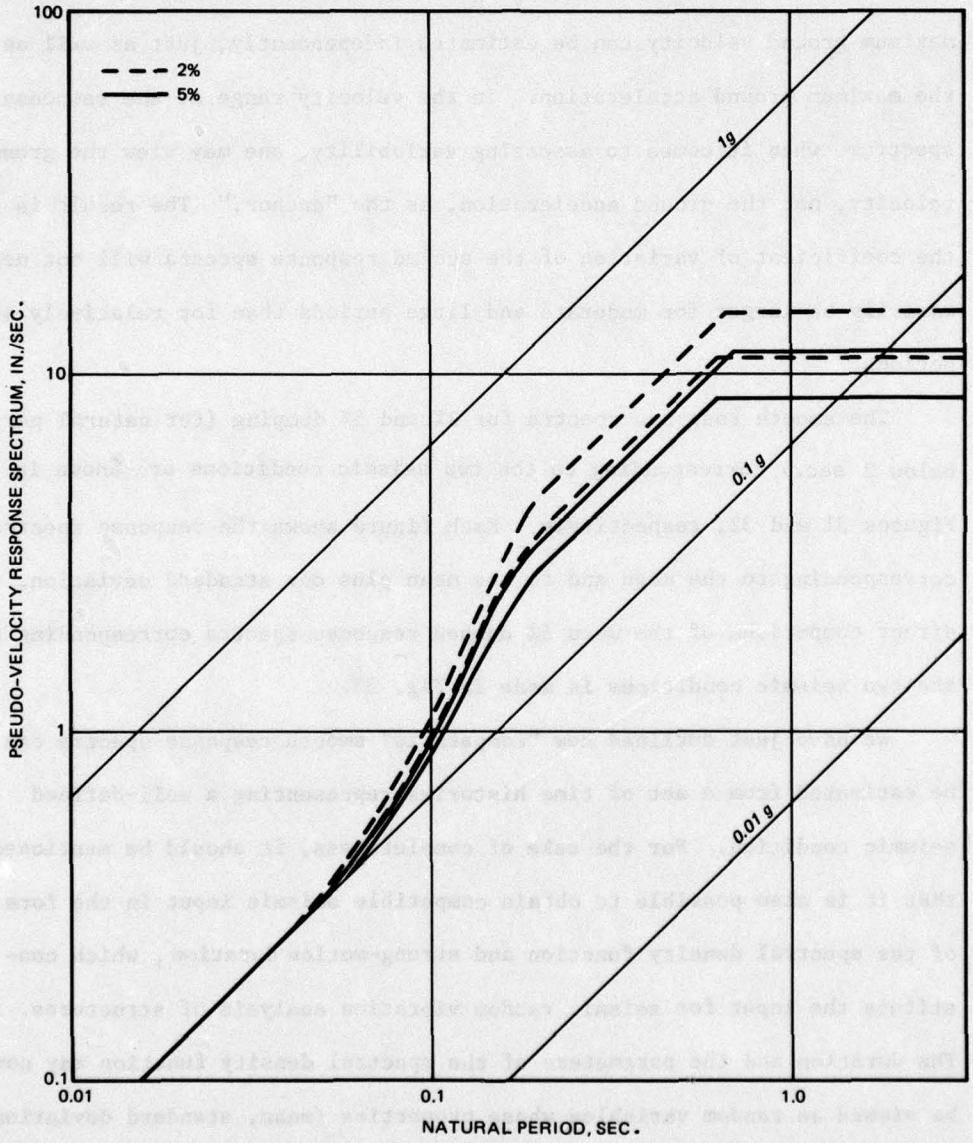

Figure 31. Smooth response spectra corresponding to mean and mean plus standard deviation for 2% and 5% damping for "Case I" site seismic condition

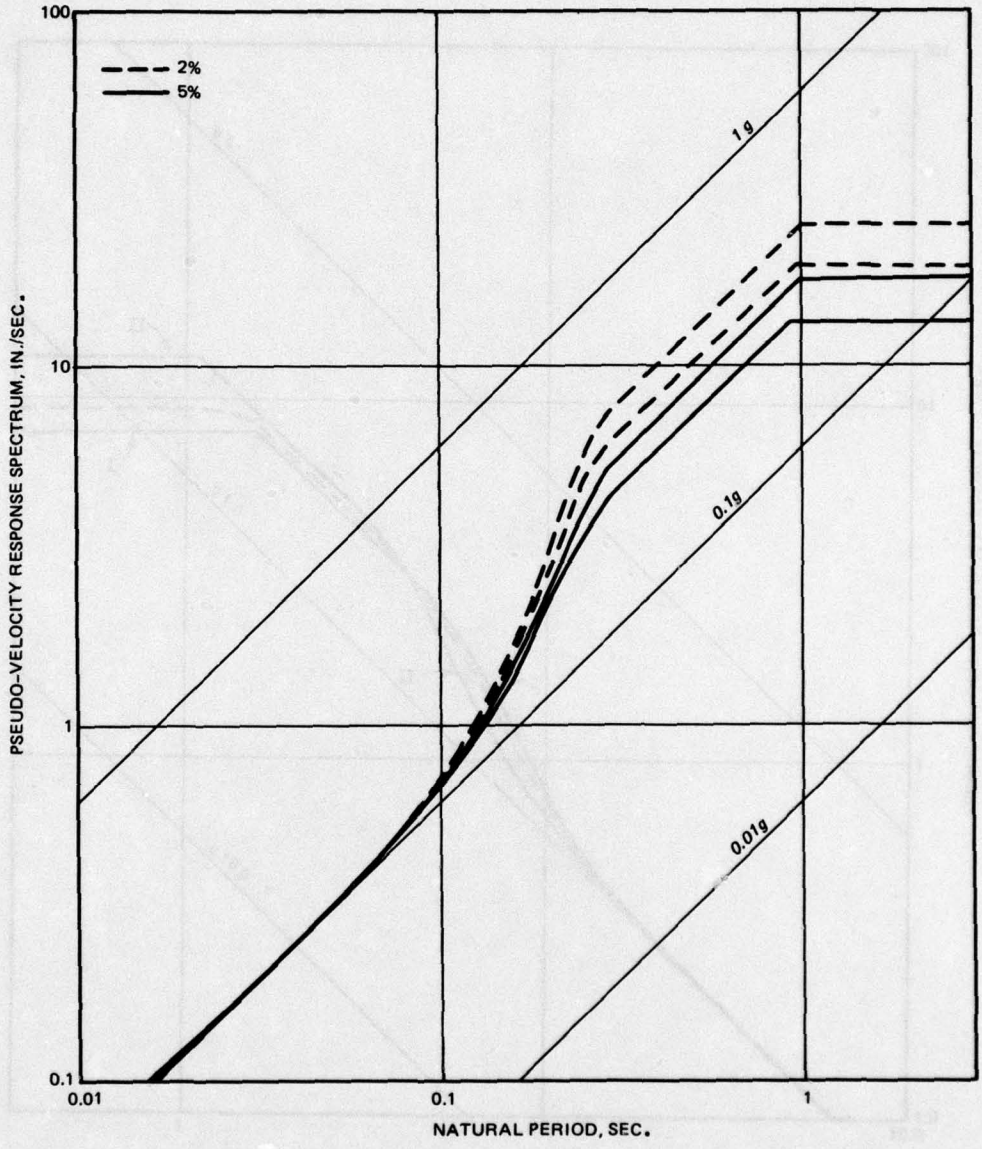

Figure 32. Smooth response spectra corresponding to mean and mean plus standard deviation for 2% and 5% damping for "Case II" site seismic condition

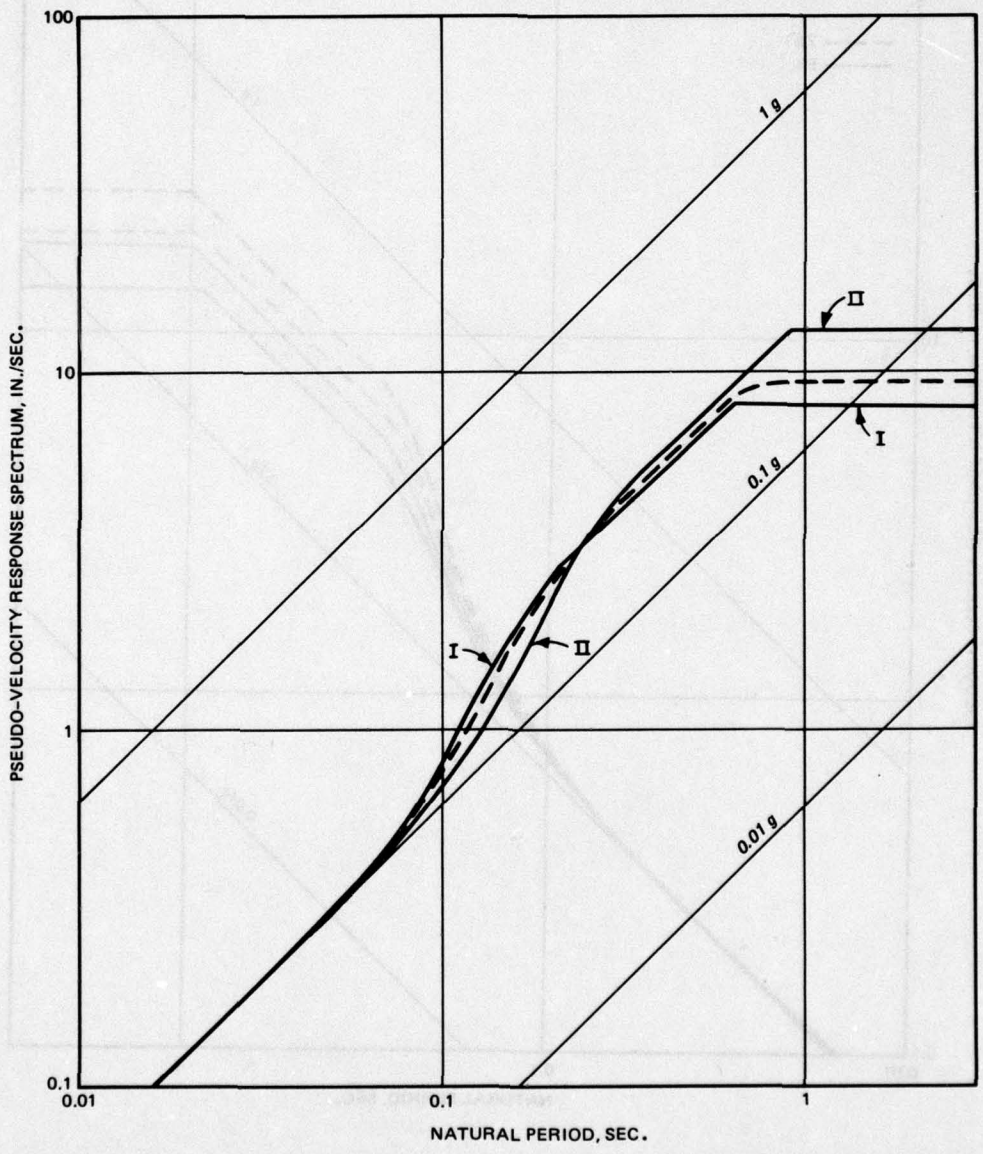

Figure 33. Mean response spectra for 5% damping corresponding to two seismic conditions at the same site. Dotted line is a design response spectrum for 50% probability of exceedance (p_I = 0.7 and p_{II} = 0.3)

partly from the specific earthquake records selected to represent the seismic condition under study. This probabilistic input representation is also a starting point for generating compatible artificial earthquake time histories. The details of these procedures are beyond the scope of this report.

Design Response Spectra

66. Throughout Part V of the report, reference has been made to compatible ground motion representations for a given site seismic condition. For purposes of illustration, two different seismic conditions (Cases I and II) were considered. The terminology "design seismic condition" or "design response spectra" was deliberately avoided. The smooth response spectra corresponding to a given seismic condition may indeed be interpreted as design response spectra if that particular condition greatly dominates the seismic risk at the site. If two or more different seismic conditions significantly contribute to the seismic risk at the site, then it becomes necessary, in order to generate proper design response spectra, to combine the information about the (conditional) responses given each seismic condition with information (provided by seismic risk assessment) about the relative likelihood of occurrence of each seismic condition. A procedure to do this is illustrated below.

67. Take as an example a "soil site" where the 0.1-g design earthquake may originate either from a moderate earthquake at moderate distance (Type I) or from a large, distant earthquake (Type II). The probabilities, p_I and $p_{II} = 1 - p_I$, that the design earthquake will be of a particular type can be obtained from a combination of seismological and geological information, sup-

ported by judgement and perhaps by formal seismic risk analysis. Ground motions and smooth site response spectra representing the two seismic conditions have been obtained before. Specifically, means and standard deviations of the amplification factors governing the shape of the response spectra in the various period ranges have been determined. From this information, one can evaluate the probability that the amplification factor S_A/a_p is less than a specified value, say r, given the type of earthquake. These conditional probabilities will be denoted by $p(r|I)$ and $p(r|II)$.

68. The probability that the design response spectra amplification factor will be less than a given value r is

$$p(r) = p(r|I)p_I + p(r|II)p_{II} .$$

This probability of no exceedance must be evaluated for a range of values of the factor r. From the relationship between p(r) and r, the engineer can then obtain the design amplification factor corresponding to a prescribed exceedance probability. To carry out the computations, a choice has to be made concerning the probability distribution of the amplification factors for each type of earthquake. This choice is not critical if probabilities of no exceedance between 0.5 and 0.9 are involved. (The normal distribution was assumed in the illustrative calculation.) Of course, the procedure needs to be repeated for a limited number of periods for each damping ratio for which response spectra are sought. As an illustration, the median design response spectra were calculated for a situation where the large, distant earthquake (Type II) was judged to carry 30%, and the closer, moderate earthquake (Type I) 70%, of the seismic risk at the 0.1-g design level. It follows that $p_I = 0.7$ and $p_{II} = 0.3$. The resulting median design response spectra for 5%

damping are shown in Fig. 33, together with the median (or mean) response spectra for the two "constituent" seismic conditions.

Conclusion

69. In Part V of the report, a procedure has been presented for developing site-specific smooth response spectra that are in agreement with (and are derived from) a set of accelerograms selected on the basis of their compatibility with a prescribed site seismic condition. Such a condition may be described in terms of an event magnitude and a distance (or a range of distances) as well as in terms of the soil conditions at the site; of course, further constraints could be imposed, e.g., on the source mechanism or the tectonic province. An alternative is to express the site seismic condition in terms of maximum ground motion amplitudes and duration. Clearly, the procedure permits all potentially significant factors to be considered in constructing site-specific spectra. It differs in this sense from the approach presented by Seed et al. (18), which singles out local site geology as the factor affecting the shape of site-specific response spectra.

70. The proposed approach to response spectra smoothing, while obviously not unique, has the following desirable features: (a) it relies on "prior" information about response spectra shapes in the acceleration, velocity (and displacement) ranges of the spectrum, (b) it permits the calculation of relatively stable estimates of the means and standard deviations based on only a small number of records, and (c) it makes full use of information about maximum ground velocity (or displacement) and about the amplification factors in the velocity (or displacement) range of the response spectra. Finally, the report outlines the steps required to obtain smooth design response spectra if two or more different types of earthquakes can cause design level shaking at the site.

REFERENCES

1. Krinitzsky, E. L. and Chang, F. K., "State-of-the-Art for Assessing Earthquake Hazards in the United States; Specifying Peak Motions for Design Earthquakes," Miscellaneous Paper S-73-1, Report 7, Jan 1979, U. S. Army Engineer Waterways Experiment Station, CE, Vicksburg, Miss.

2. Newmark, N. M., Blume, J. A., and Kapur, K., "Design Response Spectra for Nuclear Power Plants," Journal, Power Division, American Society of Civil Engineers, Vol 99, No. PO2, 1973, pp 287-303.

3. Office of Nuclear Reactor Regulation, U. S. Nuclear Regulatory Commission, "Design Response Spectra for Nuclear Power Plants," Regulatory Guide No. 1.60, Washington, D. C.

4. Vanmarcke, E. H., "Structural Response to Earthquakes," Chap. 8 in Seismic Risk and Engineering Decisions, C. Lomnitz and E. Rosenblueth, eds., Elsevier Publishing Co., Amsterdam - Oxford - New York, 1976.

5. Vanmarcke, E. H. and Cornell, C. A., "Seismic Risk and Design Response Spectra," Proceedings, American Society of Civil Engineers Specialty Conference on Safety and Reliability of Metal Structures, 1972, pp 1-25.

6. McGuire, R. K., "The Use of Intensity Data in Seismic-Hazard Analysis," Sixth World Conference on Earthquake Engineering, 1977a, New Delhi, India.

7. _____, "A Simple Model for Estimating Fourier Amplitude Spectra of Horizontal Ground Motions," Bulletin of Seismological Society of America, 1977b.

8. McGuire, R. K. and Barnard, J. A., "Magnitude Distance and Intensity Data for C. I. T. Strong Motion Records," U. S. Geological Survey Journal of Research, Vol 5, No. 3, 1977.

9. Chang, F. K. and Krinitzsky, E. L., "State-of-the-Art for Assessing Earthquake Hazards in the United States; Duration, Spectral Content, and Predominant Period of Strong-Motion Earthquake Records from Western United States," Miscellaneous Paper S-73-1, Report 8, Jan 1978, U. S. Army Engineer Waterways Experiment Station, CE, Vicksburg, Miss.

10. Newmark, N. M. and Hall, W. J., "A Rational Approach to Seismic Design Standards for Structures," Proceedings, Fifth World Conference on Earthquake Engineering, Rome, 1973.

11. Newmark, N. M. and Rosenblueth, E., Fundamentals of Earthquake Engineering, Prentice-Hall, Englewood Cliffs, N. J., 1971.

12. Seed, H. B. and Idriss, I. M., "Simplified Procedure for Evaluating Soil Liquefaction Potential," Journal, Soil Mechanics and Foundations Division, American Society of Civil Engineers, Vol 97, No. SM9, Sep 1971, pp 1249-1273.

13. Seed, H. B. and Peacock, W. H., "Applicability of Laboratory Test Procedures for Measuring Soil Liquefaction Characteristics Under Cyclic Loading," Earthquake Engineering Research Center Report No. 70-8, Nov 1978, University of California, Berkeley, Calif.

14. Lee, K. L. and Chan, K., "Number of Significant Cycles in Strong Motion Earthquakes," Proceedings, Microzation Conference, Vol 2, 1972, Seattle, Wash.

15. Crandall, S. H. and Mark, W. D., Random Vibration in Mechanical Systems, Academic Press, New York, 1963.

16. Chang, F. K., "State-of-the-Art for Assessing Earthquake Hazards in the United States; Catalogue of Strong Motion Earthquakes, Vol 1, Western United States, 1933-1971," Miscellaneous Paper S-73-1, Report 9, Apr 1978, U. S. Army Engineer Waterways Experiment Station, CE, Vicksburg, Miss.

17. Vanmarcke, E. H. and Lai, P., "Strong-Motion Duration of Earthquakes," Department of Civil Engineering Research Report R77-16, 1977, Massachusetts Institute of Technology, Cambridge, Mass.

18. Seed, H. B., Ugas, C., and Lysmer, J., "Site-Dependent Spectra for Earthquake-Resistant Design," Earthquake Engineering Research Center Report 74-12, Nov. 1974, University of California, Berkeley, Calif.

In accordance with letter from DAEN-RDC, DAEN-ASI dated 22 July 1977, Subject: Facsimile Catalog Cards for Laboratory Technical Publications, a facsimile catalog card in Library of Congress MARC format is reproduced below.

Vanmarcke, Erik H

State-of-the-art for assessing earthquake hazards in the United States; Report 14: Representation of earthquake ground motion: scaled accelerograms and equivalent response spectra / by Erik H. Vanmarcke, Department of Civil Engineering, Massachusetts Institute of Technology, Cambridge, Massachusetts. Vicksburg, Miss. : U. S. Waterways Experiment Station ; Springfield, Va. : available from National Technical Information Service, 1979.

83 p. : ill. ; 27 cm. (Miscellaneous paper - U. S. Army Engineer Waterways Experiment Station ; S-73-1, Report 14)

Prepared for Office, Chief of Engineers, U. S. Army, Washington, D. C., under Purchase Order No. DACW39-78-M-3907.

References: p. 82-83.

1. Accelerograms. 2. Earthquake engineering. 3. Earthquake hazards. 4. Earthquakes. 5. Ground motion. 6. Seismic analysis. 7. State-of-the-art studies. I. Massachusetts Institute of Technology. Dept. of Civil Engineering. II. United States. Army. Corps of Engineers. III. Series: United States. Waterways Experiment Station, Vicksburg, Miss. Miscellaneous paper ; S-73-1, Report 14.
TA7.W34m no.S-73-1 Report 14